PennWell

CELEBRATING 50 YEARS 1965-2015

November 2015

LaserFocusWorld®

Photonics Technologies & Solutions for Technical Professionals Worldwide

www.laserfocusworld.com

QCL arrays target IR spectral analysis

PAGE 36

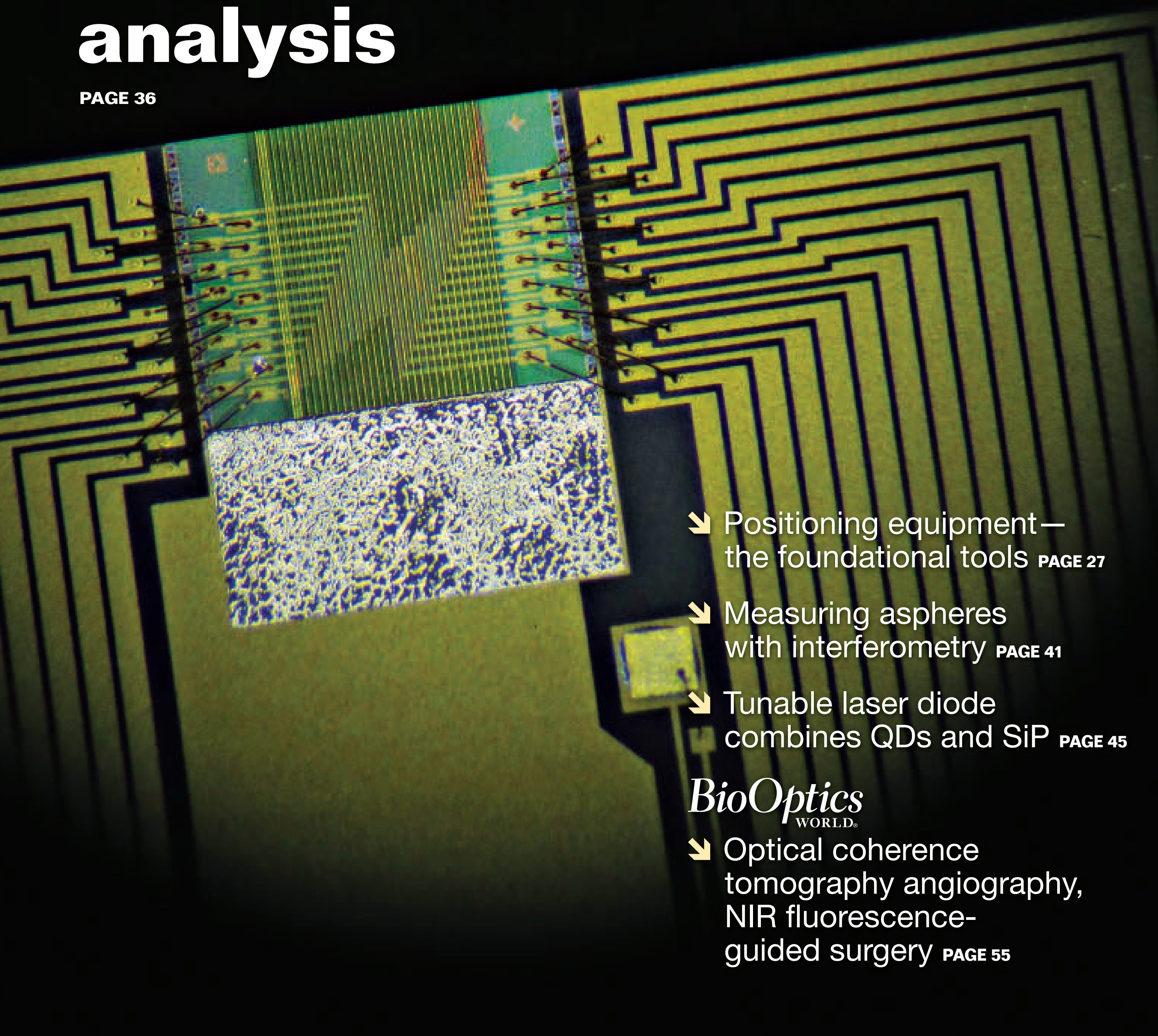

- Positioning equipment—the foundational tools PAGE 27
- Measuring aspheres with interferometry PAGE 41
- Tunable laser diode combines QDs and SiP PAGE 45

BioOptics WORLD®

- Optical coherence tomography angiography, NIR fluorescence-guided surgery PAGE 55

Optimize Your Surface Measurement and Inspection Motion

Save 40% Measurement Time and 60% Footprint

Traditional Cartesian systems require frequent, time-consuming motion reversals in X and Y to raster-scan a part, which necessitates longer travel ranges to account for inefficiencies in constantly starting and stopping. The vastly superior SMP design utilizes an industry-leading rotational motion profile to deliver smooth, continuous scanning of the part, with no starts and stops, resulting in significantly reduced measurement time and machine footprint.

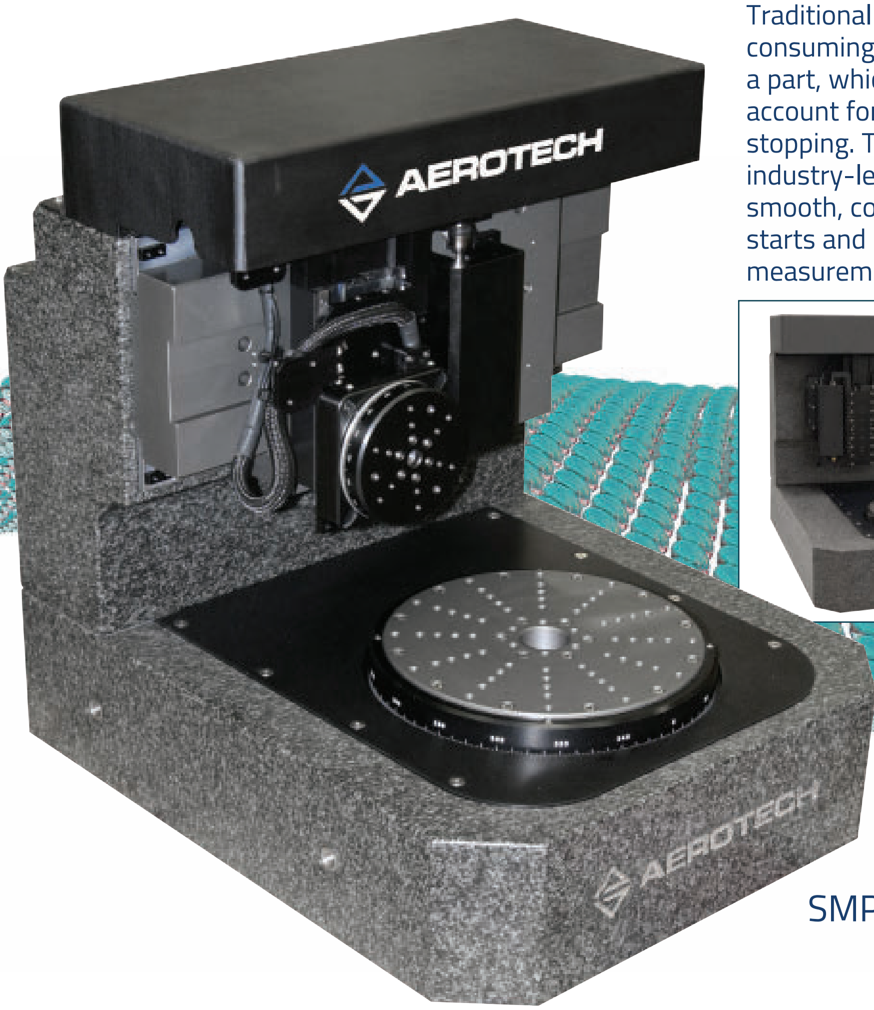

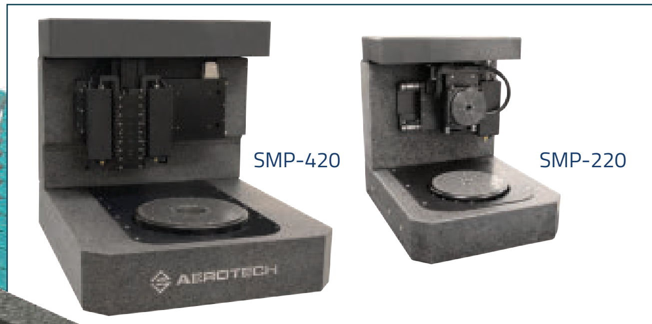

SMP-320

- Reduce measurement time by 40% compared to Cartesian systems
- Minimize footprint by 60% compared to Cartesian systems
- Axis repeatability in the low nanometer range
- Nanometer-level minimum incremental motion (resolution)
- Ultra-smooth motion even at very low velocities
- Easily customizable for customer-specific measurement processes

Spherical

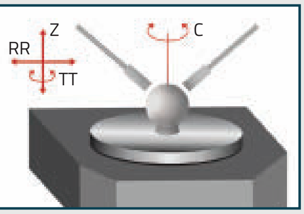

Aspheric

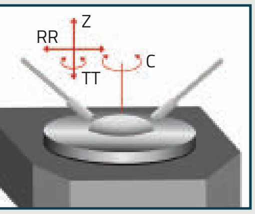

Cylindrical

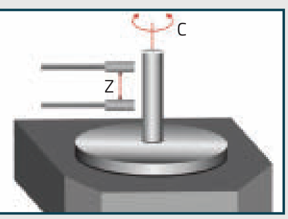

AEROTECH
Dedicated to the Science of Motion

Ph: 412-963-7470
Email: sales@aerotech.com
www.aerotech.com

Aerotech Worldwide
United States • France • Germany • United Kingdom
China • Japan • Taiwan

AF1114E-TMG

newsbreaks

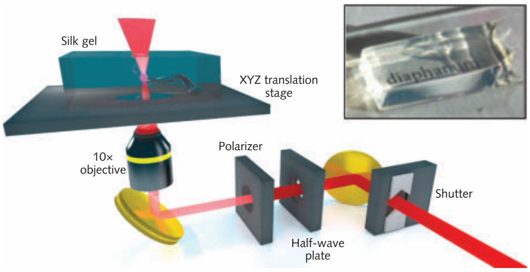

world news

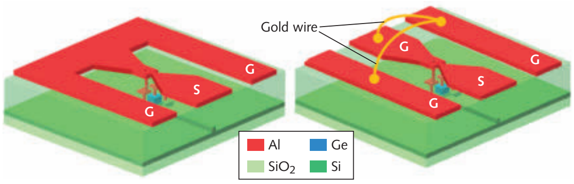

columns

departments

LASERS ▪ OPTICS ▪ DETECTORS ▪ IMAGING ▪ FIBER OPTICS ▪ INSTRUMENTATION

features

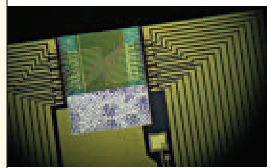

36 COVER STORY
A 200 cm^{-1} prototype quantum-cascade-laser (QCL) array with 32 QCLs is shown prior to beam combining and packaging. *(Courtesy of Pendar Technologies)*

LASER FOCUS WORLD PRESENTS
BioOptics WORLD

Coming in December

Next month includes special articles to highlight what's hot in many important areas:

- A continuation of our Looking Back/Looking Forward series will investigate the many types of optical design software.
- Senior editor John Wallace will examine the top 20 technology stories of 2015.
- Articles on magnetorheological finishing (MRF) and high-power laser calibration and characterization.

In *BioOptics World*, we will have articles on optoacoustic imaging and optical filtering for the life sciences.

laserfocusworld.online

More Features, News & Products

trending now

Focus on Positioning & Support

Laser Focus World covers optical mounting, positioning, and isolation equipment available for everything from simple optics to confocal microscopes and interferometers. Here are three of our most recent articles on this topic.

Kirigami thin-film photovoltaic cells flex to track the sun

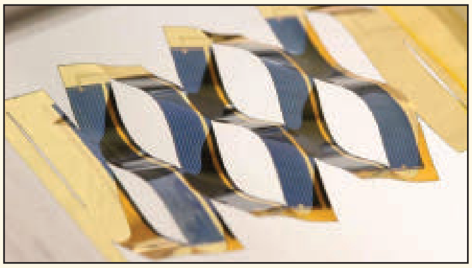

A team of researchers has come up with a way to tilt solar cells in a simple, compact way such that the whole apparatus can fit within a flat solar panel.
http://bit.ly/1LIB7ye

Get the most out of your microscope by understanding your site environment

Measuring and analyzing environmental noise before the installation of a precision microscope enables the end user to save time, money, and resources by preparing the installation location appropriately for the incoming instrument.

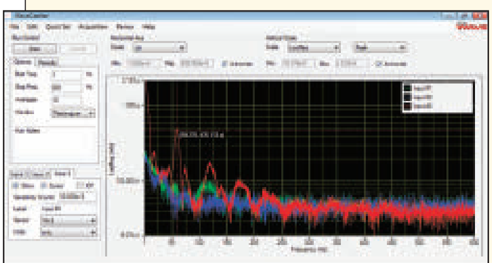

http://bit.ly/201ovMm

Matter wave interferometry cools atoms and should cool molecules

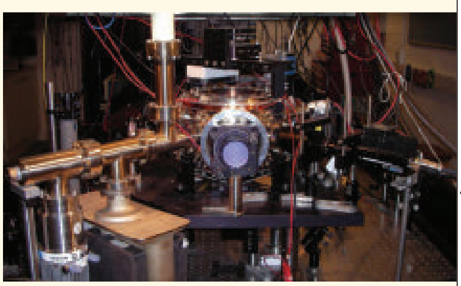

Researchers demonstrated for the first time a new laser cooling method—based upon the interference of matter waves—that could be used to cool molecules.
http://bit.ly/1RqXv2x

CORRECTION The cover photo in the October 2015 issue should have been credited to Optimax Systems and not Thin Film Center. *Laser Focus World* regrets the error.

www.laserfocusworld.com

cool content

Blog: Photon Focus

Strategies Unlimited senior analyst Allen Nogee gives his thoughts on a Kickstarter campaign for a **laser-powered razor** in development. Keep coming back to our blog for more hot topics, cool commentary, and other events-related musings!
http://bit.ly/14RIfUO

Technical Digests dig into technology topics

Laser Focus World offers free downloadable technical digests that provide an in-depth resource on photonics and optoelectronics topics, including **free-form optics** and **military laser systems**.
http://bit.ly/ViD38v

Webcasts let you make new discoveries from your desktop

Whether you are looking to learn about **laser damage to optics** or **finite element modeling of laser material processing**, we've got webcasts aplenty to meet your educational needs.
http://bit.ly/Onhs9J

White papers offer detailed tech specs on many products

Our library of technical white papers delves into performance attributes of several optics and photonics products available on the market, including **LED lens component optimization software** and **nanostructured substrates for optical diagnostics**.
http://bit.ly/1BUCpTf

editor's desk

Built on a solid foundation

Stability and precision are critical characteristics of photonics tools, and represent a recurrent theme of this issue. The characteristics are essential in interferometers, as noted by senior editor John Wallace in his Photonics Products feature exploring the different products and methods available for interferometrically measuring aspheres (see page 41). Contributing editor Jeff Hecht, continuing his 50th year celebration of *Laser Focus World*, furthers the theme by telling tales of how optical positioning equipment was developed to put interferometers, holography systems, and many other optical systems on a stable footing. As he recounts, we have come a long way from some initial lab setups that had tabletops resting on the inner tubes of truck tires (see page 27).

Greater stability and precision in biophotonics tools are also evident in our *BioOptics World* section this month, where researchers explain recent, significant advances in two fields: near-infrared fluorescence guidance for advanced surgery techniques (see page 63) and optical coherence tomography angiography (OCTA), which, aided by data processing, promises to be useful in clinical monitoring and therapeutic treatment of the retina (see page 58).

Products have always been the most reliably popular topic in our website and magazine, and of course in our Buyers Guide. They are the tools that scientists and engineers actually use or specify in their work. To illustrate, the Photonics Products article on interferometers that I described earlier is part of John Wallace's widely read, bi-monthly series on products, and I'm happy to say that the series becomes monthly in 2016, with senior editor Gail Overton also contributing with product survey articles on topics such as specialty fibers, spectrometers, high-speed cameras, and nanopositioners.

I am confident that these articles will contribute to the continued stability and precision found in *Laser Focus World* over the past 50 years.

W. Conard Holton
Associate Publisher/
Editor in Chief
cholton@pennwell.com

LaserFocusWorld

Alan Bergstein Group Publisher, (603) 891-9447; alanb@pennwell.com
W. Conard Holton Editor in Chief, (603) 891-9161; cholton@pennwell.com
Gail Overton Senior Editor, (603) 305-4756; gailo@pennwell.com
John Wallace Senior Editor, (603) 891-9228; johnw@pennwell.com
Lee Dubay Associate Editor, (603) 891-9116; leed@pennwell.com

CONTRIBUTING EDITORS
David A. Belforte Editor in Chief, *Industrial Laser Solutions*, (508) 347-9324; belforte@pennwell.com
Barbara Gefvert Editor in Chief, *BioOptics World*, (603) 891-9194; barbarag@pennwell.com
Jeff Hecht Photonic Frontiers, (617) 965-3834; jeff@jeffhecht.com

Meg Fuschetti Editorial Creative Director
Sheila Ward Production Manager
Chris Hipp Senior Illustrator
Gillian Hinkle Marketing Manager
Debbie Bouley Audience Development Manager
Alison Boyer Ad Services Manager

SUBSCRIPTION INQUIRIES
(847) 763-9540; fax (847) 763-9607; e-mail: lfw@halldata.com
web: www.lfw-subscribe.com

PennWell®
www.pennwell.com

EDITORIAL OFFICES
Laser Focus World
PennWell Corporation
98 Spit Brook Road, LL-1, Nashua, NH 03062-5737
(603) 891-0123; fax (603) 891-0574
www.laserfocusworld.com

CORPORATE OFFICERS
Robert F. Biolchini Chairman
Frank T. Lauinger Vice Chairman
Mark C. Wilmoth President and Chief Executive Officer
Jayne A. Gilsinger Executive Vice President, Corporate Development and Strategy
Brian Conway Senior Vice President, Finance and Chief Financial Officer

TECHNOLOGY GROUP
Christine A. Shaw Senior Vice President / Group Publishing Director

Pancharatnam lens acts as improved diffractive lens

In a “Pancharatnam” phase-modifying optical device, the polarization state of a circularly polarized wavefront passing through the device is modified by the device as a continuous function of the position across the device. For example, a Pancharatnam lens is basically a half-wave retarder, with the retarder’s local optical axis aligned with the azimuthal angle at that point. Such a lens—when designed as a positive lens for, say, right-handed, circularly polarized light—focuses light as a positive lens should, but becomes a negative lens when left-handed circularly polarized light is passed through the lens. Pancharatnam lenses have previously been fabricated by microrubbing, creating a space-variant subwavelength dielectric grating, or via holographic alignment. Now, a group at Kent State University (Kent, OH) has made an ultrathin (2.26 µm) *f*/2.1 Pancharatnam lens using a polarization holography alignment technique. The technique, which is low-cost, could be applicable to a wide size range.

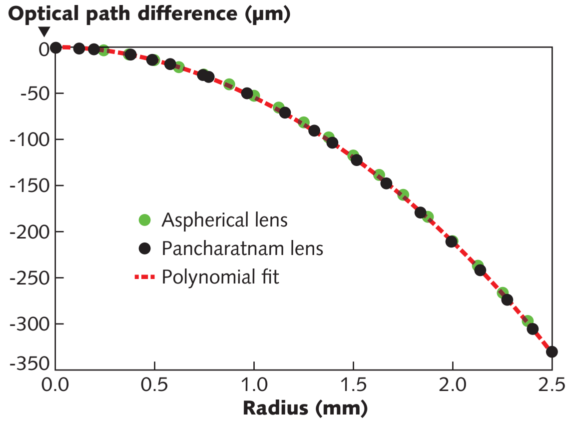

Unlike a conventional diffractive lens, a Pancharatnam lens does not diffract light into undesired orders. However, like ordinary diffractive lenses, it does have a strong wavelength dependence. The researchers fabricated an experimental device for a 632 nm wavelength using a photoalignment layer that shows a strong orientational response to the local polarization axis of light, and is exposed in a holographic setup to provide the desired half-wave retarder orientation. The result is a polarization axis that is a function of the radial distance from the center of the pattern with a gradually decreased grating pitch to the edge. The design of the fabricated device had a parabolic phase profile and showed the expected imaging properties, which were good imaging quality for low *f* numbers and some degradation for higher *f* numbers. A design modeling the optimal diffraction-limited asphere would avoid the image degradation. *Reference: K. Gao et al.,* Opt. Express, *23, 20, 26086 (Oct. 5, 2015).*

X-ray pumped laser produces 1.4 Å narrow-linewidth hard x-ray emission

In 2011, Japanese researchers achieved coherent x-ray free-electron laser emission of 1.2 Å from the SPring-8 Angstrom Compact Free Electron Laser (SACLA; Hyogo, Japan), which today routinely produces < 1 Å hard x-ray pulses (photon energy on the order of 10 keV) with 10^{20} W/cm^2 maximum focus intensity.

Now, in an effort to further the study of the movement of electrons within materials and, hence, gain crucial light-matter interaction information that governs nearly all physical processes, researchers at the University of Electro-Communications and the University of Tokyo (both in Tokyo, Japan), RIKEN and JASRI (Hyogo, Japan), and Osaka and Kyoto University have developed a 1.4 Å (0.14 nm) hard x-ray laser from a copper target with an inner-shell electron excitation scheme. By using a two-color pulse from the SACLA system, they successfully seeded the hard x-ray laser to maximize temporal coherence at almost ideal limits. The narrowest bandwidth obtained is 1.7 eV—smaller than the natural width defined by the lifetime of the atomic transition because of the uncertainty principle. The narrower linewidth denotes the effective decay time of 1 s in artificially suppressed vacancy ions. In this SACLA-seeded laser, strong induced emission occurs and the branching ratio of the relaxation process of the K-shell vacancy (Kα1, Kα2, and Auger process) is changed from its nominally constant values. This allows pure Kα1 or Kα2 laser emission with high efficiency. *Reference: H. Yoneda et al.,* Nature, *524, 446–449 (Aug. 27, 2015).*

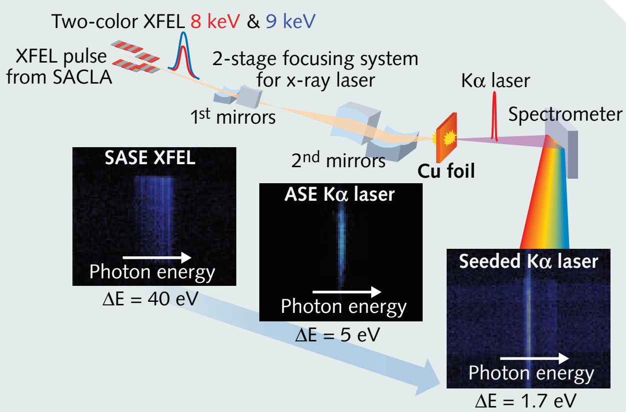

Ultrafast lasers simplify fabrication of 3D hydrogel tissue scaffolds

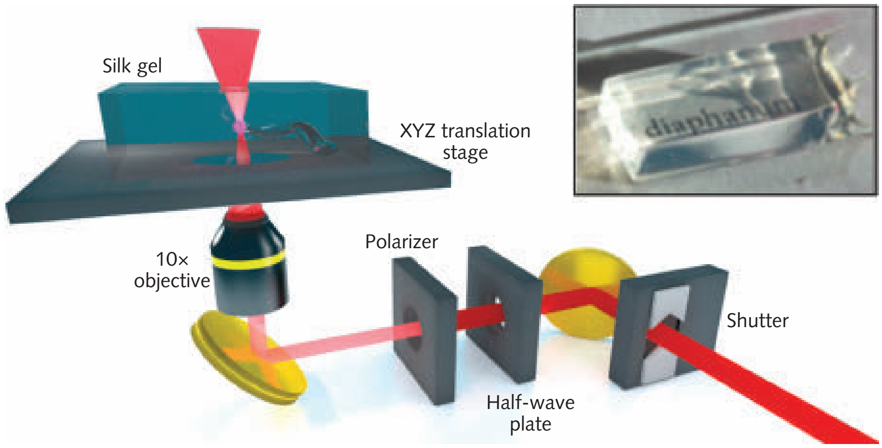

Femtosecond lasers are improving fabrication of tissue scaffolds and implants without needing nonbiocompatible photoinitiators or chemical cross-linking materials typically used in 3D printing. Direct micropatterning leveraging multiphoton absorption (MPA) of ultrafast laser light has been demonstrated by Tufts University (Medford, MA) researchers within an elastomeric silk fibroin hydrogel formula that is transparent to visible light, allows initiation of MPA at low powers (a few nanojoules) without self-focusing, is biocompatible and biodegradable, and allows laser light to create 10- to 400-μm-diameter voids (with a 5 μm lateral resolution) over a large 3D volume in the hydrogel through penetration depths up to 1 cm—1.5 orders of magnitude deeper than other biocompatible materials.

To fabricate complex features or voids within the hydrogel that function as tissue scaffolds for cell growth, the < 2 nJ output of an 810 nm, 80 MHz repetition-rate, 100 fs pulse-width femtosecond laser was input to a microscope objective and focused into the silk hydrogel fixed to a three-axis translation stage. Test patterns such as a 200-μm-diameter, two-turn helix and a blood-vessel-like branching structure beginning 300 μm deep and extending 100 μm in length were easily fabricated (in volumes up to 100 cm^3) by scanning the stage at speeds between 50 and 100 μm/s. Typical fabrication time for the helix or vessel structure is around 1 hr., depending on the shape/size of object. *Reference: M. B. Applegate et al.*, Proc. Nat. Acad. Sci., *112, 39, 12052–12057 (Sept. 29, 2015).*


Refined Tunability
NUPULSE™
Picosecond Industrial Fiber Laser
Picosecond pulses for cold processing
Tunable pulse duration
Single shot to 5 MHz
High-speed, black marking on metals
NUPULSE
NUFERN®
info@nufern.com
FIBER LASERS & AMPLIFIERS | OPTICAL FIBERS | FIBER GYRO COILS | DEFENSE TECHNOLOGY

Multimode holographic waveguides tackle *in vivo* biological imaging

The ability to image biological structures and tissues deep within the human body is met with varying levels of success through such methods as optical coherence tomography (OCT), multiphoton microscopy, and endoscopy. Challenged by the tradeoff of imaging resolution vs. depth, a researcher at the University of Dundee (Dundee, Scotland), with support from the Scottish Universities Physics Alliance (Glasgow, Scotland), has built on earlier work to improve understanding of holographic light transport processes through optical fibers, enabling *in vivo* imaging through flexible multimode fibers—a feat not previously possible.

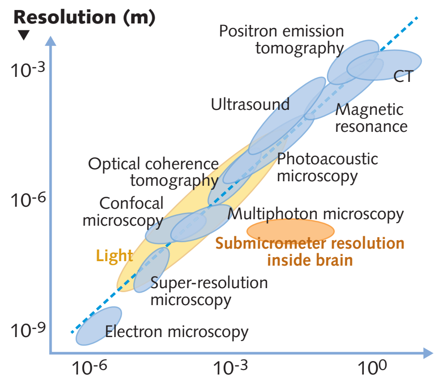

Because today's flexible endoscopes with 1 mm diameter or larger fiber bundles are too invasive for sensitive tissues, hair-thin multimode optical fibers were selected to transmit image information along the fiber via several concurring optical modes propagating at different phase velocities. Although the output optical fields are randomly appearing superpositions of these modes with highly complex phase relations, digital holography can characterize these scrambled images empirically, revealing the transmission matrix of the optical system and the details of the image. The most common approach is based on phase-shifting of the input modes such that they interfere constructively at a selected point behind the fiber output facet, thus creating a diffraction-limited focal point. A matrix of such focal points is then used to raster-scan the object to form its image. Currently available components can be used to achieve sub-micron resolution with typically tens of kilopixels at a few frames per second, but the performance is likely to grow steeply in the near future. *Reference: M. Plöschner et al.*, Nat. Photonics, *9, 8, 529–535 (2015).*

Fiber Y-splitter
See page 20

Got News? Please send articles to johnw@pennwell.com

ORBITAL ANGULAR MOMENTUM

Natural catenary structures create perfect OAM beams

The natural curve formed by a free-hanging chain, known in architectural circles as a catenary structure, had no known applications in photonics until researchers at the Chinese Academy of Sciences (Chengdu, China), Swinburne University of Technology (Hawthorn, Victoria, Australia), and the National University of Singapore created planar catenary arrays capable of generating optical beams with various degrees of orbital angular momentum (OAM).[1]

Unlike OAM beams formed by spiral phase plates, computer-generated holograms, optical nanoantenna arrays, ring resonators, and even chiral forms, catenary OAM beams have broader bandwidth and can be created from nanometers-thick structures.

Broadband OAM

Orbital angular momentum has emerged as a useful attribute for applications in optical communications, quantum information processing, and so many other emerging applications that it now has a dedicated annual conference venue.

With a goal to generate light with a geometrical phase and spatially continuous and spectrally achromatic distribution, the researchers fabricated two-dimensional (2D) structures on metallic surfaces using varying patterns of catenary structures. The structures consisted of repeating scales or petals of volumes bordered by two catenary curves, with a length Λ and a separation at the midsection (or shift) called Δ (see figure). Phase and polarization equations define how the catenary parameters produce light with a particular OAM value.

To evaluate broadband performance of the resulting OAM beams, three lasers with wavelengths of 532, 632.8, and 780 nm were adopted to illuminate the catenary structures and the resultant beams were analyzed. An analysis of the efficiency of conversion—defined as the ratio of the OAM-carrying beam to the overall transmitted power—for the ascending wavelengths revealed conversion efficiency values of 23.2, 39.8, and 54.4%, which is at least a 30-fold enhancement compared to circular nanoslit structures.

Subsequently, the catenary structures were used to realize more complex functionalities involving OAM. Except for the phase control being in the azimuthal direction, the researchers added additional phase variations along the radial direction. In such a way, the OAM beam could be either focused into a small doughnut or converted to a high-order Bessel beam, which is famous for its nondiffractive property.

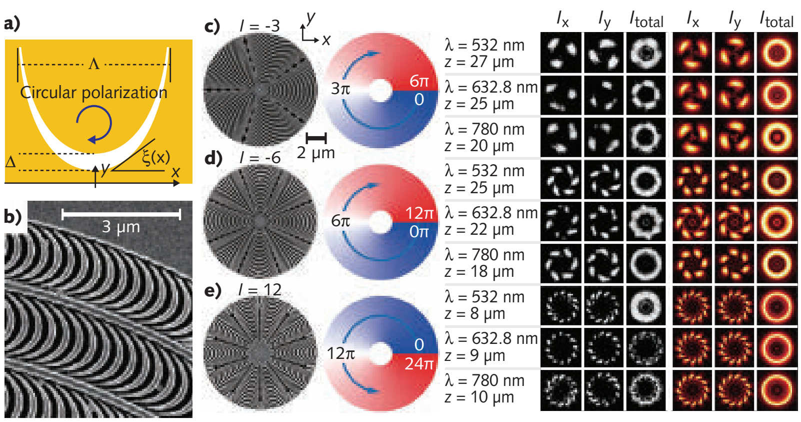

Two catenary curves enclose a volume (a) with length Λ and mid-axis separation of Δ. The structures are arranged in a repeating scallop pattern (b) and in a series of concentric or spiraling circles that define a particular phase distribution. Different patterns (c-e) with different topological charges define different types of OAM or circularly polarized beam profiles. *(Image credit: Chinese Academy of Sciences)*

It is also possible to construct catenary structures using dielectric rather than metallic materials as a way to enhance energy efficiency, albeit with a sacrifice in achievable bandwidth.

"The generation of OAM is just one of the many applications of optical catenaries," says Xiangang Luo, director of the State Key Laboratory of Optical Technologies on Nano-Fabrication and Micro-Engineering at the Chinese Academy of Sciences. "In fact, we have recently extended the concept of catenary optics to other applications, such as polarization-controlled surface plasmon manipulation and invisibility cloaking."—*Gail Overton*

REFERENCE

1. M. Pu et al., *Sci. Adv.*, 1, 9, e1500396 (Oct. 2, 2015).

SILICON PHOTONICS

Standard wire-bonding technique doubles waveguide Ge detector bandwidth

Some forms of active silicon photonic circuits benefit from the use of germanium (Ge) as a photodetector material, creating a hybrid system. These Ge waveguide-coupled photodetectors can take the form of either vertical or lateral *p-i-n* junction structures. While lateral structures have reached a 3 dB bandwidth of 120 GHz, the easier-to-make vertical structures have had difficulty exceeding a 3 dB 30 GHz bandwidth using many but very complicated techniques.

Now, researchers from the Huazhong University of Science and Technology (Wuhan, China) and Huawei Technologies (Shenzhen, China) have come up with a straightforward way of boosting the speed of conventional vertical *p-i-n* junction Ge detectors from 30 to 60 GHz.[1] The technique involves using standard wire-bonding technology to introduce gold wires into the detector's discrete ground electrodes.

The so-called RC parasitic parameter (R and C refer to the photodetector equivalent circuit's resistance and capacitance components, respectively) places a limit on how fast a detector can operate. However, introducing an inductor (L) into the detector's RC circuit to create a so-called RLC circuit can help high-speed operation because the introduced inductance counteracts part of the influence of the capacitance.

Avoiding the creation of any complicated on-chip inductors, the research group simply wire-bonds gold wires to the Ge detector, creating an "off-chip" inductor (although the wires actually reside at the Ge detector itself). To do this, they change the detector's single conventional integral electrode to three separate parts (see figure), leaving the actual photodetection section unchanged. Then, they introduce two gold wires to connect the two discrete ground electrodes—the section of wire forms the inductor, with its inductance value depending on the size and length of the wire.

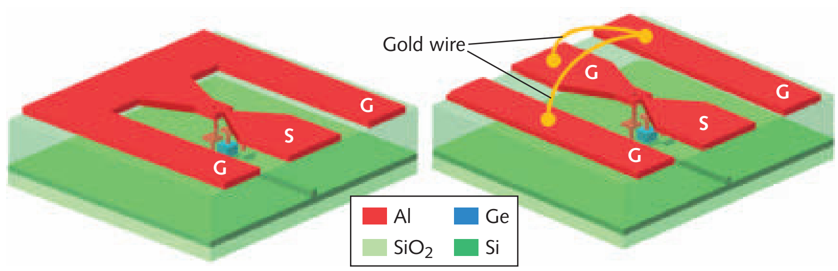

A conventional vertical *p-i-n* junction Ge detector, with its single integrated electrode, is seen at left. A modified Ge detector with three separate electrodes is shown at right—these electrodes can be connected with gold wires via the standard wire-bonding process to form a single electrode that has increased inductance, raising the bandwidth of the detector.

For example, a detector can be made using a gold wire about 450 μm long and with a 25 μm diameter, which provides an inductance and resistance of 1 nH/mm and 2 Ω/mm, respectively, over a wide frequency range. For this device, calculations show the doubling of the detector's bandwidth from 30 to 60 GHz.

Experiment verifies concept

An experimental Ge photodetector was fabricated on a silicon wafer using a 0.18 μm CMOS process at the Institute of

Microelectronics in Singapore. First, a single-mode channel waveguide with a 500 nm width was fabricated in the silicon, along with a grating coupler etched to a depth of 70 nm for vertically coupling light into the detector. Next, doped layers of Ge totaling about 700 nm were deposited and then etched, and metals were deposited to form the electrodes. Post-fabrication bonding of two pieces of gold wire totaling about 450 μm in length completed the device.

Bonding of the wires slightly decreased the detector's responsivity from 1 to 0.85 A/W at 1550 nm under a –3 V bias voltage, attributed to the resistance of the wires. At a bias voltage of –0.5 V, the bonded wires actually slightly reduced the dark current from 64 to 61 nA.

The detector's frequency response was measured by coupling light at a 1550 nm wavelength to the device through a cleaved fiber at a power of about 5 dBm. While some jitter was seen in the measurements at higher frequencies because of bandwidth limitations in the electrical cable and connections used in the measurement, a 3 dB response out past 60 GHz was seen.

The researchers note that because wire-bonding technology is a standard part of a Ge waveguide detector's construction anyway, their method adds no extra fabrication process. In addition, the bonded wire can easily be removed and a new wire of same or different length and diameter rebonded.—*John Wallace*

REFERENCE

1. G. Chen et al., *Opt. Express* (2015); doi:10.1364/OE.23.025700.

MID-INFRARED LASERS

CMOS silicon-on-sapphire process produces broad mid-IR supercontinuum

Beyond its well-known photonic capabilities in the telecommunications wavelength band around 1.5 μm and its functionality in silicon-on-insulator (SOI) form up to 2.5 μm, silicon has now entered a new frontier: silicon-on-sapphire (SOS) nanowires have been used to demonstrate octave-spanning mid-infrared (mid-IR) supercontinuum generation from 1.9 to just beyond 6 μm.[1]

This broadband supercontinuum source is realized using a complementary metal-oxide semiconductor (CMOS) process and is the collaborative effort of researchers from the Center for Ultrahigh Bandwidth Devices for Optical Systems (CUDOS) at the University of Sydney, Macquarie University, and Silanna Semiconductor (all in Sydney,

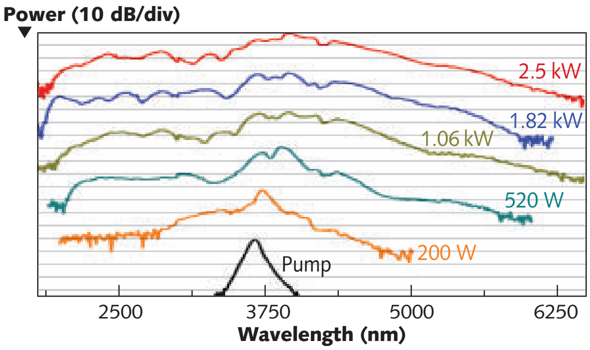

The power output spectra from a silicon-on-sapphire (SOS)-based supercontinuum source are shown for input power levels ranging from 200 W to 2.5 kW. *(Image credit: CUDOS)*

NSW, Australia), the CUDOS Laser Physics Center at Australian National University (Canberra, ACT, Australia), the Institut des Nanotechnologies de Lyon, CNRS (Lyon, France), and RMIT University (Melbourne, Victoria, Australia). The team of researchers says that this mid-IR supercontinuum source represents "both the widest spectrum and longest wavelength generated to date in any silicon platform."

Compact, inexpensive mid-IR sources are becoming more and more important, especially for applications in molecular sensing at part-per-billion and even part-per-trillion levels. Although supercontinuum generation using chalcogenide glass fibers has been demonstrated out to 13 µm, the CMOS-compatible SOS platform offers scalability and promises new nonlinear integrated (and cost-effective) silicon devices such as this mid-IR supercontinuum source that operates well beyond the legacy silicon window.

Supercontinuum SOS

The first SOS waveguides fabricated in 2010 had 4.3 dB/cm losses at 4.5 µm.[2] To avoid higher multiphoton absorption that normally occurs in silicon beyond 2.5 µm, the researchers engineered SOS nanowires that minimized dispersion and optical loss at the pump wavelength via a 2.4 × 0.48 µm nanowire. By treating the nanowire with chemical oxidation and oxide stripping to reduce surface roughness, and by using a relatively wide nanowire to improve mode confinement, propagation losses are minimized to a level of 1.0 ± 0.3 dB/cm at 4 µm.

For supercontinuum generation, the 3.7 µm, 320 fs pulse-width, 20 MHz repetition rate output from a tunable optical parametric amplifier (OPA) was input to the TE mode of the nanowire, collimated and sent to a monochromator, and detected with two detectors: lead selenide (PbSe) from 1.5 to 4.8 µm and mercury cadmium telluride (MCT) from 4 to 6.5 µm. For coupled input peak powers from 200 W to 2.5 kW, the widest continuous output spectrum spans 1.53 octaves from 1.9 to 5.5 µm at the -30 dB signal level for a 1.82 kW input. Even well above the noise floor at -45 dB, light is generated beyond 6 µm (see figure).

To achieve a flatter dispersion profile over a wider bandwidth, SOS-based pillar waveguides could be constructed. Furthermore, improvements to epitaxial growth of the SOS nanowires are expected to minimize near-IR losses by reducing lattice mismatch at the silicon/sapphire interface. The researchers say that these improvements will make it possible to demonstrate supercontinuum generation over the full transparency spectrum of silicon using a single nanowire.

"The silicon-on-sapphire platform paves the way for integration of electronics and photonics on a single device," says Neetesh Singh of CUDOS, University of Sydney. "This would lead to electrically tunable, on-chip, linear, and nonlinear ultrawide optical operation from near-IR to mid-IR range."—*Gail Overton*

REFERENCES

1. N. Singh et al., *Optica*, 2, 9, 797–802 (September 4, 2015).
2. T. Baehr-Jones et al., *Opt. Express*, 18, 12, 12127–12135 (2010).

FIBER-OPTIC COMPONENTS

Fiber Y-splitter handles seven-core optical fiber

In the past few years, data-transmission rates for experimental fiber-optic systems has reached deep into the terabit-per-second range. Some configurations that have helped to achieve such rates are a combination of orbital angular momentum (OAM) and wavelength-division multiplexing (WDM), which reached 100 Tbit/s over a short length of fiber; hybrid integration with differential-quadrature phase-shift keying, reaching 14 Tbit/s over a single 160 km fiber; an optical fast-Fourier-transform (FFT) scheme that enabled 26 Tbit/s over a single 50 km fiber; and the use of multicore single-mode fiber, which allowed transmission of 255 Tbit/s over a 1 km fiber length.

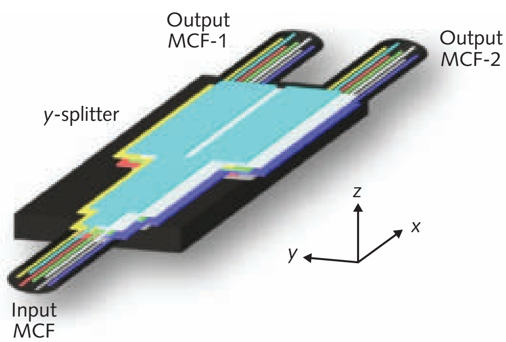

Light from the seven cores of an input multicore fiber (MCF) is split individually by a Y-splitter based on seven layers of gradient-index waveguide optics. Both the input and output MCFs are simply cut and placed in contact with the Y-splitter.

The last approach, which often takes the form of a seven-core triangular array, is a relatively straightforward fiber design that can greatly boost data rate (as long as crosstalk between cores is minimized). One thing that is not straightforward about using seven-core fiber, though, is the design of the components that couple light into and out of the fibers, as well as manage the light during transmission. To help in this respect, Ehab Awad of King Saud University (Riyadh, Saudi Arabia) has designed a 2.4-mm-long Y-splitter for multicore fibers that requires no separation of the fiber's multiple cores.

Numerically simulated

The design, which so far has been numerically simulated for a seven-core

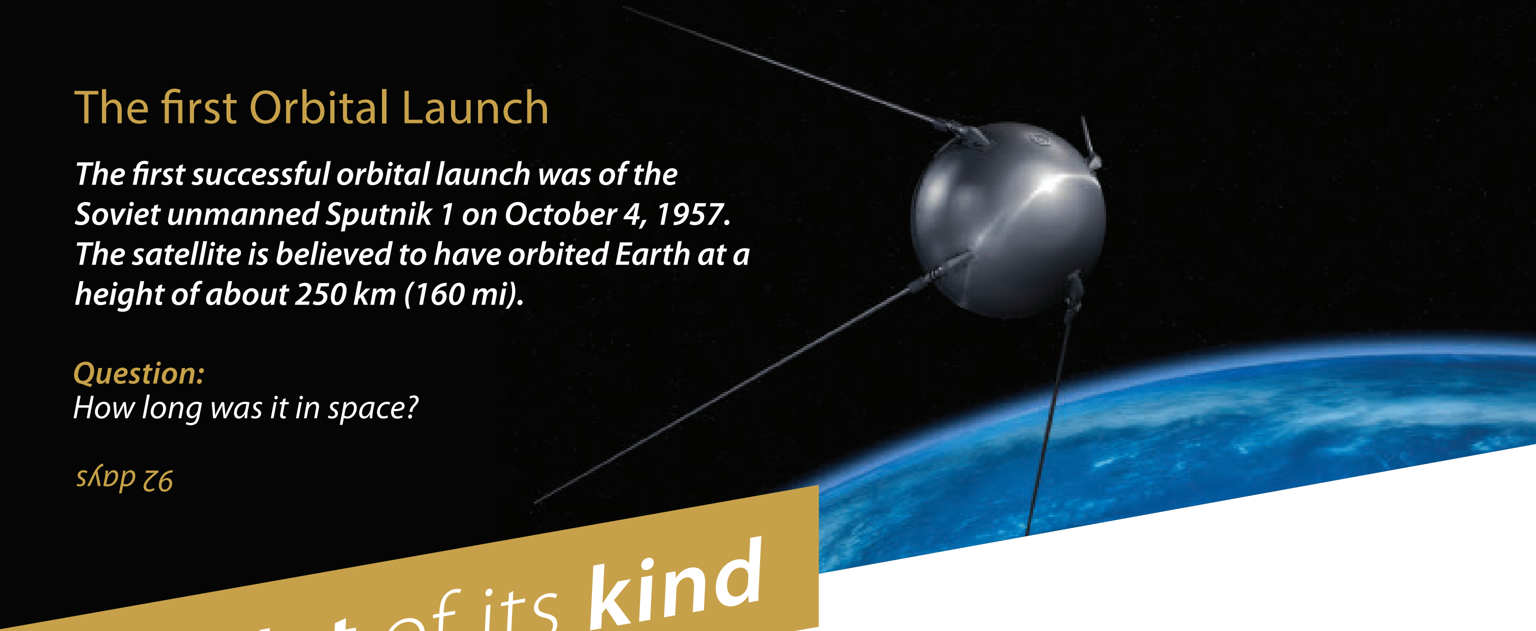

The first Orbital Launch

The first successful orbital launch was of the Soviet unmanned Sputnik 1 on October 4, 1957. The satellite is believed to have orbited Earth at a height of about 250 km (160 mi).

Question:
How long was it in space?

92 days

The **1st** of its **kind**

Full Range of Laser Power & Energy Sensors

Thermal sensors
- 100nw - 120KW & 15µJ - 4000J
- Power & single shot energy
- High damage threshold
- Apertures up to 200X200mm

Pyroelectric and Photodiode sensors
- 10pJ - 40J
- Laser energy at up to 25kHz
- High damage threshold

Photodiode sensors
- 10pW - 3W
- High sensitivity, high accuracy power sensors
- Radiometric, photometric & integrating sphere products available

www.ophiropt.com/photonics 1-866-755-5499

OPHIR® Photonics
A Newport Company

The True Measure of Laser Performance ™

fiber but not yet constructed, relies on a number of differing Y-splitting waveguide layers—one for each core—with all layers having a novel double-hump graded-index (DHGI) profile that splits optical power equally into two halves (see figure). The input and two output fibers are rotated about their axes with respect to the Y-splitter until all of the seven cores reside in different horizontal planes with respect to the splitter. This allows a separate waveguide layer to access each of the seven cores.

Each single Y-splitter layer contains an expander, a DHGI space-division splitter (SDS), and a separator. The seven individual Y-splitters are surrounded by a 400 × 125 μm cladding region. The fiber in the numerical model has seven identical step-index single-mode cores with a 40 μm separation between adjacent cores, a cladding refractive index of 1.45, and a core refractive index of 1.4551.

Each splitter has a waveguide height of 9 μm, is separated from the adjacent waveguide layer by 4 μm of cladding, and splits the input light into two outputs separated by 250 μm (twice the diameter of the multicore fiber). The input and output fibers are rotated by 19° about their axis to create a line-of-sight view between cores of each single splitter.

The waveguide lens embedded in each splitter layer is 280 × 60 × 9 μm in size and has a gentle parabolic refractive-index profile that expands the beam adiabatically to minimize the production of higher-order modes. Light from the lens enters the DHGI SDS portion of the device, which has two parabolic graded-index humps, each with a size of 995 × 60 × 9 μm. The dimensions are sized to reliably split the input beam 50%/50%. The two beams are then sent to two separate waveguides and then on to the two output fibers.

In the process of designing the Y-splitter, Awad ran finite-difference time-domain (FDTD) simulations of the electromagnetic-field distribution in the device and associated optical fibers at 1555 nm and other wavelengths, as well as eigenmode expansion (EME) solutions using software from Lumerical Solutions (Vancouver, BC, Canada). These simulations showed no significant cross-coupling between waveguide layers or cores.

The simulations indicated that the splitter would work well over a broadband region from 1460 to 1675 nm with polarization-insensitive operation, showing an insertion loss of around 0.12 dB over all wavelengths, excess loss of 0.13 dB, polarization-dependent loss of less than 0.02 dB, and a worst-case return loss of 35.8 dB. The optimum 3 dB splitting ratio fluctuated by less than 0.1 dB over the entire wavelength range. A tolerance analysis showed that low-loss performance was achieved for maximum misalignments of about 0.5 to 1.0 μm (depending on the type of loss modeled).—*John Wallace*

The simulations indicated that the splitter would work well over a broadband region from 1460 to 1675 nm with polarization-insensitive operation, showing an insertion loss of around 0.12 dB over all wavelengths, excess loss of 0.13 dB, polarization-dependent loss of less than 0.02 dB, and a worst-case return loss of 35.8 dB.

REFERENCE

1 E. Awad, *Opt. Express* (2015); doi:10.1364/OE.23.025661.

I just read Jeff Hecht's article in *Laser Focus World* titled "Spectrometers and Spectroscopy: Looking Back/Looking Forward: Spectrometers and spectroscopy get faster, better, and cheaper," and I thought the article was very well written and covered many of the key points in the evolution of miniature spectrometers. I was also excited to see that he cited an article that I co-authored in *LFW* back in May 2013.

I think you left out one of the major milestones in the miniaturization of Raman spectrometers—the commercialization of the volume Bragg grating (VBG)-based external cavity diode laser by Innovative Photonic Solutions (IPS) in 2003. I know this statement may seem biased because I am currently employed by IPS, but I had been a customer of IPS for six years prior to joining the company in fall 2013, so I can speak with both perspectives. The reason why this laser was so important is it allowed systems integrators to have a compact, low-cost, and low-power-consumption excitation source that was wavelength- and power-stabilized over a wide ambient temperature range. This resulted in the IPS laser being used in most of the first-generation "handheld" Raman spectrometers. Since then, the VBG-stabilized diode laser has become the industry standard in Raman spectroscopy—in both handheld and laboratory systems.

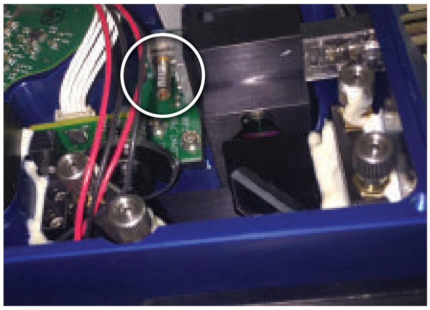
A VBG-stabilized laser diode integrated into a portable Raman spectrometer. *(Courtesy of Snowy Range Instruments – Laramie, WY)*

A few years after the initial release of the VBG-based diode laser, IPS again revolutionized the world of handheld Raman when they came out with the first fully integrated, VBG-stabilized diode laser with a collimated output in a TO-56 package (see photo). This even further reduced the size and power consumption, allowing for the smartphone-size Raman spectrometers that now fit in the palm of your hand and run off AA batteries.

IPS has historically been really bad with PR and over the years, our sales have primarily been OEM and private label; therefore, outside of the Raman spectroscopy community, not too many people are aware of IPS's impact. I know it's too late to get any of this into the article, but I figured it couldn't hurt to fill the gap in the story.

Again, overall I really liked the article and I have already sent it to a few friends.

Robert V. Chimenti *is a product line manager at Innovative Photonic Solutions, Monmouth Junction, NJ; e-mail: rchimenti@innovativephotonics.com.*

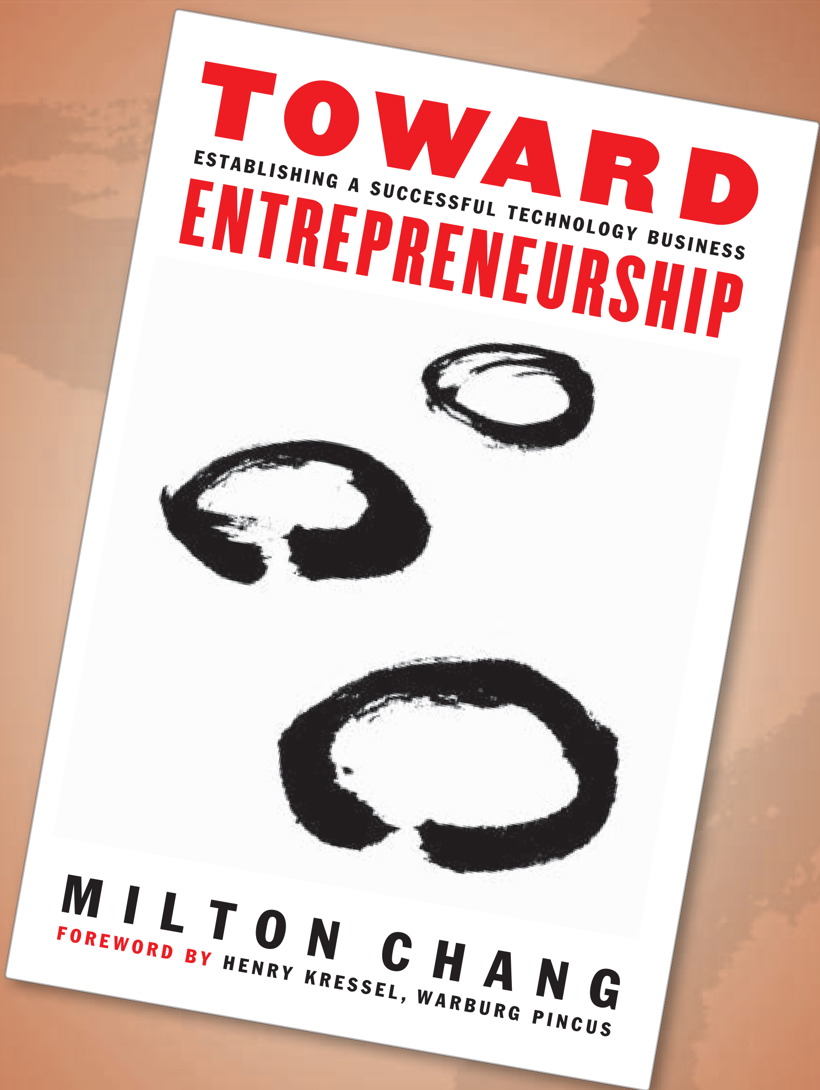
TOWARD
ESTABLISHING A SUCCESSFUL TECHNOLOGY BUSINESS
ENTREPRENEURSHIP
MILTON CHANG
FOREWORD BY HENRY KRESSEL, WARBURG PINCUS

LOOKING BACK/LOOKING FORWARD:

Positioning equipment—the challenge of building a solid foundation for optics

JEFF HECHT, Contributing Editor

Stability and precision have been crucial for optics since the 19th century. The birth of holography and other precision laser measurements brought a new generation of equipment, which is now feeding the needs of nanotechnology.

Positioning and stabilizing optics may seem a humble task, but it paid off in a big way for Albert A. Michelson in 1907, when he received the Nobel Prize in Physics "for his optical precision instruments and the spectroscopic and metrological investigations carried out with their aid."

His most famous experiment was an 1887 attempt with Edward Morley to measure how the Earth's motion affected the speed of light. The measurement required exacting precision, so they assembled a multipass Michelson interferometer on a foot-thick slab of sandstone measuring 5 ft^2 that floated on liquid mercury in the basement of a massive stone building to isolate it from thermal variations and vibrations from passing horse traffic (see Fig. 1). They could detect shifts as small as 1% of a fringe—but they failed to find the ether drift predicted by classical physics, and thus helped launch modern physics.

Holography demands stability

Early laser experiments didn't require such extreme stability, and typically were performed on laboratory tables. Ordinary optical measurements were made on optical benches, essentially long, straight rails holding optical mounts to align a series of lenses.

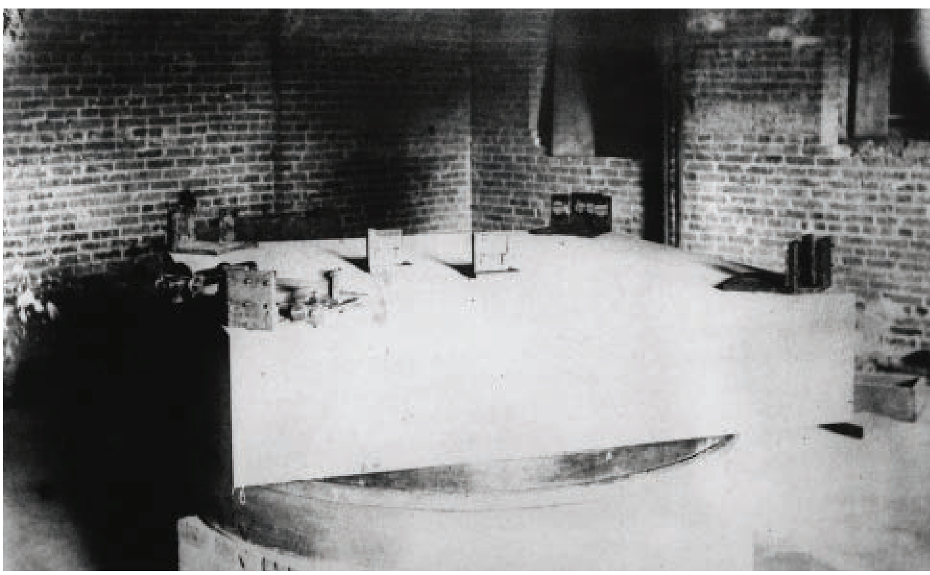

FIGURE 1. The Michelson-Morley experiment was performed on this slab in the basement of a stone dormitory at Western Reserve University in Cleveland. *(Courtesy of the Special Collections & Archives Department, Nimitz Library, U.S. Naval Academy)*

The first issue of *Laser Focus* in January 1, 1965 didn't mention tables, mounts, or other positioning equipment. But it did include a lengthy report on the then-new subject of three-dimensional (3D) laser holography. We noted that recording holograms with then-available continuous-wave (CW) lasers required long exposures. During that time, we wrote, "the reflecting objects must remain stationary to less than about 1/8 wavelength of the illumination of the exposure." To achieve that high stability, Emmett Leith and Juris Upatnieks had to fill the HO-gauge toy train engine in their iconic hologram with epoxy and glue it to the tracks (see Fig. 2).

FIGURE 2. Leith and Upatnieks' iconic toy train hologram. It looked so good because the inside was filled with epoxy to stabilize it.

"Before holography, you never had to worry about the stability of the tabletop," recalls Milton Chang, who earned a PhD for holographic research at Caltech under Nicholas George. He and fellow grad student John Matthews worked on a homemade optical bench made by floating a massive steel plate on a pair of heavy-duty truck inner tubes.

I spent the summer after my junior year working in that lab, and was quite impressed by the setup. But it didn't provide the several minutes of absolute stillness needed for serious holography. The lab was on the first floor, so it picked up vibrations when the elevator went up and down, and from passing traffic. The only way to record good holograms was in the middle of the night, when no one else was in the building and the elevator slept.

After he graduated, Matthews set out to develop better optical tables for holography. He and Dennis Terry, a supervisor in the Caltech machine shop, decided to form their own company while spending a day at Newport Beach in 1969. The name Newport Research was inspired by the beach and their interest in the scientific market. Matthews developed ways to damp vibrations in the tables, and adapted a honeycomb structure used in aerospace for its rigidity and light weight. They earned $46,000 in their first year working in a garage, and then moved into a shop

in nearby Fountain Valley. Chang joined them in 1972 as marketing manager.

Artists making holograms took a low-end approach to vibration isolation. In 1970, Canadian artist Jerry Pethick and laser physicist and holographer Lloyd Cross stuck plastic pipes and concrete blocks into a box filled with sand, and attached optics to them with C clamps. Soon, holographic art was emerging from basement holographic sandboxes.

FIGURE 3. By January 1975, optical positioning equipment had become an important business, as this ad from Aerotech in the issue described an "optical erector set" for holding components.

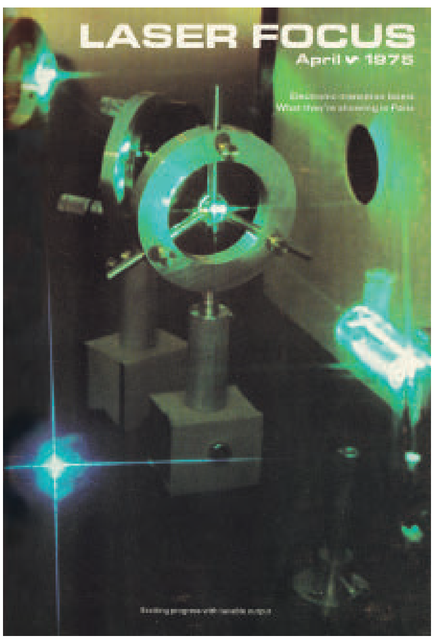

FIGURE 4. Optical mounts have a supporting role on our April 1975 cover.

FIGURE 5. A 20-ft vertical optical table built to support a fiber draw tower, outside Newport's plant in Fountain Valley, CA. *(Courtesy of Newport/Jim Fisher)*

A foundation for lasers

Optical positioning equipment had become an important business by the time of our January 1975 issue. Newport ran a full-page ad dense with information in small type, many photos, and two graphs of vibration isolation and damping. They had plenty of competition. Information-rich ads from Aerotech (Pittsburgh, PA; see Fig. 3) and Burleigh Instruments (East Rochester, NY) described "optical erector sets" for holding components. Modern Optics (El Monte, CA) advertised optical tables starting at $1000 and precision mirror mounts for $49. And Scientech (Boulder, CO) offered magnesium-alloy optical benches for $100 per meter in lengths to 5 m.

Our main editorial coverage of positioning equipment was in the products section. One January 1975 entry described CVI Laser mirror mounts with manual adjustments offering 0.5 arcsec angular resolution. But optical mounts sometimes played supporting roles on the cover, as shown on our April 1975 cover (see Fig. 4).

The optical table business was set on end by the fiber-optic boom of the late 1970s. "We built some vertical tables for Corning in the 1970s to support drawing towers," recalls Larry Mayhew, a senior manufacturing engineer at Newport. The first vertical table stood 20 ft tall (see Fig. 5), and later Corning brought assemblies up to 54 ft tall.

Another new application emerged in the early 1980s. Mayhew visited a mysterious southern California customer called WED Enterprises to make measurements for a new optical table—and found the WED stood for Walt E. Disney. The optical tables were replacing an assembly of 4 × 4 boards floating on inner tubes in creating special effects for movies like *Tron*.

Robotics and programmable positioners

The 1980s brought numerical control to positioning equipment for optics and to industrial laser systems. "The first U.S. industrial laser robot system was installed in 1984. By 1989, industry sources predict that several hundred laser robot systems could be in place performing spot welding and cutting operations," wrote David Belforte in our October 1984 issue.

Flipping through the rest of that issue showed the emerging trend. An ad from Oriel Corp. (Stratford, CT) mentioned computer-compatible stepping motors and drives with active control to maintain constant speed for motorized micropositioners, and Newport advertised a motorized drive with a keypad control. Our products section described a positioning system that Anorad (Hauppauge, NY) had developed for automated laser drilling and cutting of printed-circuit boards.

Nanotechnology and mountaintop optical tables

Our editorial coverage of positioning equipment expanded in the 1990s. A feature in our January 1995 issue (see Fig. 6) listed options for table surfaces that still sound familiar. "Stainless steel is by far the


eagleyard
photonics
NEED FOR SEED
Pure Power.
www.eagleyard.com
Pulsed Laser Diodes for Fiber Lasers
eagleyards new DFB 1030 nm seed laser complements the already worldwide successfully established DFB 1064 nm pulse laser.
• Outstanding spectral performance under pulse mode
• Pulse peak performance up to 1 Watt
Its high efficiency in conjunction with the compact housing and robust design makes both DFB1030 and DFB1064 laser diodes perfectly suited for the use in fiber lasers for high precision material processing.
Detailed information at: www.eagleyard.com/products/single-frequency-laser-diodes/
eagleyard

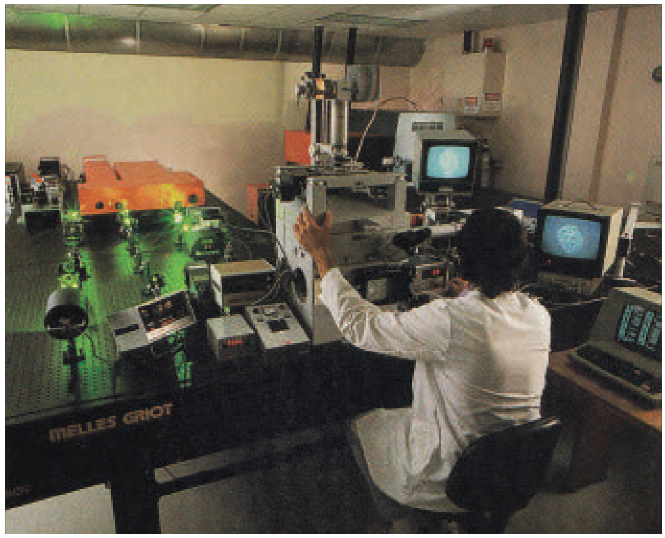

FIGURE 6. Skin material options for table surfaces included stainless steel, aluminum, and granite, as reported in January 1995.

most common top-skin material because steel has a high stiffness-to-weight ratio and can be laminated, machined, drilled and tapped, then damped with reasonable effort," wrote Jerry Hobbs. Aluminum skins are light and easy to machine, but are more prone to deformation and contamination. Granite can be polished flatter, but it is more massive and amplifies a broader range of vibrations.

"Nano" had begun to emerge as a buzzword. Burleigh Instruments (Fishers, NY) used the headline "Nanopositioning" for an ad in our January 1995 issue (see Fig. 7) promoting its "inchworm" piezoelectric positioners, able to move up to 200 mm at speeds of 1 nm to 2 mm/s. A September 1999 feature by Scott Jordan of Polytec PI (Auburn, MA) told how piezoelectric positioners could automate alignment of single-mode optical fiber for communication systems.

FIGURE 7. Burleigh Instruments' "inchworm" piezoelectric positioners were able to move up to 200 mm at speeds of 1 nm to 2 mm/s.

The late 1990s also saw optical tables reaching new heights at the Keck Observatory on Mauna Kea, Hawaii. Newport supplied more than 50 tables for an optical delay line used for interferometry with the twin 10 m telescopes. Getting the tables up the


WHAT CAN WE
MAKE FOR YOU?
CUSTOM
OPTIONS
LENSES
OBJECTIVES
FILTERS
ASPHERES
COATINGS
Optics for your
LIFE SCIENCES APPLICATIONS
27,200 Stock Optics
Quick Modifications 2-3 Week Delivery
Custom Design and Manufacturing
Stephan Briggs
Biomedical Engineer and
Life Sciences Expert
Best-Selling Products:
Hard Coated Bandpass Filters
Broadband AR Coated Optics
Precision Prisms
Laser Optics
www.edmundoptics.com/life-sciences
Contact Us Today!
Edmund optics | worldwide
1-856-547-3488

mountain was a picnic compared to installing and testing them in the thin air at 14,000 ft, recalls Warren Booth, a senior manufacturing engineer at Newport.

The age of nanopositioning

A March 2004 feature (see Fig. 8) by Steve Kidd of Melles Griot UK and two colleagues from LNL Optenia (Ottawa, ON, Canada) described a six-axis stage with active alignment that could align a probe to a 2 μm waveguide with 10 nm resolution within a second or two. That marked a dramatic advance over the 10 minutes needed manually. An ad from Mad City Labs (Madison, WI) offered nanopositioning systems with subnanometer precision.

FIGURE 8. A six-axis stage with active alignment could align a probe to a 2 μm waveguide with 10 nm resolution within a second or two.

New cutting-edge research required new positioning techniques. Exacting precision was needed to prevent any relative motion between the ultrashort laser and the acceleration chamber in the Berkeley Laboratory Laser Accelerator (BELLA) at the Lawrence Berkeley Laboratory in California, which we described in June 2013. That required tuning vibration damping of the optical tables at the site rather than in the factory for the first time ever, says Booth of Newport.

Vibration isolation is finding applications far beyond optics. The oddest Booth recalls was at a biotechnology company trying to produce genetically engineered rats. The rodents were so finicky that they wouldn't breed if they could feel any vibration, and the company was near active train tracks. The baby rat population boomed after he installed an isolation table as a foundation for a rat housing project. (Booth called it a "rat brothel," but somebody might find that offensive.)

Looking forward

One emerging trend is the "smart table," with a control system that actively identifies resonant frequencies and damps them with faster settling time than standard tables. "Some semiconductor companies are

looking for that now, as a way to improve throughput," says James Fisher, vice president for optical components and vibration control at Newport, which recently introduced one. Figure 9, from our March 2015 issue, shows how that system improved the quality of nanostructures fabricated by Steven Koo at MIT in a fifth-floor laboratory.

So far, the market for active systems has been limited to the most sensitive equipment, including atomic force and scanning-probe microscopes as well as semiconductor fabrication. But Fisher says active systems will become more affordable as sensor costs drop and electronics become more powerful, and "people will need more active systems" as their demands for extreme stability and precision increase.

New technology offers other options. The same March 2015 feature described totally passive negative-stiffness vibration isolators developed by Minus K Technology (Inglewood, CA). Based on a combination of coiled springs and negative-stiffness flexures, they have a low natural frequency of 0.5 Hz, making them more effective at such low frequencies than air or active damping, says Steve Valma, operations manager at Minus K. They don't require an air supply or power. They are finding growing applications as sensitive instruments have become small enough to be installed on higher floors, where they are more vulnerable to low-frequency building vibrations. One recent inquiry came from a person in the 20th floor of a Hong Kong building who was having problems making measurements with an atomic force microscope.

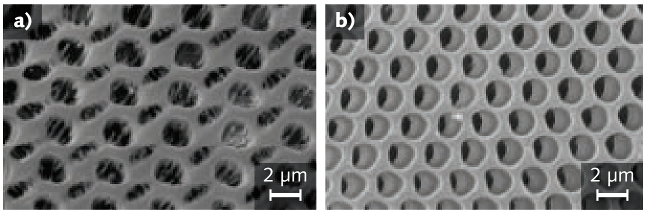

FIGURE 9. Without active damping, nanostructures fabricated at MIT were irregular (a). Turning on the active damping system produced the more regular patterns (b).

Valma says the passive negative-stiffness isolators can be made on a wide range of scales. NASA's Johnson Space Flight Center is using six custom-made isolators with capacity of 10,000 pounds each to test the James Webb Space Telescope on the ground. On the other end of the scale, their smallest units can handle 25 pounds each. Their most interesting application so far has been to isolate the high-end Döhmann Helix 1 audio turntable just introduced by Audio Union. At $40,000, the turntable is designed for serious audiophiles who are very affluent—a far cry from a stable table to coddle fussy rats.

Monolithic DFB QCL array aims at handheld IR spectral analysis

MARK F. WITINSKI, ROMAIN BLANCHARD, CHRISTIAN PFLUEGL, LAURENT DIEHL, BIAO LI, BENJAMIN PANCY, DARYOOSH VAKHSHOORI, and FEDERICO CAPASSO

Many QCLs combined on a single chip demonstrate fully electronic wavelength tuning for stand-off IR spectroscopy of explosives and other materials.

Advances in infrared (IR) laser sources, optics, and detectors promise major new advances in areas of chemical analysis such as trace-gas monitoring, IR microscopy, industrial safety, and security. One key type of photonic device that has yet to reach its full potential is a truly portable noncontact (standoff), chemically versatile analyzer for fast Fourier-transform infrared (FTIR)-quality spectral examination of nearly any condensed-phase material.

The unique challenges of standoff IR spectroscopy actually extend beyond advances in IR hardware, requiring the proper combination of several areas of expertise: cutting-edge optical design and laser fabrication, integrated laser electronics, thermally efficient hermetic packaging, statistical signal processing methods, and deep chemical knowledge.

At the core of the approach we have taken at Pendar Technologies is the monolithic distributed feedback (DFB) quantum-cascade laser (QCL) array. Invented in Federico Capasso's group at Harvard University (Cambridge, MA) and licensed exclusively to Pendar, the continuously wavelength-tunable QCL array source is a highly stable broadband source that can be used for illumination in reflectance spectroscopy. Each element of the array is individually addressable and emits at a different wavelength by design.

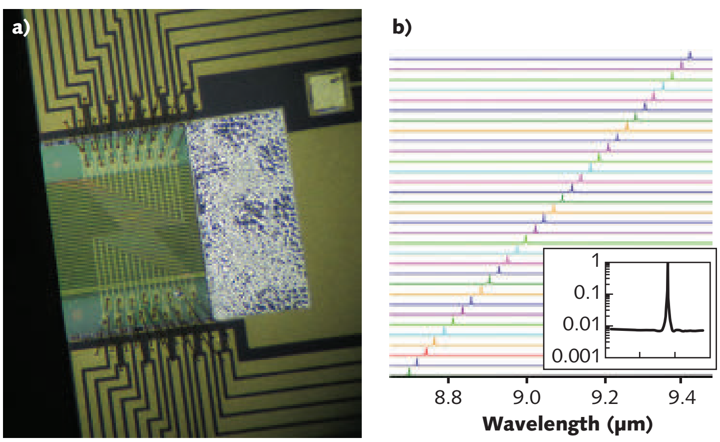

FIGURE 1. A 200 cm^{-1} prototype QCL array with 32 QCLs is shown prior to beam combining and packaging (a), and experimental spectra from 32 adjacent QCLs are seen (b). *(Courtesy of Pendar Technologies)*

The advantages of these QCL arrays over external-cavity (EC) QCLs stem from (1) the monolithic structure of QCL arrays and (2) their fully electronic wavelength tuning—that is, no moving gratings, allowing for much-higher-speed acquisition through improved amplitude and wavelength stability. When integrated into a system, the result is robust, stable, and field-deployable.

One of the key advances that has enabled this technology to be fielded is the high-yield fabrication of each laser ridge in the QCL array from a single wafer such that every channel simultaneously meets the specified wavelength, power, and single-mode suppression ratio. Each of these parameters is critical to both efficient beam combining and to obtaining high-quality molecular spectroscopy once integrated.

With these hurdles largely overcome, the payoff in terms of spectrometer performance lies largely in a demonstrated shot-to-shot amplitude stability in pulsed mode of <0.1%—a factor of 50 more stable than is typical for EC QCLs, even when used in the lab. Most importantly, the DFB QCL noise is random, and averages toward an Allan variance limit quickly such that detector-noise-limited, high-quality spectra can be obtained for trace levels (for example, 1–50 μg/cm^2) of typical powders in just 100 ms.

More DFB array advantages

While the stability advantage of DFBs vs. EC configurations has been well established, there are a few less-obvious aspects to DFB arrays that make them more suitable to real-world spectroscopy tools and, in particular, portable spectroscopy tools. For one, the laser array as a whole can maintain a 100% duty cycle while each laser in the array requires operation only over a 100/*n* (%) duty cycle, where *n* is the number of lasers in the array. Put another way, a laser array consisting of only pulsed QCLs can operate as a truly continuous-wave (CW) system, allowing for high-measurement duty cycle while possibly reducing the cost of fabrication.

In a related way, generating light for an array that has a 100% aggregate duty cycle (by using, for instance, 32 lasers at 3% duty cycle), the thermal heat-sinking requirements of the source are dramatically reduced. Indeed, our packaged prototypes do not even require active cooling to keep the system cool enough to run. A thermoelectric cooler is built into the package only to stabilize the temperature, which therefore stabilizes the 32 wavelengths (see Fig. 1).

Finally, the arbitrary programmability of the QCL array opens up many new possibilities for experimental optimization. Certain lasers can be skipped, multiple lasers can fire at once, repetition rates and pulse durations can be set for each element, and so on. These advantages are only truly realized when the QCL array is instrumented into a full system.

Looking holistically at how best to integrate this new capability into a full system, it is critical to draft the link equations that govern the use of electrons to produce photons, the collection of photons scattered back, and finally the conversion from raw spectral information to chemical identification. In the case of mid-IR material identification, it becomes clear that three aspects are particularly consequential: (1) How broad a wavelength range is needed for the tool to be of maximum specificity without producing redundant or useless chemical information (that is, how many laser channels should be used, how should they be spaced with respect to one another, and over what total wavelength regime should they be spaced); (2) the mechanical and electro-optical design of the instrument; and (3) how to get the highest performance regressions against reference spectra while maintaining the high-speed identification that the QCL array actually enables.

With regard to the wavelength regions of interest (see Fig. 2), most of the spectral richness of an IR spectrum is centered in two bands, generally referred to as the functional group region (about 3.3–5.5 μm) and the fingerprint region (about 7–11 μm). The first is typically dominated by the stretch modes of certain common bond groups, while the latter includes bending modes of some functional groups as well as lower frequency modes that are characteristic of the macromolecule "backbone"—for instance, the torsional modes of a toluene ring found in many highly energetic materials. With support from the Department of Homeland Security (DHS)'s Widely Tunable Infrared Source (WTIRS) program and from the Army Research Lab, Pendar is developing a compact array module that fully covers 7–11 μm (900–1430 cm^{-1}).

System architecture drivers

To maximize signal-to-noise (SNR) while minimizing the required acquisition time, the system architecture is driven by the following first-order considerations:

1. Increasing the laser power enabled by relaxed thermal constraints as the heat load is distributed over several modules (arrays) and laser waveguides.

2. Maximization of the measurement duty cycle enabled by the fast purely electronic control of the array, allowing close to zero-delay switching between lasers—that is, a laser is on at any time. This is also enabled by the distributed heat load among the laser units.

3. Improved source stability, wavelength accuracy, pulse-to-pulse amplitude, and frequency repeatability—all of which are needed to ensure that the source noise is not the limiting form of noise (compared to detector or speckle noise). Other researchers have studied the source-noise problem of commercial EC QCLs as well and concluded that the order-of-magnitude advantage in minimum detectable absorbance (MDA) offered by a DFB QCL carries through the full experiment.

Finally, once the spectra are digitized, the system must use complex chemometrics algorithms to ensure confident identification of threats in the presence of chemical clutter, deliberate interferents, and unknown backgrounds, without the intervention of an expert user. Our approach to real-time chemometrics is centered on the fact that for chemically cluttered situations, spectral libraries alone—no matter how large—cannot constitute the sole basis for chemometric analysis. Microphysics modeling and experimentation are also required, particularly in regard to crystal size distribution, clutter interactions, and chemical photolysis/reactions. The key advance lies in the incorporation of chemical and physical understanding of the targets and their co-indicators. We are currently developing a four-tiered approach to the spectroscopic algorithms challenge:

1. *Physics-based models.* Reliable chemical detection from standoff measurements will involve transformation of the chemical signatures in the reference spectral library to reflect the physical and environmental conditions of the experiment. A physics-based model will thus be included in the detection algorithm to help us model the variability in a reference spectrum as a function of effects such as vapor pressure, deliquescence, photochemical lifetime, reactive lifetime, decomposition products, and so on to facilitate better comparison with the measured spectrum.

2. *Situational effects.* Effects of different substrates and their properties on the chemical signatures and the angular dependence of spectra that are not clearly linked to equations of physics and chemistry will be experimentally evaluated and included in the

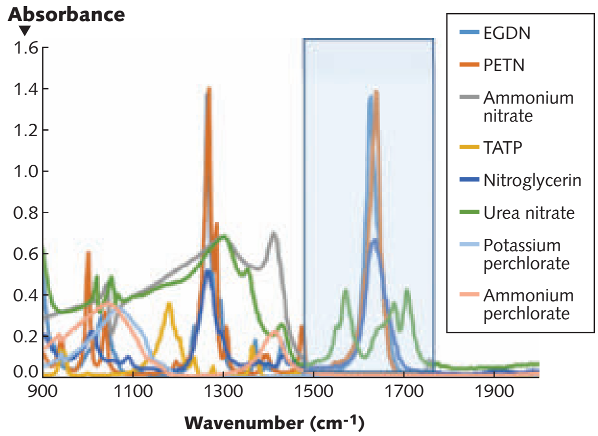

FIGURE 2. An assemblage of IR spectra of many common explosives shows that each has at least one unique absorption feature in the wavelength ranges selected. The blue shaded box indicates strong water interference in the troposphere. The figure intentionally spans beyond 1800 cm^{-1} so as to illustrate that no new information is gained for this chemical class by shifting the longwave-IR (LWIR) source further to the blue until the midwave-IR (MWIR) is reached.

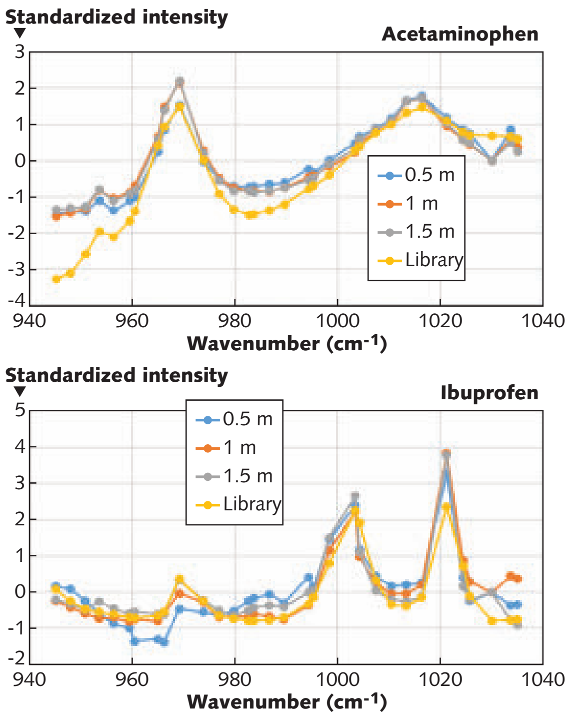

FIGURE 3. Standoff spectra of of acetaminophen and ibuprofen for three target distances. The black line shows the FTIR of the same using a diffuse reflectance accessory. The only data processing shown is the normalization of the curve areas to a common value.

detection algorithm. In particular, experimentally measuring such variability will help us algorithmically model the variability of chemical signatures from some "gold standard" reference signature, which—in addition to the physical model—will enable better detection strategies.

3. *Feature-based classification.* Extraction of relevant feature vectors from the reference library spectra and the knowledge of the chemistry to form a hierarchical decision tree that will help us provide different levels of classification based on the customer requirements. For instance, if a customer is only interested in finding out whether a given chemical is an explosive, then we might save on computational cost by avoiding searching through the leaves of the decision tree to find out the exact chemical.

4. *Real-time atmospheric measurements.* Once validated, the model will be suitable for field implementation by the inclusion of an integrated sensor suite that simultaneously records atmospheric pressure, temperature, relative humidity, solar flux, wind magnitude, and water-vapor mixing ratio.

With these design drivers considered, Pendar recently completed the build of a handheld demonstration system. Figure 3 shows the experimentally obtained spectra for two nonhazardous chemical targets as a function of stand-off distance. The yellow line in each panel shows the library FTIR ("true") spectrum for each. Agreements of $r^2 > 0.9$ were typical. With the prototype system as an extrapolation point, continued, focused advances in the technology are now underway to open myriad frontiers in molecular spectroscopy.

ACKNOWLEDGEMENT

Pendar Technologies was formed in August 2015 through a merger between Pendar Medical (Cambridge, MA), a portable spectroscopy company founded by Daryoosh Vakhshoori (who was previously at Ahura Scientific and CoreTek), and QCL sensing startup Eos Photonics (Cambridge, MA), a Harvard spinoff founded by professor Federico Capasso and his postdocs.

Mark F. Witinski is vice president of the Chemical Analysis and Security Unit, **Romain Blanchard** is a systems architect, **Biao Li** is a senior scientist, **Christian Pfluegl** is vice president of engineering for the Infrared Systems Unit, **Laurent Diehl** is vice president of the Mid Infrared Platform, **Benjamin Pancy** is an optical engineer, **Daryoosh Vakhshoori** is chief executive officer, and **Federico Capasso** is a board member and advisor at Pendar Technologies, Cambridge, MA; e-mail: witinski@pendar.tech, www.pendartechnologies.com. Capasso is also a professor of applied physics at Harvard University, Cambridge, MA.


SPIE. PHOTONICS WEST
CONNECTING MINDS. ADVANCING LIGHT.
2016
PHOTONICS WEST.
THE PREMIER EVENT FOR THE PHOTONICS AND LASER INDUSTRIES
REGISTER TODAY
WWW.SPIE.ORG/2016PW
BiOS—Biomedical Optics
Translational Research
LASE—Lasers and Sources
OPTO—Optoelectronic Devices
Green Photonics
3D Printing
Industry Panels and Keynotes
The Moscone Center
San Francisco, California, USA
Conferences & Courses
13–18 February 2016
Photonics West Exhibition
16–18 February 2016
BiOS EXPO
13–14 February 2016

Numerous ways exist to interferometrically measure aspheres

JOHN WALLACE, Senior Editor

Aspheric optics can be measured using a Fizeau interferometer, or by using an optical profiler containing an interferometer; both approaches have a variety of forms.

Because aspheric optics—from large precision one-off designs to mass-produced small elements for consumer devices—are growing in use, the testing of aspheres is currently a very active area in optics, with improvements to the technology occurring rapidly and with impressive results. Optical testing of aspheres takes two major forms: interferometric testing and noncontact profilers (which can contain their own interferometers).

The archetypal laser interferometer—the type that has been used in optical labs for decades—is a Fizeau interferometer that uses laser light at 633 nm to measure spherical optics. For added flexibility, today's interferometers can be obtained with laser sources operating at wavelengths ranging from ultraviolet (UV) to longwave-infrared (LWIR).

Measuring aspheric surfaces or optical components on a standard laser interferometer, however, quickly becomes challenging as the asphericity of an optic increases. While weak aspheres can be measured with a standard interferometer, stronger aspheres require the use of a null lens, which is placed in the interferometer to counteract the optic's asphericity. Such a null lens often takes the form of a computer-generated hologram (CGH), a diffractive element that can be easier to fabricate than a refractive null lens. This approach is widely used.

However, null lenses do add complexity to the interferometric setup—not only do they have to be precisely made, but they have to be properly placed and aligned with respect to the interferometer and the optic under test. In response, techniques have been developed to allow testing of even strong aspheres without the use of null lenses.

In an optical profiler, a spot of laser light is scanned across the surface of an optic to determine its 3D shape point by point. In some cases, the profiler's own optical system includes a laser interferometer to characterize the spot displacement. Optical profilers are capable of measuring very steep surfaces, including hemispheres.

The Fizeau interferometric approach

Today's Fizeau interferometer is an instrument well suited for asphere surface-form characterization. For example, the Verifire Asphere (VFA), produced by Zygo (Middlefield, CT), an Ametek company, is a noncontact interferometric metrology tool based on the Verifire Fizeau interferometer that Zygo has produced for many years.

As described by Tyler Steele, product manager at Zygo, the instrument contains a five-axis motorized stage and two-axis displacement measuring interferometer (DMI) that enables automatic alignment and acquisition of an aspheric surface under test. A full 3D surface-error map and an array of numerical outputs are available to characterize surface error for final

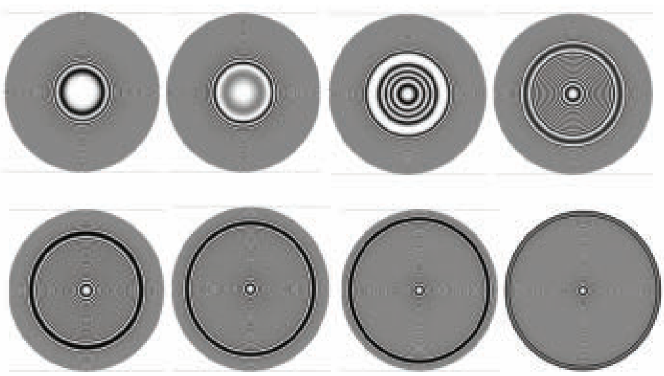

FIGURE 1. Data from different zones of an aspheric surface measured by a Verifire Asphere interferometer are combined in software to obtain the optic's shape. *(Courtesy of Zygo)*

metrology or provide feedback for deterministic polishing.

"An aspheric surface that is aligned to a Fizeau interferometer produces annular zones of null interference," says Steele. "The zone radial position is a function of Z position of the test surface relative to the interferometer. As the test part is translated in Z with feedback from the DMI, zones are acquired across the test surface (see Fig. 1) and the aspheric surface is reconstructed in software. The output is a deviation from the ideal design, or an optimized asphere base radius and conic constant can be calculated from the as-measured best fit surface."

The VFA is best suited for rotationally symmetric aspheres with departure from spherical of less than 800 μm and radius of curvature less than 800 mm, notes Steele. "The ophthalmic market has benefited from this metrology technique, as contact lens surfaces fit within these conditions," he says. "Many new contact-lens designs are based on aspheric surfaces that slightly deviate from spherical in order to achieve multifocal effects. Accurate metrology of these designs is critical in ensuring the proper prescription, as well as defect inspection and process management."

Large-volume manufacturing areas such as the contact-lens market have driven the development of an automation capability for the VFA: a 150 × 150 mm stage and automation software enable multiple test parts to be placed in a tray and automatically measured. Relevant results and a surface-error map are reported, with a graphical pass/fail interface controlled by an operator. In addition to asphere metrology, the VFA is capable of precision spherical radius and surface measurements, as well as toric surfaces—each a key surface shape in the ophthalmic contact-lens industry, says Steele.

One way to allow a Fizeau interferometer to measure strong aspheres without resulting in an unmeasurably high number of fringes is to divide the full aperture into subapertures, measure each one, and combine the data. This approach, developed at QED Technologies (Rochester, NY) and termed subaperture stitching interferometry (SSI), is a mainstay of the company's interferometer systems.

"Our systems combine a precision motion platform, interferometer, novel stitching algorithms, and custom software," says Paul Murphy, senior optical engineer at QED. "SSI technology enables testing spheres of large size (150–400 mm convex lenses) and high-numerical-aperture (hemispherical) optics that have traditionally challenged conventional full-aperture interferometry. Finally, SSI technology makes aspheric measurement possible without dedicated null lenses."

The Aspheric Stitching Interferometer with QIS [ASI(Q)] is the latest offering from QED, notes Murphy. The QIS, a coherent imaging, 6-in.-aperture Fizeau interferometer, is mounted in a multiaxis machine. The user enters information on the part and the software automatically recommends a transmission element, designs an appropriate subaperture layout (lattice), and collects and stitches the subaperture data (see Fig. 2).

"The QIS allows for greater than 50% more slope capture than a conventional, incoherent system," explains Murphy. "This is critical for asphere measurement, as many prescriptions have large slopes (many fringes) over any given subaperture. The ASI(Q) also can be configured with the optional variable optical null (VON). The VON corrects for known amounts of coma and astigmatism for any given subaperture, allowing for data capture in subapertures that would otherwise have fringe densities too high for reliable interferometric acquisition. Achievable measurement specifications are part- and environment-dependent, but QED has demonstrated results in the single-nanometer range."

The ASI can handle steep surfaces; in one example by Murphy (which happens to be for a sphere rather than for an asphere), a 150-mm-diameter lens with an approximately 500 mm radius was measured and polished. "A 6 in. interferometer cannot cover a convex part of these dimensions, says Murphy. "For a concave part, an *f*/3 or faster transmission sphere is needed to cover the part without stitching. With stitching, however, we were able to employ a slower diverging transmission sphere to obtain higher magnification and thus superior lateral resolution. Furthermore, we took advantage of the ASI's automatic random reference calibration to enable mid-spatial-frequency measurements at tenth-nanometer levels. These measurements allowed magnetorheological finishing (MRF) corrections to improve

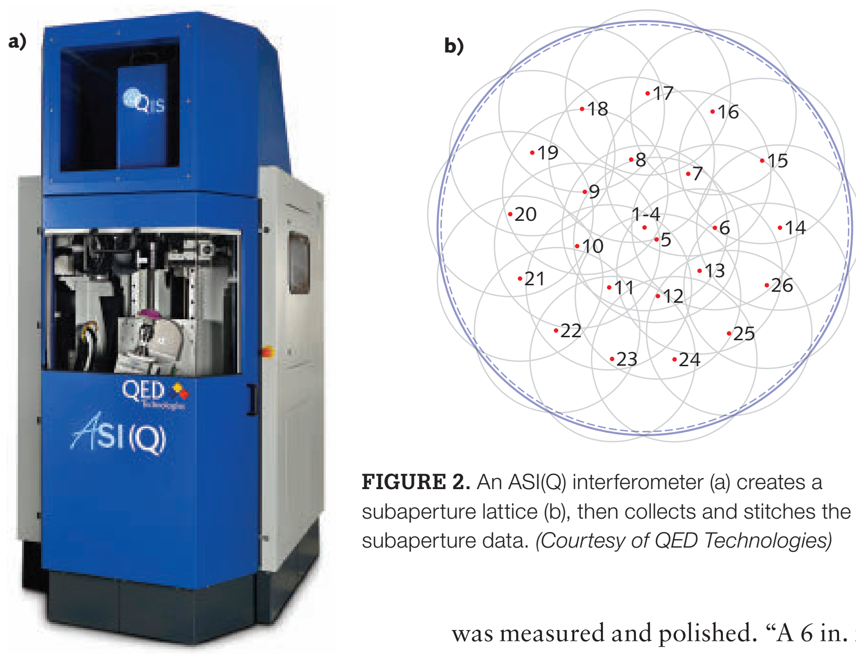

FIGURE 2. An ASI(Q) interferometer (a) creates a subaperture lattice (b), then collects and stitches the subaperture data. *(Courtesy of QED Technologies)*

the surface form and mid-frequencies to better than 1 nm root-mean-squared (RMS), as well as monitor submillimeter lateral features."

Surface profiling by scanning

Measuring the surface of an asphere by scanning an optical spot across it in a predetermined pattern is another important noncontact technique (contact profilometry, which is yet another important technique, will not be covered in this article).

The UltraSurf noncontact metrology system, made by OptiPro Systems (Ontario, NY), uses focused light from an optical probe to scan aspheric surfaces for 2D and 3D surface figure error analysis for either ground or polished optical surfaces (see Fig. 3). Noncontact point sensors can include a low-coherence interferometer to measure inside and outside surfaces at the same time, or a white light confocal system to measure individual optical surfaces.

"The UltraSurf 4X 300 has the capability to measure virtually any asphere up to 300 mm in diameter," says Ed Fess, R&D manager at OptiPro. "The 4X 300 model number denotes four axes of motion (X, Z, B, and C) with 300 mm of X-axis travel. To achieve high-precision metrology, all axes are driven by the latest air-bearing and linear-motor technology. Each linear axis has nanometer resolution, while both rotary axes have subarcsecond resolution. In addition, the UltraSurf 4X 300 can accommodate a variety of probes operating at different wavelengths."

Fess notes that the unit's flexibility in both travel and probe compatibility makes it ideal for measuring large aspheric surfaces as well as aspheres with radical departure. "The UltraSurf is also capable of measuring both surfaces of near-meniscus shapes simultaneously," he adds. "In this case, it can measure the convex, concave, and thickness maps in one measurement scan. The thickness map can provide a detailed 3D map of any wedge and decenter that might be between the two surfaces."

For More Information

Companies mentioned in this article include:

OptiPro Systems
Ontario, NY
www.optipro.com

QED Technologies
Rochester, NY
www.qedmrf.com

Taylor Hobson
Leicester, East Midlands, England
www.taylor-hobson.com

Zygo
Middlefield, CT
www.zygo.com

FOR A COMPLETE LISTING OF COMPANIES *making interferometers, visit the* Laser Focus World *Buyers Guide (http://buyersguide.laserfocusworld.com/index.html).*

Fess gives two example applications in which the UltraSurf's capabilities helped in a manufacturing process. The first involved a customer who was manufacturing an asphere with aspheric departure on the order of 1000 waves. "The customer had an issue during their manufacturing process that caused the form error of the optic to exceed what they could measure with their interferometer and hologram setup," says Fess. "We were able to use the UltraSurf to measure the optic and provide them with a data map to use with their subaperture polishing process. This allowed them to correct the surface shape and utilize their process again. We also had a customer purchase an UltraSurf for the simple fact that it was not slope-limited like contact profilometers, and was not limited to how aspheric the profile was."

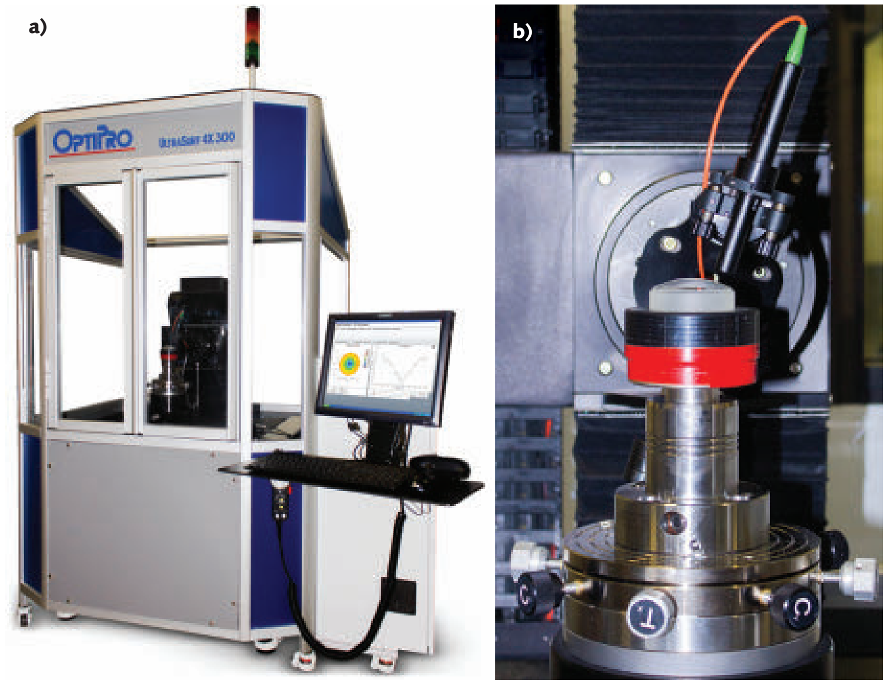

FIGURE 3. An UltraSurf 4X 300 noncontact metrology system (a) scans an aspheric surface using a stage-mounted single-point optical probe (b). *(Courtesy of OptiPro Systems)*

Zygo has developed and commercialized a 3D surface mapping system, called the Compass, that is specifically designed to inspect small aspheres typically used in consumer electronics devices. Eric Felkel, product manager at Zygo, says the Compass asphere metrology tool uses both coherence scanning interferometry (CSI) and 2D vision analysis to make subnanometer 3D measurements of optical surfaces, as well as 2D inspection of relevant mounting and alignment parameters of both lenses and injection-molding tooling molds.

"The technique is entirely noncontact and results in 3D topography, deviation, and texture results," he says. "Users can create recipes that automate the process of characterizing the entire lens. The noncontact CSI technology leverages the short coherence length of white-light illumination to compare the surface of a test region to a reference surface built into the microscope objective. Overlapping regions of the surface are measured and then stitched together to form a full 3D map of the lens topography. The 3D map can then be compared to the optical prescription and a deviation map can be presented, showing both qualitatively and quantitatively how different the optical element is from the design parameters."

The noncontact measurement is important, notes Felkel. "While small plastic lenses can be made in sufficient volumes to be expendable for metrology, the precise molds used to manufacture them require significantly more care," he explains. "A noncontact solution allows a finished lens mold to be measured and immediately used, without a final finishing step to remove evidence of metrology. In addition, because Compass measures the entire surface of the asphere, it can detect problems that may escape notice of other techniques."

For example, one issue uncovered by an inspection with the Compass tool was that a customer's plastic injection process was actually underfilling the lens mold, resulting in an asymmetric lens surface as well as an incorrect surface shape. Line-profiling-based techniques could see the incorrect surface shape, but it wasn't until the lens was measured with the Compass that the underfill became obvious.

Multiwavelength interferometry

A scanning-interferometer-based asphere-measurement system produced by Taylor Hobson (Leicester, East Midlands, England), another Ametek company, is based on multiwavelength interferometry (MWLI), which has the capability of measuring absolute distances. As noted by Erik Stover, business development manager at Taylor Hobson, the LuphoScan system contains a four-wavelength probe.

The system contains a fiber-based interferometer with four wavelengths that lie in the 1530–1610 nm range, with all light coincident at the same point on the test optic. The resulting four independently measured interference signals are digitized and their information combined to produce an absolute distance measurement. The optic under test is scanned by rotating it on a 360° rotary stage while moving the interferometer probe radially and in Z.

The absolute-measurement capability allows the system to correlate data measured successively on different surfaces, such as the front and back of a lens, enabling the system to determine decenter, wedge, lens thickness, and lens-mount positioning as well as asphere surface shape.

Quantum dots and silicon photonics combine in broadband tunable laser

TOMOHIRO KITA and NAOKATSU YAMAMOTO

A new wavelength-tunable laser diode combines quantum-dot (QD) technology and silicon photonics with large optical gains around the 1310 nm telecom window and is amenable to integration of other passive and active components towards a truly integrated photonic platform.

A new heterogeneous wavelength-tunable laser diode, configured using quantum dot (QD) and silicon photonics technology, leverages large optical gains in the 1000–1300 nm wavelength region using a scalable platform for highly integrated photonics devices. A cooperative research effort between Tohoku University (Sendai, Japan) and the National Institution of Information and Communication Technology (NICT; Tokyo, Japan) has resulted in the demonstration of broadband tuning of 44 nm around a 1230 nm center wavelength with an ultrasmall device footprint, with many more configurations with various performance metrics possible.

Recently developed high-capacity optical transmission systems use wavelength-division multiplexing (WDM) systems with dense frequency channels. Because the frequency channels in the conventional band (C-band) at 1530–1565 nm are overcrowded, the frequency utilization efficiency of such WDM systems becomes saturated. However, extensive and unexploited frequency resources are buried in the near-infrared (NIR) wavelength regions such as the thousand (T) and original (O) bands between 1000 and 1260 nm and 1260 and 1350 nm, respectively.

Quantum dot-based optical gain media have various attractive characteristics, including ultrabroad optical gain bandwidths, high-temperature device stability, and small linewidth enhancement factors, as well as silicon photonic wire waveguides based on silicon-on-insulator (SOI) structures that are easily amenable to constructing highly integrated photonics devices.[1-4]

The photonic devices used for short-range data transmission are required to have a small footprint and low power consumption. Therefore, compact, low-power wavelength-tunable laser diodes are key devices for use in higher-capacity data transmission systems that have been designed to use these undeveloped frequency bands, and our heterogeneous tunable wavelength laser diode consisting of a QD optical gain medium and a silicon photonics external cavity is a promising candidate.[5]

Quantum dot optical amplifier

Ultrabroadband optical gain media spanning the T- and O-band are effectively fabricated by using QD growth techniques on large-diameter gallium-arsenide (GaAs) substrates. Our sandwiched sub-nano-separator (SSNS) growth technique is a simple and efficient method for obtaining high-quality QDs (see Fig. 1).

In the SSNS method, three monolayers (each around 0.85 nm thick) of GaAs thin film are grown in an indium GaAs (InGaAs) quantum well (QW) under the QDs. We had previously observed many large, coalescent dots that could induce crystal defects in QD devices using a

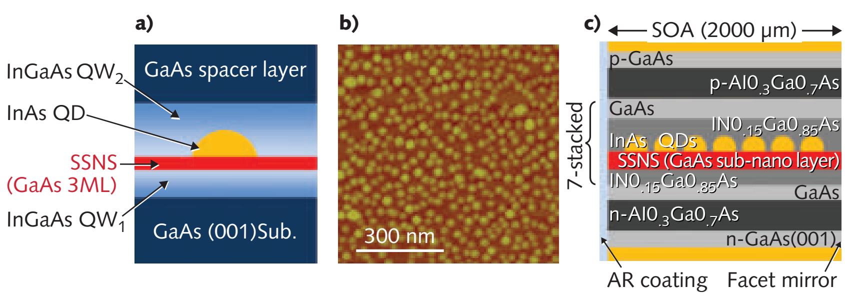

FIGURE 1. A cross-section (a) shows a quantum dot (QD) device grown using the SSNS technique, resulting in a high-density, high-quality QD structure (b) that is used to create a typical SOA (c) using QD optical gain.

conventional growth technique without SSNS. Now, we can obtain high-density (8.2×10^{10} cm^{-2}), high-quality QD structures since the SSNS technique successfully suppresses the formation of coalescent dots.

For single-mode transmission, a ridge-type semiconductor waveguide was fabricated for single-mode transmission. The cross-section of the semiconductor optical amplifier (SOA) has an anti-reflection (AR) coating facet to connect a silicon photonics chip with low reflection and a cleaved facet used as a reflecting mirror in the laser cavity.

To fabricate the SOA, the SSNS growth technique was combined with molecular beam epitaxy. Quantum dots comprised of indium arsenide (InAs) with 20–30 nm diameters were grown within an InGaAs QW. Seven of these QD layers are stacked to achieve broadband optical gain. Subsequently, this QD-SOA is used as an optical gain medium for the heterogeneous laser, which can be complemented by other communication technology devices such as a high-speed modulator, a two-mode laser, and a photoreceiver.[6,7]

Silicon photonics ring resonator filter

With the QD-SOA fabricated, a wavelength filter is fabricated next using silicon photonics techniques. It includes a spot-size converter that has a silicon oxide (SiOx) core and a tapered Si waveguide that connects the QD-SOA to the Si photonic wire waveguide while minimizing optical reflections and coupling losses (see Fig. 2).

The wavelength-tunable filter consists of two ring resonators of different size. The Vernier effect of these two ring resonators allows only light of a specific wavelength to reflect to the QD-SOA. Furthermore, Tantalum micro-heaters formed above the resonators provide a means whereby the laser wavelength can be tuned through application of the thermooptic effect.

Essentially, the wavelength tuning operation of the double ring resonator wavelength filter is achieved through Vernier effects wherein a ring resonator acts as a wavelength filter with constant wavelength interval called the free spectral range (FSR), which is inversely proportional to the circumference of the ring. The tuning wavelength range is determined from the FSR difference of the two rings with *FSR1* and *FSR2*.

A smaller difference in the FSR provides a wider wavelength tuning range, even when the transmittance difference between the main and side peaks is small. On the other hand, a sufficiently large transmittance difference is required to achieve stable single-mode lasing and is obtained using large FSR ring resonators.

Silicon photonics allows us to fabricate an ultrasmall ring resonator with large FSR because of the strong light

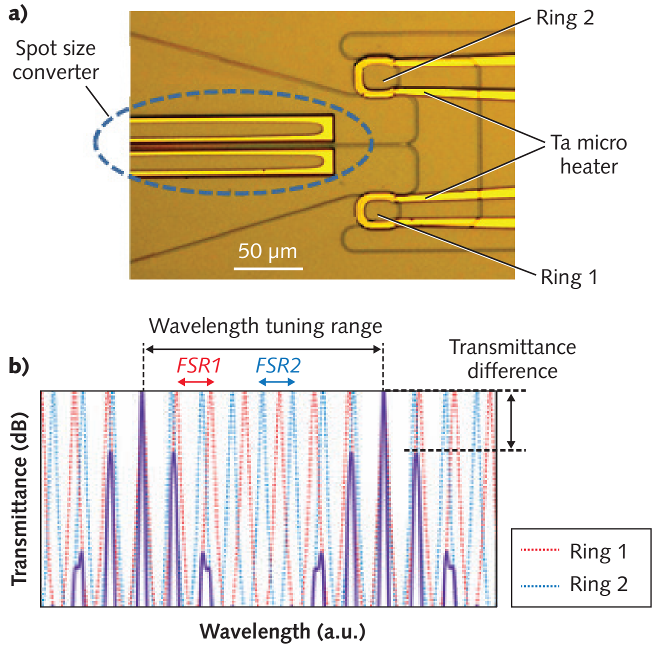

FIGURE 2. A microscope image (a) shows a silicon-photonics-based wavelength-tunable filter. In a transmittance analysis (b), the red and blue dotted lines indicate the transmittance of a small ring resonator with free spectral range *FSR1* and a large ring resonator with *FSR2*, respectively, and the solid line indicates the product of each transmittance. The tuning wavelength range is determined from the FSR difference of the two rings. A smaller difference in the FSR provides a wider wavelength tuning range, even when the transmittance difference between the main and side peaks is small.

confinement in the waveguide. The ring resonator consists of four circle quadrants and four straight lines and the radius of the circle was chosen to be 10 μm to avoid bending losses. The FSRs of the ring resonators and the coupling efficiency between the bus-waveguide and the ring resonator are optimized to obtain wide wavelength tuning range and sufficient transmittance difference.

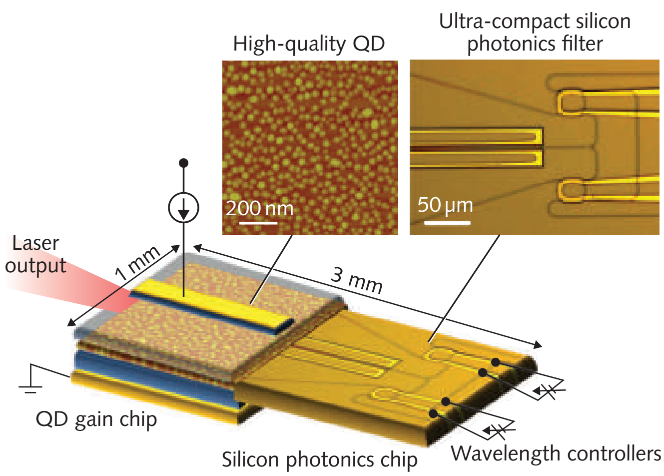

FIGURE 3. A schematic shows how the heterogeneous wavelength-tunable laser diode is constructed.

The FSRs and the coupling efficiencies of the double ring resonators are designed to obtain a 50 nm wavelength tuning range and 1 dB transmittance difference. We have since fabricated various wavelength-tunable laser diodes, including a broadband tunable laser diode, a narrow spectral-linewidth tunable laser diode, and a high-power integrated tunable laser diode by using a silicon photonics wavelength filter and a commercially available C-band SOA.[8, 9]

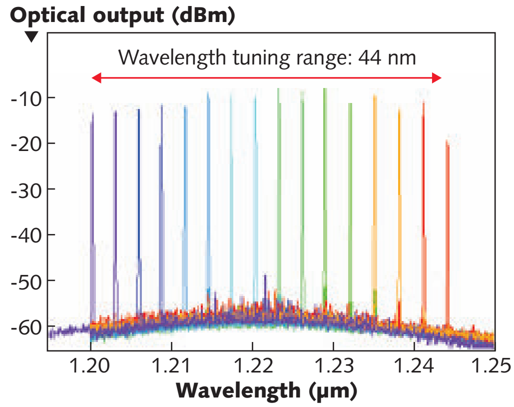

FIGURE 4. The heterogeneous wavelength-tunable laser diode has a broad tuning range about its center wavelength.

The tunable laser diode

Using stepper motor controllers, the QD-SOA—kept at approximately 25°C using a thermoelectric cooler—and the silicon photonics wavelength filter are butt-jointed (see Fig. 3). The lasing wavelength is controlled by the temperature of a micro-heater placed on the ring resonators. With physical footprints of 600 μm × 1 mm and 1 × 2 mm for the wavelength filter and the QD-SOA, respectively, the total device size of the tunable laser diode is just 1 × 3 mm.

Measured using a lensed fiber, the laser output from the cleaved facet of the QD-SOA shows single-mode lasing characteristics with a laser oscillation threshold current of 230 mA. Maximum fiber-coupled output power is 0.4 mW when the QD-SOA injection current is 500 mA.

As the ring resonator temperature is increased by a heater with 2.1 mW/nm power consumption, the superimposed lasing spectra show a 44 nm wavelength tuning range with more than a 37 dB side-mode-suppression ratio between the ring resonator's modes. The 44 nm wavelength tuning range of our heterogeneous QD/Si photonics wavelength-tunable laser is, to our knowledge, the broadest achieved to date. The 44 nm tuning range around 1230 nm corresponds to 8.8 THz in the frequency domain, which is far larger than the 4.4 THz frequency that is available within the C-band.

Our heterogeneous laser is suitable for use as a light source on a silicon photonics platform that includes other optical components such as high-speed modulators and germanium (Ge)-based detectors. In addition to application as a single-chip broadband optical transceiver for telecommunications, the laser could also be applied to biomedical imaging applications such as optical coherence tomography (OCT), considering the low absorption of NIR light at 1310 nm in the presence of water. ◀

ACKNOWLEDGEMENTS

This research was partially supported by the Strategic Information and Communications R&D Promotion Program (SCOPE), of Japan's Ministry of Internal Affairs and Communications and a Grant-in-Aid for Scientific Research of the Japan Society for the Promotion of Science.

REFERENCES

1. Y. Arakawam and H. Sakaki, *Appl. Phys. Lett.*, 40, 11, 939–941 (1982).
2. D. L. Huffaker et al., *Appl. Phys. Lett.*, 73, 18, 2564–2566 (1998).
3. R. A. Soref, *Proc. IEEE*, 81, 12, 1687–1706 (1993).
4. B. Jalai and S. Fathpour, *J. Lightwave Technol.*, 24, 12, 4600–4615 (2006).
5. T. Kita et al., *Appl. Phys. Express*, 8, 6, 062701 (2015).
6. N. Yamamoto et al., *Jpn. J. Appl. Phys.*, 51, 2S, 02BG08 (2012).
7. N. Yamamoto et al., *Proc. OFC*, Los Angeles, CA, paper W2A.24 (Mar. 2015).
8. T. Kita et al., *Appl. Phys. Lett.*, 106, 11, 111104 (2015).
9. N. Kobayashi et al., *J. Lightwave Technol.*, 33, 6, 1241–1246 (2015).

Tomohiro Kita is assistant professor in the Department of Electrical Engineering at Tohoku University, Sendai, Japan; e-mail: tkita@ecei.tohoku.ac.jp; www.ecei.tohoku.ac.jp. **Naokatsu Yamamoto** is director of the Lightwave Device Laboratory at the National Institution of Information and Communication Technology, Tokyo, Japan; e-mail: naokatsu@nict.go.jp; www.nict.go.jp.

Tell us what you think about this article. Send an e-mail to LFWFeedback@pennwell.com.

Shack-Hartmann wavefront sensor enables flexible characterization of lenses

RALF DORN and JOHANNES PFUND

A Shack-Hartmann wavefront sensor can replace an interferometer or stylus profilometer for measuring lens properties in a lab or production environment.

Many devices in today's market make use of optics; in particular, aspherical elements are on the rise because they allow optical systems to be designed more compactly and easily. Although functional and quality demands on optics are continuously increasing, maintaining quality of optics often lags behind because of the lack of sufficiently flexible measurement technology. Here, the use of a Shack-Hartmann wavefront sensor provides a solution, enabling a rapid and flexible recording of the characteristic values of optical lenses. A great number of different measurement processes and modalities can be integrated into one device so that it works efficiently both in manual and automated production environments.

There are several methods available to test an optical device. The simplest (and at the same time also the slowest) is to sample the optics using tactile methods such as stylus-based surface profilometry. However, optics can be damaged by tactile methods and the measuring device quickly approaches its limits for cases of high curvature.

In contrast, a Shack-Hartmann wavefront sensor assesses optics quickly using current computer power, and can operate using low-coherence light sources. The Shack-Hartmann sensor has a very high dynamic measurement range and functions rapidly enough that the measurement process is insensitive to environmental vibrations, and as a result is suitable for use in the vicinity of operating machines.

Sensor configuration

A Shack-Hartmann wavefront sensor consists of a 2D array of microlenses and a CCD camera detector. After passing through the microlens field, a flat wavefront generates a regular grid of points on the detector whose spots have the same array separation distance as the microlenses. If the wavefront has a curvature, the spots generated by the microlens are displaced in *x* and *y* correspondingly. From the shifts of these grid points, the wavefront can be reconstructed. With strongly curved wavefronts, however, the spots in the proximity of adjacent spots can move out of their "home aperture," or the immediate region surrounding the reference point's location.

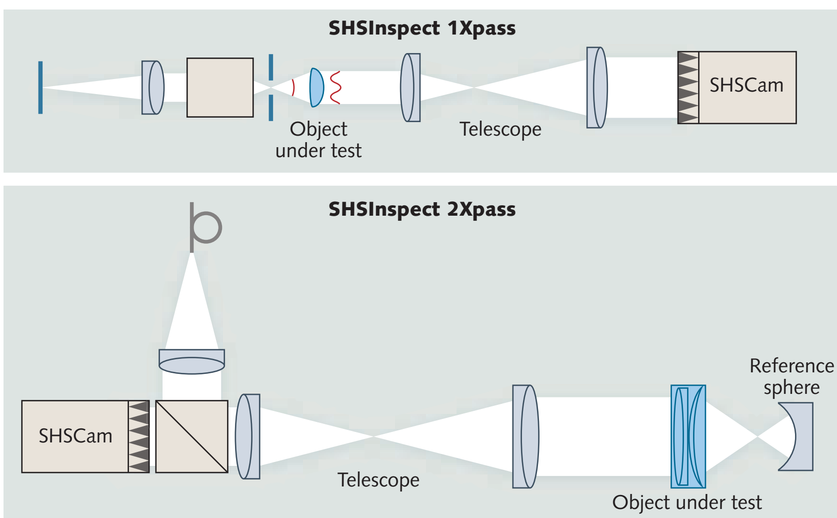

FIGURE 1. Schematic shows sensor-system configurations for measurement in single (SHSInspect 1Xpass; a) and double pass (SHSInspect 2Xpass; b).

Optocraft has developed a Shack-Hartmann wavefront-sensing system (SHSLab) that contains a solution to this problem—a process that reliably assigns the displaced spots to their proper reference points in the case of high wavefront curvatures (see Fig. 2). The process requires only a single camera image and is thus very fast and simple to use. The local radius of curvature of a wavefront impinging on the microlens array can be as small as 5 mm, allowing wavefronts with extreme curvatures to be measured.

The sensor (SHSCam) can accommodate up to 240 × 160 spots as well as an evaluation rate of up to 1000 Hz. By means of associated software (SHSWorks), a great number of optical measurement variables can be tested, such as wavefront aberrations, imaging quality (Strehl, MTF, etc.), focal length, and laser quality.

One of the complete measurement systems based around SHSLab is called SHSInspect (see Fig. 3). The system has two configurations: with "1Xpass," the measurement beam runs through the test specimens only once, while with "2Xpass," the light passes twice through the test specimen (see Fig. 1). In the latter case, the light is reflected back after the first transition of a mirror.

One strength of 2Xpass is that its influence on the measurement beam is doubled because of the twofold transition through

For testing of chromatic effects, a single wavefront sensor can be used over a wide wavelength range. The basic optical principle of the Shack-Hartmann sensor makes it possible to use the sensor not only with light sources of different wavelengths, but also with sources having low coherence. As a result, low-cost LEDs can be used as a source that provides a large range of wavelengths for testing.

the test specimen. The resulting increase in measurement sensitivity allows the whole measurement configuration to be calibrated simply by means of a plane mirror and a reference sphere.

Integration into R&D and production environments

For the optical industry, this type of system offers high accuracy and can also be easily integrated into an automated production environment. One important characteristic is that the system works fast enough to measure in real time during the production cycle. The 1Xpass and 2Xpass systems reach, according to sensor size, frame rates between 1 and 50 Hz and, in special applications, up to 1000 Hz. Ultimately, the time required for the insertion of the test specimen into the measuring equipment determines the measuring rate.

Production environments naturally vibrate, induced by running machines or motors in the device itself. The high vibration tolerance of the Shack-Hartmann sensor system allows the expense of vibration damping to be avoided. A further important requirement for production quality control is a sufficiently high level of measurement precision. The Shack-Hartmann sensor head by itself achieves a typical uncalibrated base accuracy of $\lambda/15$ peak-to-valley (PV). Depending on the optical structure of the test system, an even higher precision can be achieved by suitable calibration measures. In the case of the 2Xpass, a value of $\lambda/20$ PV is about typical.

For testing of chromatic effects, a single wavefront sensor can be used over a wide wavelength range. The basic optical principle of the Shack-Hartmann sensor makes it possible to use the sensor not only with light sources of different wavelengths, but also with sources having low coherence. As a result, low-cost LEDs can be used as a source that provides a large range of wavelengths for testing.

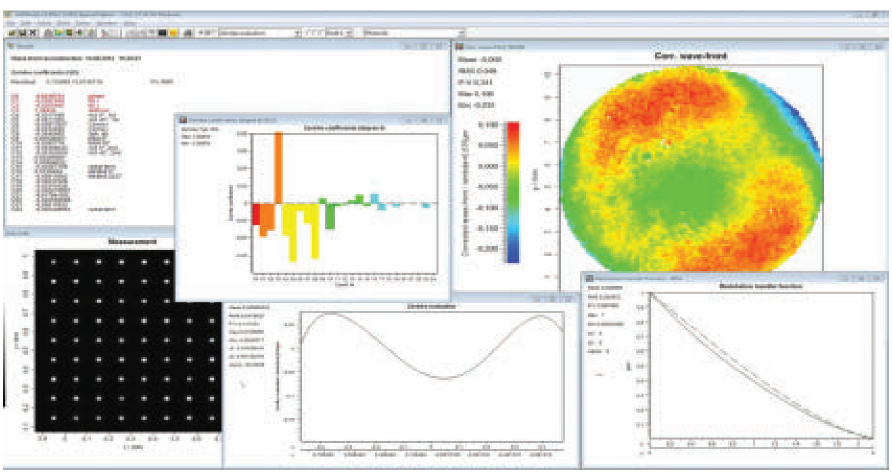

FIGURE 2. A screen capture shows various forms of data captured and produced by SHSLab, including the spot array imaged at the CCD sensor, a 2D wavefront representation, a wavefront cross-section, and a Zernike evaluation.

Multifunctional systems

SHSInspect (especially in its 2Xpass form) is adaptable to the requirements of the user. Currently, on-axis and off-axis measurements with field angles up to 50° are possible. Larger angles are feasible. By measuring the mechanical and optical characteristics of a lens, both the back focal length (BFL) and the effective focal length (EFL) can be determined.

Many objective lenses include an adjustable lens provided at a location that can be targeted, displaced, and/or tilted,

FIGURE 3. SHSInspect operates over a large wavelength range and also works with low-coherence light sources such as LEDs.

for example, to compensate form and position faults of the other fixed-assembly lenses. With the 2Xpass, the adjustment of such sliding lenses in microscope lenses is done rapidly, enabled by the motorized centering function of the return sphere to automatically adjust the return sphere to its ideal position. This allows the operator to concentrate on the adjustments of the test specimen.

In production, measurements can be implemented partly or fully automatically. In the first case, the test specimen is inserted manually into the measuring system—the measurements then progress automatically in accordance with a test protocol. However, this loading and unloading can also be implemented by means of a robot.

Because of their speed and the reliability of their measurements, Shack-Hartmann wavefront sensors are suitable for the testing of optics both in research and in production. Even wavefronts with extreme curvatures can be measured precisely using corresponding evaluation software in combination with special sensor models. However, to select the proper sensor configuration, it is important to first evaluate the required measurement sensitivity, as well as the requirements for integration into the production environment.

Ralf Dorn and **Johannes Pfund** are at Optocraft GmbH, Erlangen, Germany; e-mails: j.pfund@optocraft.de and r.dorn@optocraft.de; www.optocraft.de.

Computer modeling boosts laser device development

RÜDIGER PASCHOTTA

A full quantitative understanding of laser devices is boosted by computer modeling, which is not only essential for efficient development processes, but also for identifying the causes of unexpected behavior.

Computer modeling can give valuable insight into the function of laser devices. It can even reveal internal details that could not be observed in experiments, and thus allows one to develop a comprehensive understanding from which laser development can enormously profit. For example, the performance potentials of certain technologies can be fully exploited and time-consuming and expensive iterations in the development process can be avoided. Some typical examples clarify the benefits of computer modeling for improved laser device development.

Example 1: *Q*-switched lasers

The basic dynamics of pulse generation in a *Q*-switched laser can be described with helpful formulas that reveal the influence of various laser parameters on certain performance parameters such as pulse energy and duration. However, it is often important to understand the impact of additional effects. For example, what effects will thermal lensing and gain guiding have on the performance of a *Q*-switched, single-transverse-mode laser?

Obviously, such questions cannot simply be addressed with experimental tests since these at most reveal what laser output is achieved in a few situations, but neglect the full impact of particular effects on the performance and do not allow a full system optimization.

A computer model that takes into account the transverse dimensions concerning beam profiles and excitation in the laser crystal can show in detail how the thermal lens with its aberrations affects the beam quality, for example, and to what extent the transverse dependence of the laser gain (gain guiding) influences the performance in high-gain situations. Note that the transverse gain profile changes substantially within the pulse duration because of saturation of the gain medium. Without such a model, it is close to impossible to properly quantify the importance of such effects.

The transverse beam profile in a typical actively *Q*-switched Nd:YAG laser varies with the number of resonator round trips (see Fig. 1). In addition to significant variations of beam size during the pulse, much stronger effects of that kind associated with a dramatic reduction in beam quality are observed if the path length in air is increased from 20 to only 25 mm, which would still be well within the stability range of that laser resonator.

This path length increase causes a frequency degeneration for higher-order modes—knowledge that could not be gained through experiments, but could be garnered through modeling exercises that quantify the sensitivity of the laser to gain-guiding effects, which depend strongly on the resonator design and not only on the magnitude of gain and the pump beam size. Such knowledge is essential for an efficient optimization process.

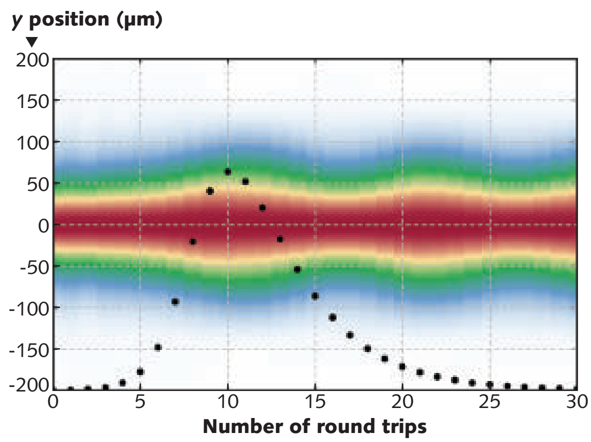

FIGURE 1. Evolution of the transverse beam profile (shown with a color scale) and the optical power (black circles, in arbitrary units) in an actively *Q*-switched laser is simulated with RP Fiber Power software using numerical beam propagation. The color scale is normalized for each round trip according to the time-dependent optical power so that the variation of the beam diameter can be seen.

Example 2: Mode-locked lasers

Today, even fiber lasers can have impressive performance characteristics in the area of ultrashort pulse generation. This, however, requires operation in regimes where strong nonlinear and dispersive effects occur. Particularly in such cases, the relationships between device parameters and performance are often far from obvious.

Among other details, suitable parameters of saturable absorbers for passive mode locking—namely, the required modulation depth and the acceptable recovery time—need to be determined. Only a numerical model makes it practical to explore the limits of pulse stability and optimize performance. A "blind flight" trial-and-error approach in the lab can easily lead to time-consuming, costly, and frustrating iterations, making it nearly impossible to develop optimized designs.

Example 3: Ultrashort-pulse fiber amplifiers

High-energy optical pulses can be generated by amplifying low-energy seed pulses from a pulsed laser diode in a sequence of fiber amplifier stages. Between the amplifier stages, bandpass filters, Faraday isolators, and/or optical switches can suppress light resulting from amplified spontaneous emission (ASE). It is not obvious to which extent the mentioned methods are required.

Also, it is essential to know about other aspects such as occurring optical intensities, pulse distortions because of gain saturation, and possible nonlinear effects, amongst others. For many reasons, an uninformed trial-and-error approach is again inefficient.

Also, diagnosing problems in an experiment can be rather difficult because one cannot easily measure various essential quantities within the optical fibers or find out in the lab why such a system does not work well.

A comprehensive computer model of a multistage amplifier system can therefore be extremely helpful. It can be constructed in a much shorter time than an experimental prototype and at much lower cost. By revealing all relevant internal details, it allows one to refine the system design such that all known potential problems are safely avoided. The likelihood of unwelcome surprises in the subsequent laboratory experiments is then much reduced. One does not have to order expensive components without knowing whether they will work in practice.

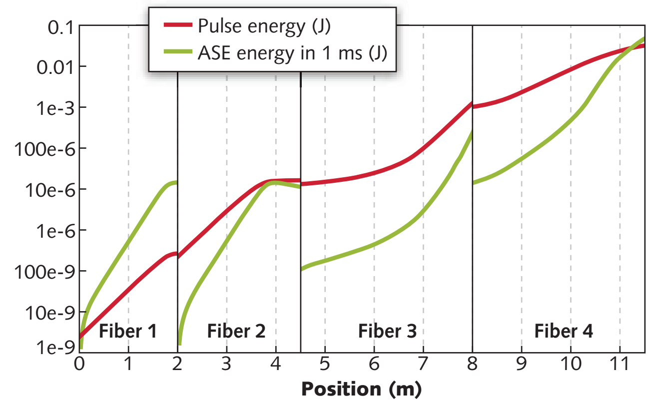

FIGURE 2. The evolution of pulse energy and forward ASE powers in a four-stage fiber amplifier system with various types of ASE suppression between the stages, calculated with a comprehensive computer model.

Modeling can reveal how the pulse energies and forward ASE levels evolve in a four-stage amplifier system (see Fig. 2). The ASE is essentially removed by acousto-optic modulators after the first and second stages, and reduced with a bandpass filter after the third stage. The output is substantial in terms of average power, although the peak power of the amplified pulse is far higher. The same model also calculates the temporal shape of the resulting pulses (with strong distortions because of gain saturation) and many other quantities of interest.

How to get started

Although laser development can greatly profit from computer modeling, many engineers and scientists hesitate before using this powerful method. But some tips and simple steps to follow based on practical experience can ease apprehensions about the method.

First, an important step is to identify the questions that should be answered by a model. For example, one may identify the need to understand the evolution of ASE powers along amplifier fibers, including their time dependencies.

Next, a suitable person should be found to actually develop the model—perhaps just one person within an R&D team or a research group. If there is no such person around (or no one has spare time), or if such needs do not arise often enough to justify the effort, an external consultant may be the right choice. Then, the consultant can evaluate the calculated results together with interpretations and recommendations and pass those to the team.

In many cases, an R&D team or research group will prefer to do the modeling work internally using some suitable software tools. In that way, the internal developers gain the most solid in-house expertise. They just need to select software tools that will serve multiple modeling needs in the future.

Different user interfaces

The easiest way to get started is by using software that consists of forms in which the developer enters various device and operation parameters like fiber length, input power levels, and wavelengths desired, and then obtains an output in text and graphical form that shows, for example, how optical power evolves within the device or how it changes with time (see Fig. 3).

Using these simple tools, models can be set up quickly and leverage a number of predefined diagrams that can make various adjustments through the available forms. For example, a developer could calculate the output power of an amplifier as a function of the pump power.

A common disadvantage of forms, however, is their lack of flexibility. The types of models and generated diagrams are more or less limited to those considered by the developer of the software. It may not be practical to put together multi-stage

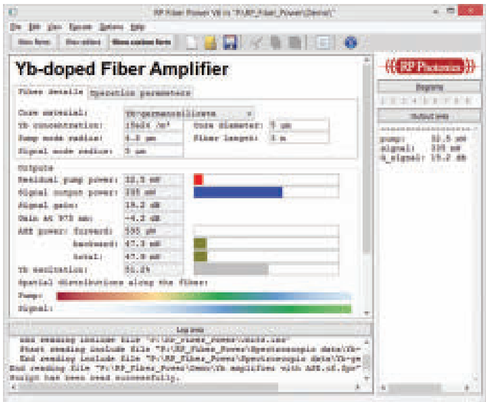

FIGURE 3. Form-based software can be used to model laser devices such as a fiber amplifier. It is essential that such forms be made or modified by the user or by technical support, so that they can be tailored to specific applications.

amplifier systems and to simulate complex operation cycles if the software developer did not offer these variants.

Much greater flexibility is obtained if modeling software also offers a script language that can be used to define the considered setup, to trigger calculations, and to generate the text or graphical outputs in any desired form. With a powerful script language, one can freely implement even the most sophisticated models and operation modes. For example, one could simulate multiple amplification and pumping cycles of an amplifier system as the output parameters stay constant, or automatically modify system parameters such that certain goals are met. However, potential users may have concerns that such a language would take too long to learn.

These two approaches—modeling software with forms or with a script language—are so fundamentally different that moving from forms to scripting may appear overwhelming. Fortunately, there are ways to conveniently combine the two approaches.

One possibility is that the software, when controlled with forms, can generate scripts based on the form inputs. The user can then go as far as possible using simple forms, but when the limits of that approach are met, the user can easily switch to script programming, starting with the automatically generated script rather than writing one from scratch. Also, forms may allow the user to inject small pieces of script code into the generated script, so that certain details (such as additional, special plots in a diagram) can be added without moving to script programming altogether.

Another possibility is that forms can be defined within scripts. This means that input and output fields, possibly including convenient graphical control elements such as selection boxes, can be defined in text form and associated with certain variables or functions rather than being hard-coded in the software. This allows the user to construct forms tailored to a certain modeling purpose, rather than being limited to those forms created by the software developer.

Advanced simulation and design software is an easy path to device modeling without being limited to basic tasks. The valuable time of laser engineers and scientists can be saved for more complex tasks rather than being used in overly time-consuming learning exercises.

Documentation and support

For any modeling task, documentation of methods and results is essential. The documentation must not only explain details of the user interface, but must inform the user what kind of physical model was used, what simplifying assumptions were made, and what limitations need to be considered. Unfortunately, software documentation is often neglected.

In case of doubt, competent technical support should be available—not only for helping with the handling of the software, but also offering detailed technical and scientific advice. For example, a beginner may find it difficult to decide which kind of model should be implemented for a certain purpose and which possibly disturbing effects need to be considered. Such support should come from a competent expert in the field rather than just a programmer.

Rüdiger Paschotta is founder and executive of RP Photonics Consulting, Bad Dürrheim, Germany; e-mail: paschotta@rp-photonics.com; www.rp-photonics.com.

STATEMENT OF OWNERSHIP, MANAGEMENT, AND CIRCULATION

1. Publication title: Laser Focus World. **2. Publication number:** 922-380 **3. Filing date:** October 1, 2015. **4. Issue frequency:** Monthly. **5. Number of issues published annually:** 12. **6. Annual subscription price:** $162.00. **7. Complete mailing address of known office of publication:** PennWell Corporation, 1421 South Sheridan Rd., Tulsa, OK 74112, Tulsa County. **7a. Contact person:** Traci Huntsman. **7b. Telephone:** 918-831-9435. **8. Complete mailing address of headquarters or general business office of publisher:** PennWell Corporation, 98 Spit Brook Rd., Nashua, NH 03062. **9. Full names and complete mailing addresses of Publisher, Editor and Managing Editor:** Publisher: Alan Bergstein, 98 Spit Brook Rd., Nashua, NH 03062. Editor: W. Conard Holton, 98 Spit Brook Rd., Nashua, NH 03062. Managing Editor: W. Conard Holton, 98 Spit Brook Rd., Nashua, NH 03062. **10. Owner:** PennWell Corporation, 1421 So. Sheridan Rd., Tulsa, OK 74112, Tulsa County; Successors to the Estate of Helen B. Lauinger, 1421 So. Sheridan Rd., Tulsa, OK 74112, Tulsa County. **11. Known Bondholders, Mortgages, and Other Security Holders Owning or Holding 1 Percent or More of Total Amount of Bonds, Mortgages, or Other Securities:** None. **12.** N/A. **13. Publication Title:** Laser Focus World. **14. Issue Date for Circulation Data:** September 2015.

15. Extent and Nature of Circulation:

	Average No. copies each issue during preceding 12 months:	No. copies of single issue published nearest to filing date:
a. Total number of copies	38,302	38,308
b. Legitimate paid and/or requested distribution		
1. Outside county paid/requested mail subscriptions stated on PS form 3541	32,398	32,798
2. In-county paid/requested mail subscriptions stated on PS form 3541	0	0
3. Sales through dealers and carriers, street vendors, counter sales, and other paid or requested distribution outside USPS®	2,529	2,320
4. Requested copies distributed by other mail classes through the USPS®	0	0
c. Total paid and/or requested circulation	34,927	35,118
d. Non-requested distribution		
1. Outside county nonrequested copies stated on PS form 3541	1,971	1,926
2. In-county nonrequested copies stated on PS form 3541	0	0
3. Nonreqeusted copies distributed through the USPS by other classes of mail	0	0
4. Nonrequested copies distributed outside the mail	960	820
e. Total nonrequested distribution	2,931	2,746
f. Total Distribution	37,858	37,864
g. Copies not Distributed	444	444
h. Total	38,302	38,308
i. Percent paid and/or requested circulation	92.26%	92.75%

16. Electronic Copy Circulation

a. Requested and Paid Electronic Copies	33,027	37,423
b. Total requested and paid print copies + requested/paid electronic copies	67,954	72,541
c. Total requested copy distribution + requested/paid electronic copies	70,885	75,287
d. Percent paid and/or requested circulation	95.87%	96.35%

☑ I certify that 50% of all my distributed copies (electronic and print) are legitimate requests or paid copies.

17. Publication of Statement of Ownership: Will be printed in the November 2015 issue of this publication.

18. Signature and title of Editor, Publisher, Business Manager, or Owner: Traci Huntsman, Manager Corporate Assets and Postal Compliance. **Date:** 10/01/2015.

I certify that all information furnished on this form is true and complete. I understand that anyone who furnishes false or misleading information on this form or who omits material or information requested on the form may be subject to criminal sanctions (including fines and imprisonment) and/or civil sanctions (including civil penalties).

LASER FOCUS WORLD PRESENTS

BioOptics WORLD

Advances in lasers, optics, and imaging for the life sciences

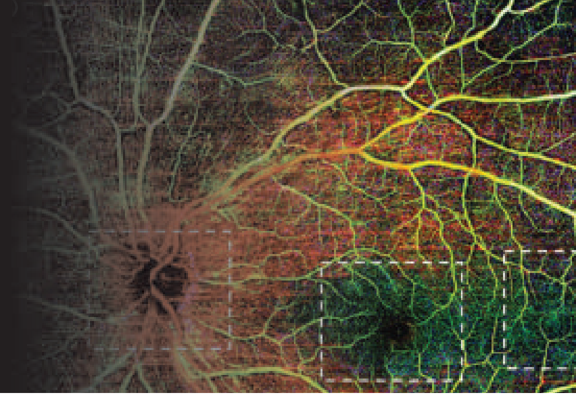

Optics profile up among neuroscientists

Barbara Gefvert
Editor in Chief
barbarag@pennwell.com

While the technology behind amazing advances in neuroscience is still often hard to discern in the conference at the Society for Neuroscience (SfN) annual meeting, two things have recently helped bring it out of the shadows: the U.S.'s Brain Research through Advancing Innovative Neurotechnologies (BRAIN) Initiative and a trend toward interdisciplinary research.

At the 2015 event (October 17-21)—which attracted approximately 30,000—optogenetics was a star as the focus of nearly 30 dedicated conference sessions and even an SfN-sponsored an Optogenetics Social. (Optogenetics was mentioned as well in sessions dedicated to other topics.) Optical imaging was another hot topic, as several sessions specifically discussed approaches such as two-photon and light-sheet microscopy (and others discussed optical imaging-enabled discoveries), and super-resolution pioneer and Nobel Laureate Stefan Hell was one of seven luminaries to deliver Special Lectures.

online@biopticsworld.com

Startup to provide access to low-cost super-resolution microscopy

A new startup is working to introduce imaging reagents that provide super-resolution microscopy capabilities on standard single-molecule microscopes. **http://bit.ly/1LX43pz**

Protein-based sensor detects viral infection, can kill cancer cells

A modular system of proteins can detect a particular DNA sequence in a cell and then trigger a specific response, such as cell death. **http://bit.ly/1LwVMap**

IR thermography can detect joint inflammation, helping to improve work ergonomics

A study has found that infrared (IR) thermography can detect joint inflammation and, therefore, help improve work ergonomics. **http://bit.ly/1GDr0h5**

* Daily news * New products * Financial information * More features * Webcasts * Videos * eNewsletters * Blog

Neuro15 exhibitors meet exacting demands: Part 1

Increasingly, neuroscientists are working with researchers in disciplines such as chemistry and physics. This trend has been noticed by exhibitors at the Society for Neuroscience (SfN) annual meeting (October 17-21, 2015; Chicago, IL), and was in evidence throughout the conference program (see figure). Perhaps such collaboration is why the field of neuroscience seems better able to appreciate the capabilities of technology. For sure, exhibitors at Neuroscience dished up plenty to entice them.

Many developers have innovated to ease the use of sophisticated tech. For instance, durable-equipment developer Sutter Instrument has paired with high-performance filter developer Semrock to offer filter changers specially designed for wavelength selection over a wide spectral range to any given nanometer value. Now, with the release of Semrock's VersaChrome Edge filter technology, which allows selection of bandwidth as well as center wavelength (and blocking outside the passband with an additional filter), Sutter has released the VF-1 Edge system to ease selection of both the long and short ends of the bandpass via the instrument or device such as a computer. Also new from Sutter is its first major new product line in two decades: a suite of electrophysiology recording hardware and software (Integrated Patch Amplifier) to enable efficient, low-noise, whole-cell recordings.

Neuroscience 2015 featured rotating poster presentations in the exhibit hall. *(Courtesy of Coherent)*

Smile for the camera innovations

Speaking of low noise, Photometrics demonstrated how onboard software in its Prime sCMOS camera can improve outcomes: Its PrimeEnhance feature promises to reduce active shot noise by 300–500%, while PrimeLocate automatically detects and transfers regions of interest, and easy cropping reduces file sizes.

And Hamamatsu upped the imaging ante with its ORCA-Flash 4.0 V2 sCMOS, promising not only improved read noise, but also quantum efficiency (QE) up to 82% to detect very faint signal and reduce exposure times. Other enhancements include enhanced frame rate (100 frames/s max at full resolution) and dynamic range. To help you gauge the actual QE that you will achieve (the 82% is at about 600 nm wavelength), the company gave away slide rules that show the camera's photon output using grey levels or analog-to-digital units (the measure that your imaging software uses to report intensity) in any region of an image.

Advanced spatial light modulators

While the average neuroscientist may not have known that spatial light modulator (SLMs) can have dramatic impact on his/her experiments, a few exhibitors demonstrated just that. Boulder Nonlinear Systems (BNS) showed how next-generation SLMs are helping to drive scientific advances. The company displayed PocketScope, a portable single-photon SLM microscope able to image or photostimulate different regions of a sample simultaneously, with 3D precision and at high frame rates. BNS is preparing the instrument, developed in the lab of Columbia University neuroscience pioneer Rafael Yuste, for commercial release. Future SLM development promises more exciting applications.

Meadowlark Optics, a development partner of BNS, also showed how high-speed SLMs increase the number of 3D neuronal ensembles able to be excited simultaneously. And Phi-Optics promoted Spatial Light Interference Microsopy (SLIM) as an add-on to all major brands of optical microscopes for quantitative cell imaging.

ASI drew attention with an impressive display of its dual inverted selective plane illumination microscopy (diSPIM), which offers light-sheet excitation and emission from both the right and left. And Mad City Labs showed off its Kohler Illumination Tower, providing an extra-long working distance (>30 mm!) for use with live-cell chambers. Prior Scientific displayed a precision-control setup that included a super compact 3-axis manipulator from Sensapex.

Optogenetics

Among the many companies exhibiting optogenetics offering was Mightex, which showed its Optical Activation, Stimulation and Imaging System (OASIS) for *in vivo* and *in vitro* research, and its new optogenetics starter kits—turnkey solutions for ChR2 stimulation offering super-high output power (up to 7.2 mW with a 200 µm fiber) and ultra-low power variation (<2%) during rotation.

Coherent discussed optogenetics research based on multiphoton excitation principles for *in vivo* work: Its Chameleon and Fidelity products support standard imaging with fluorescent proteins, optogenetic activation, and monitoring of neuron activity using genetically encoded Ca^{+} indicators.

For Part 2 of our Neuroscience coverage, please visit www.biopticsworld.com/worldview-blog.html.—*Barbara Gefvert*

OCT angiography: A new approach with 'gold standard' capabilities and more

CHIEH-LI CHEN, QINGIN ZHANG, ANQI ZHANG, and **RUIKANG K. WANG**

Optical coherence tomography angiography (OCTA) is a new imaging technique enabling the visualization of microcirculation in vivo *with high resolution. Aided by data processing, it promises usefulness in the clinical monitoring and therapeutic treatment of various retinal pathologies.*

Since its first demonstration in a biomedical application in 1991, optical coherence tomography (OCT)[1] has become an indispensable tool in routine clinical practice for anatomical (structural) imaging and therapeutic monitoring—especially in ophthalmology.[2] Recent advances in light sources and detection techniques have enabled OCT to advance and extend dramatically, to the point of enabling functional imaging. Now, a newly developed technique, OCT angiography (OCTA), is allowing the functional visualization of blood vessel networks in the eye. Inheriting all the advantages of OCT—such as the ability to generate cross-sectional images of biological structures in three dimensions (3D) with high sectioning resolution (1–10 μm)[1]—OCTA can provide functional information about the dynamics of blood vessel networks *in vivo*, without exogenous intravenous dye-injection.[3]

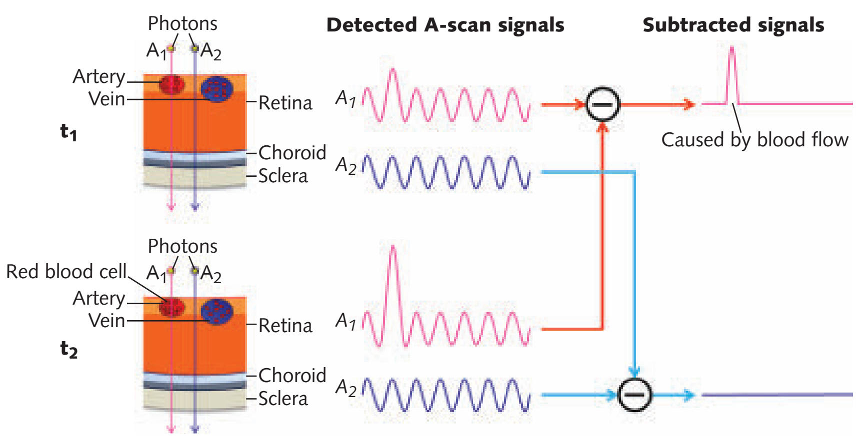

FIGURE 1. How OCTA works: As moving blood cells pass through vessels, they generate changes in OCT signals. Based on this concept, a blood flow signal can be extracted by subtracting the OCT signals from the same location but at different time points (red path). The OCT signals will be different at these locations, while OCT signals from surrounding retinal tissues will remain steady (blue path).

The concept of OCTA is to use changes in OCT signals caused by moving particles (for example, red blood cells) as the contrast mechanism for imaging functional flows. To give a brief description of its operation, imagine two OCT signals—one backscattered from static structural tissue and the other backscattered from moving particles (such as red blood cells) in vessels. The signal from structural tissue remains steady, while the signal from flowing blood changes over time. To differentiate the moving particles from static tissue, repeated cross-sectional scans (B-scans) are performed at the same location. Temporal changes of the OCT signal in adjacent scans caused by moving particles generate the angiographic contrast and allow visualization of the microvasculature in OCTA (see Fig. 1).

Compared to the 'gold standards'

Compared with other functional imaging techniques, a key advantage of OCTA is that it is non-contact and noninvasive. Fluorescein angiography (FA) and indocyanine green angiography (ICGA) are the current "gold standards" for diagnosing vasculature abnormality in clinical practice. However, the invasiveness of the dye injection combined with possible adverse reactions, such as nausea or anaphylactic response in some rare cases, makes them unsuitable for widespread ophthalmic screening applications and for frequent monitoring. By contrast, OCTA enables visualization of ocular vessels by detecting the differences between cross-sectional scans without intravenous contrast agent or dye injection. Thus, OCTA may be a better alternative in longitudinal disease monitoring—especially for progressive diseases showing high correlation with vessel dysfunction (such as age-related macular degeneration, diabetic retinopathy, and glaucoma) that may benefit from early intervention or treatment.

In addition, OCTA is more time-efficient. It takes 10–30 min. for FA and ICGA imaging, while only a few seconds for OCTA to complete one volumetric scan. Thirdly, OCTA provides visualization of *in vivo* vasculature in 3D with microscopic resolution. Though FA and ICGA provide images with a wide field of view, the images are two-dimensional and therefore cannot provide depth information of vasculatures. As a depth-resolved imaging technique, OCTA allows visualization of vessel networks at various depths. These vessel networks can be segmented into specific retinal and choroidal layers to determine where the disease originates. Furthermore, the high axial and transversal resolution of OCT systems enable detection of capillaries and visualization of microcirculation.

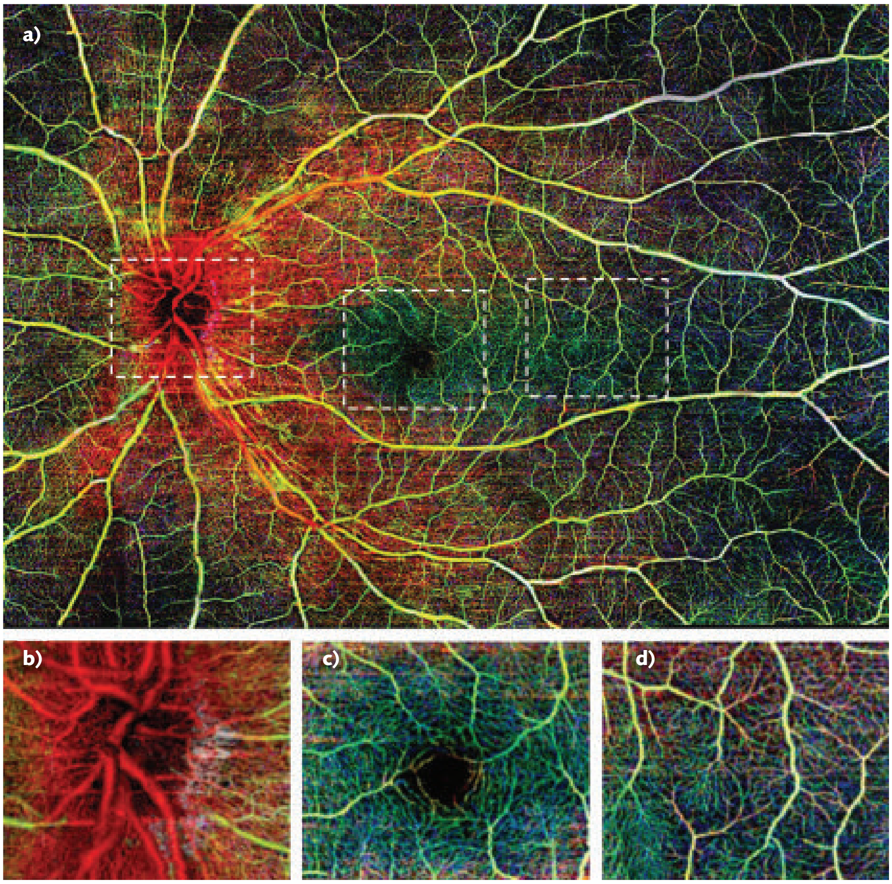

FIGURE 2. (a) Wide-field imagery of the retinal vasculature of a healthy young woman was obtained by montage scanning protocol of optical microangiography (OMAG). Data are coded with different colors for each of three layers: red represents NFL, green is SRL, and blue is DRL. (b-d) exhibit the magnified angiograms located in the white dashed boxes in (a), which better illustrates the high sensitivity of OMAG. OMAG angiograms corresponding to the white dashed boxes in (b) are shown in (b-d), magnified to demonstrate the detail of blood vessels in different regions, including (b) optic nerve head, (c) fovea, and (d) temporal region. The size of (a) is 12 × 16 mm^2, while the size of (b-d) is 2.0 × 2.4 mm^2. *(Adapted from Q. Zhang et al. with permission[5])*

Data processing

Increased interest in OCTA has spawned the development of numerous data-processing algorithms. To classify them, the basic concept of OCT signal should be introduced: Raw data in Fourier-domain OCT consists of spectral interferograms captured by the detector. Fourier transformation is applied to the raw data to obtain depth-resolved signals. After Fourier transformation, the OCT signal contains both magnitude and phase information, which have both been explored, individually and together, to develop angiographic methods for the purpose of contrasting blood flow within living tissue. Therefore, the various OCTA approaches can be roughly categorized, but not limited into three groups:

1. OCTA based on both the magnitude and phase of OCT signal (complex signal);
2. OCTA based on the magnitude of OCT signal; and
3. OCTA based on the phase of OCT signal.

Optical microangiography (OMAG)-based OCTA is one of the leading techniques, employing the change of complex signal (both intensity and phase changes) to contrast blood flow information. OMAG has been shown to have ultra-high sensitivity to the

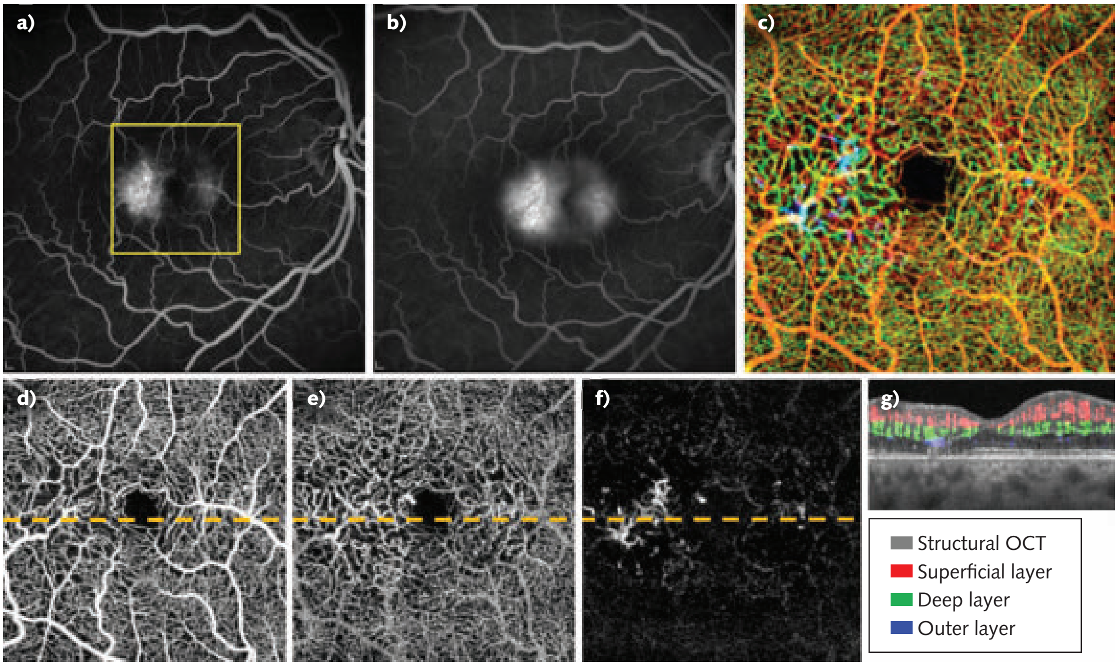

FIGURE 3. Optical microangiography (OMAG) and fluorescein angiography (FA) images illustrate intermediate, non-proliferative MacTel2. (a) An early-phase FA image shows hyperfluorescence in the temporal juxtafoveal region, while (b) a late-phase FA image shows increased and diffuse hyperfluorescence and leakage. (c) A composite *en face* color-coded OMAG demonstrates abnormalities that correspond well to the microvascular abnormalities seen in the early-stage FA image. (d) An *en face* OMAG image from the superficial retinal layer shows microvascular abnormalities in the juxtafoveal region, while (e) an *en face* OMAG from the deep retinal layer shows the telangiectatic and dilated vessels in the middle retinal layers. (f) And an *en face* OMAG image from the outer retinal layer shows subtle microvascular alterations in the outer retinal layers. (g) Finally, a horizontal central B-scan shows the microvascular flow in different colors corresponding to the different segmented layers of the retina. Thinning of the retina and disruption of the inner segment/outer segment/ellipsoid boundary are observed temporally in an area of abnormal retinal flow (green and blue). The size of (c-f) is 3 × 3 mm^2.

microcirculation.[3,4] OMAG algorithm has been implemented both in a 100 kHz 1 µm swept-source OCT (SS-OCT) prototype and a CIRRUS HD-OCT 5000 system (both by Carl Zeiss Meditec, Dublin, CA) to conduct clinical evaluations. The CIRRUS HD-OCT 5000 system with AngioPlex OCT angiography, which uses the OMAG algorithm, operates at a central wavelength of 840 nm and a speed of 68,000 A-scans/s, and is the first and only OCTA technology to have received clearance from the U.S. Food and Drug Administration (FDA).

A key feature of CIRRUS HD-OCT 5000 is an active eye-tracking mechanism able to trace and compensate eye motion in real time, and provide motion-artifact-free angiographic images.[5] It allows wide-field imaging (>10 × 10 mm^2) without sacrificing resolution (that is, the same spatial sampling rate as in the typical 3 × 3 mm^2 field of view), which increases effectiveness of OMAG for clinical practice.

Application in human studies

OMAG has been widely applied in human eye diseases to provide more information about retinal and choroidal circulation. Several studies were conducted using both a CIRRUS HD-OCT 5000 prototype with active motion-tracking capability and a prototype 1 µm SS-OCT system (with center wavelength at 1060 nm).[6] For the CIRRUS HD-OCT 5000 prototype, a montage scan protocol enabled by motion-tracking capability centered at the fovea was used to acquire volumetric datasets with 10% area overlap between adjacent dataset for later montaging.[5] For the SS-OCT prototype, a single volumetric scan was acquired from the subjects. Four consecutive B-scans along the transverse direction were acquired at each fixed longitudinal location before the scanning probe proceeded to the next location along the longitudinal direction. A sampling interval of approximately 9.8 µm was achieved in both directions to guarantee high-resolution angiograms. The time difference between two adjacent B-scans was approximately 3.6 ms. A single-volume dataset can be acquired in ~4 s.

For later data processing, OMAG uses a complex value differentiation algorithm to extract *in vivo* blood flow information. Retinal layer segmentation can be performed to isolate specific retinal and choroidal layers. Typically, three main retinal layers are segmented: a superficial retinal layer (SRL) that includes the ganglion cell layer and the inner plexiform layer; a deep retinal layer (DRL) that includes the inner nuclear layer and the outer plexiform layer; and an outer retinal layer (ORL) that includes the outer nuclear layer and the external limiting membrane. The segmentation can also be used to separate the choroid into choriocapillaris and deep choroid layers. The segmented layers can be adjusted to provide a better presentation of the vasculature for various ocular pathologies. Finally, the *en face* vascular images are created by using a maximum (or average) projection method within the layer of interest and then used to correlate the findings between OMAG and conventional methods (FA/ICGA images).

Figure 2 shows a wide-field OMAG angiogram enabled by real-time motion-tracking of normal retinal vasculature, captured with CIRRUS HD-OCT 5000 system.[5] Three layers were segmented to give a better demonstration according to depth. Figure 2a shows the results of the wide-field OMAG angiogram (~12 × 16 mm^2), including nerve fiber layer (NFL), SRL, and DRL.

Macular telangiectasia type 2 (MacTel2) is a bilateral retinal disease that presents with asymmetric severity during the fifth to seventh decades of life and affects the juxtafoveal region of the macula. The pathogenesis of the disease is unknown and currently, there is no proven treatment. Until recently, OCT has been unable to provide information on the functional microvasculature in the central macula and unable to provide information about blood flow involvement in this disease. But the results provided by OMAG hold promise for the evaluation of patients with MacTel2 and other diseases affecting the microvasculature (see Fig. 3).[6] One 3D dataset processed with OMAG takes <4 s to acquire and has none of the potential adverse events associated with FA. Further studies are needed to quantitate vascular caliber, density, and blood flow in the central macula and identify whether changes in these parameters predict disease progression or response to future therapeutic interventions.

The vascular *en face* images from OMAG are comparable to the current gold standard, and further provide angiograms with high resolution and the depth information of pathologies. Though currently there is no standard way of evaluating OCT angiography and new clinical endpoints must be established with larger studies, OMAG has demonstrated its potential as being a useful and powerful tool for diagnosis, detection, and monitoring of various ocular pathologies. ◂

REFERENCES

1. D. Huang et al., *Science*, 254, 1178–1181 (1991).
2. C. R. Baumal, *Curr. Opin. Ophthalmol.*, 10, 182–188 (1999).
3. R. K. Wang, *IEEE J. Sel. Top. Quantum Electron.*, 16, 545–554 (2010).
4. R. K. Wang, L. An, P. Francis, and D. Wilson, *Opt. Lett.*, 35, 9, 1467–1469 (2010).
5. Q. Zhang et al., *J. Biomed. Opt.*, 20, 066008 (2015).
6. M. R. Thorell et al., *Ophthalmic Surg. Lasers Imaging Retina*, 45, 369–380 (2014).

Chieh-Li Chen, *Ph.D.*, **Qinqin Zhang**, *Ph.D., and* **Anqi Zhang**, *Ph.D., are senior research fellows, and* **Ruikang K. Wang**, *Ph.D., is a professor, all in the Bioengineering & Ophthalmology Department at the University of Washington, Seattle, WA; e-mail: wangrk@uw.edu; http://depts.washington.edu/wangast.*

Advanced surgery: NIR fluorescence guidance arrives

DAVID J. BURRINGTON

To resect an entire tumor while avoiding healthy tissue, surgeons must be able to see relevant details invisible to the naked eye. Optical imaging with targeted contrast agents have demonstrated efficacy in clinical trials to enable better visualization for better outcomes—now, refinement and commercialization efforts aim to eventually bring them to the surgical suite.

As much as surgeons might wish for "x-ray vision," the reality is that the human brain and eyes are restricted to perceiving a very narrow sliver of the electromagnetic spectrum called visible light, which spans roughly 400–700 nm. Because of this, many objects able to provide helpful information during surgery are invisible to the unaided eye. Even a thin layer of blood or tissue, just hundreds of microns in depth, can completely obscure a surgeon's vision.

Some objects, such as malignant tumors, need to be resected fully for cure, but finding small collections of cells in the context of normal tissue remains a significant challenge. For example, even today, between 30 and 40% of all breast cancers are left behind during the initial surgery,[1] resulting in the need for either repeat surgery and/or adjuvant therapy. Conversely, objects such as blood vessels, nerves, and bodily lumens need to be avoided, as damage to them during surgery results in high morbidity.[2,3]

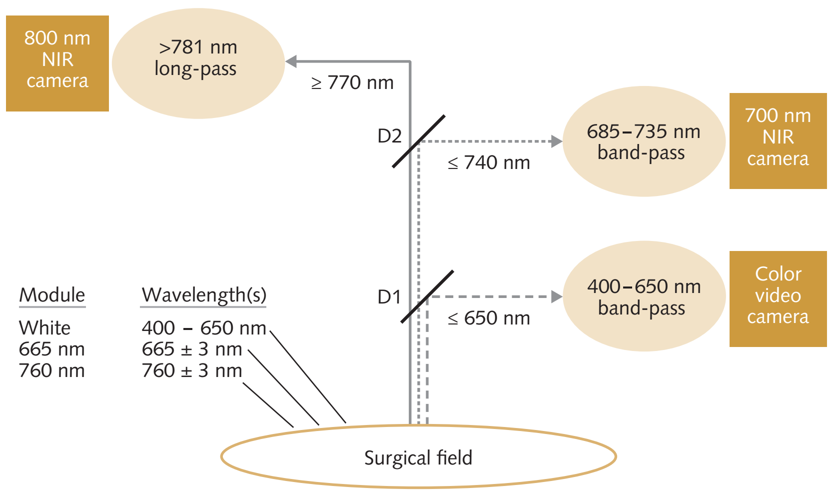

FIGURE 1. All FLARE imaging systems permit simultaneous, real-time acquisition of color video and provide two independent channels of NIR fluorescence without moving parts.

Expanding the surgeon's view

There is a constant tension in modern oncologic surgery between the diametrically opposed goals of maximizing both tissue resection and tissue avoidance:

- Take out too much tissue and the cancer might be cured, but complications from the surgery create a lifetime of suffering caused by a combination of physical and/or emotional pain and follow-up care costs; or
- Remove too little tissue and the cancer may spread and kill the patient.

Solving this conundrum is the reason John V. Frangioni, M.D., Ph.D., developed FLuorescence-Assisted Resection and Exploration (FLARE) technology[4] while he was a full-time Professor of

Medicine and Professor of Radiology at Harvard Medical School (Boston, MA). FLARE is an optical imaging platform that combines state-of-the-art engineering and chemistry to solve important biomedical problems. Rather than being constrained to visible light, FLARE expands the spectrum of the surgeon's vision up to 900 nm. In fact, this critical region from 700 to 900 nm, termed the near infrared (NIR) "window," is where the absorbance curves for biomolecules that constitute living tissue all reach local minima.

But absorbance is not the only reason the NIR window is so important. Wavelength-dependent scatter and autofluorescence are also much lower in the NIR compared to the visible. The final key property of NIR light is invisibility itself. Because the surgeon can perceive NIR light only as a faint red glow without assignment of wavelength or intensity, light used for both excitation and fluorescent emission can be made invisible. Being invisible means no change to the look of the surgical field—so surgeons can operate as they normally do.

Because of the invisibility of NIR light, two innovations are needed to make the technology work: an imaging system that generates and "sees" otherwise invisible NIR fluorescent light, and targeted contrast agents having the desired NIR emission wavelength. FLARE accomplishes the former using the optical system shown diagrammatically in Fig. 1 (which is the subject of issued patents in the U.S. and Europe). NIR-depleted white light and two independent channels of NIR excitation light illuminate the field-of-view (FOV), while three independent sensors image the FOV simultaneously and in real time. The table summarizes the system's optical characteristics.

Every FLARE imaging system is able to display four independent video streams, including a color video image of the surgical field (i.e., what the surgeon is accustomed to seeing), two independent channels of NIR fluorescence emission (one centered at 700 nm and one at 800 nm), and a merge of all three (see Fig. 2). The merged image permits a range of options, from simple overlay of images to real-time ratiometric imaging—which unlocks the potential of next-generation contrast agents that respond to environmental stimuli.

In fact, FLARE's dual-NIR channel capability solves that longstanding problem of opposing goals: One NIR channel can be dedicated to tissue resection and highlighted using one color in the merged image, while the other independent channel can be dedicated to tissue avoidance and highlighted with a different color—all in real time.

Optical characteristics of FLARE

Aberration correction	400–900 nm
Parfocality	400–900 nm
Transmission	≥ 90% (400–850 nm)
Distortion	< 1%
Vignetting	< 5%
Telecentricity	< 5°
Working distance	12–18 in. (variable)
FOV	0.9 cm diameter at 12 in. WD to 25 cm diameter at 18 in. WD
Zoom	15X (motorized)
Focus	Motorized
System resolution	70 μm (max. zoom) to 700 μm (min. zoom) at 15 in. WD

Wavelength with targeting

Developing NIR fluorescence contrast agents that have the desired emission wavelength and desired targeting is a daunting task. FLARE accomplishes this in two ways. The first is the traditional approach of covalently conjugating a targeting ligand to a NIR fluorophore. Unlike conventional NIR fluorophores, however, FLARE uses a novel and proprietary class of "zwitterionic" NIR fluorophores that have geometrically balanced, electrically neutral polyionicity.[5-7] These physicochemical properties result in extremely low non-specific binding and uptake *in vitro* and *in vivo*, and thus extremely low non-specific background. Zwitterionic NIR fluorophores are

Dream in *color* this fall

From only
5.995€
Delivery time: 1 week

Quick fantasy

The SuperK COMPACT is the most affordable way to true single mode white light laser performance. Use the 450-2400 nm output as is or convert it to a broadband tunable laser with one of our computer controlled filters.

From only
29.995€
Delivery time: 2 weeks

Day dream

Recognized as the best on the market, the SuperK EXTREME lasers gives you all you can dream of with 260-2400 nm coverage and a large accessory range. Get the special campaign model for only 29.995€ and a quick upgrade later if you need more power.

-20%
On new systems
-40%
On demo lasers

Lucid dreaming

When only the best spectral coverage and beam quality can get you there! Get any of our market leading SuperK EXTREME models with 20% discount or one of our many demo lasers with 40% discount and get closer to your dream.

+1 732 972 9937 / +49 (221) 99511-0 / +45 4348 3900
www.nktphotonics.com/dream
sales@nktphotonics.com

SuperK customers
Leica MICROSYSTEMS
HORIBA Scientific

NKT Photonics
the power of light

available at 700 nm (e.g., ZW700-1 Forte and its derivatives) and 800 nm (ZW800-1 and its derivatives; see Fig. 3), as well as in a variety of conjugation and linker chemistries. The Forte line of zwitterionic NIR fluorophores also provides extraordinarily high (>90% at 24 h) stability in warm serum.

The second approach to targeted NIR fluorophores is called "structure-inherent targeting."[8] For this class of FLARE molecules, the targeted moieties are grafted onto the resonant backbone of a NIR fluorophore such that targeting and fluorescence is accomplished as a single molecular entity. To date, peer-reviewed literature from Dr. Frangioni's company, Curadel, has addressed structure-inherent targeting to cartilage, bone,

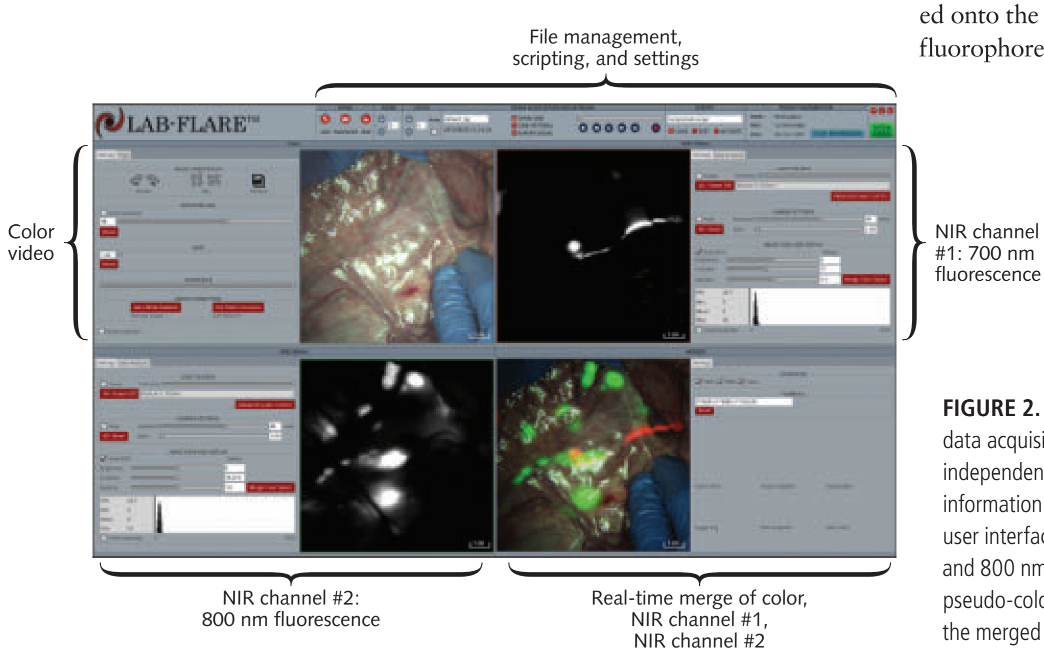

FIGURE 2. FLARE provides real-time data acquisition and data analysis of four independent video streams, and presents this information through a streamlined graphical user interface. For this example, the 700 and 800 nm NIR fluorescence channels are pseudo-colored green and red (respectively) in the merged image.

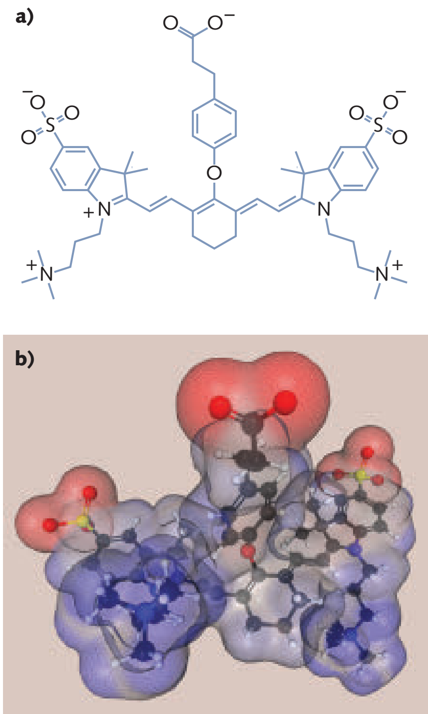

FIGURE 3. The carboxylic acid form of zwitterionic NIR fluorophore ZW800-1 (CAS #1239619-02-3) in two dimensions (a) and 3D with positive (red) and negative (blue) charges geometrically and electrically balanced over the molecular surface (b).

parathyroid glands, thyroid glands, and adrenal glands, to name a few applications.

Availability

Curadel is currently refining and commercializing FLARE technology. Because of the future clinical potential of the technology, and to avoid any possible confusion by consumers, the company conducts its development and commercialization activities through two separate companies, with separate product offerings and labeling.

Curadel ResVet Imaging (CRV) already manufactures and sells NIR fluorescence imaging systems and contrast agents under the Lab-FLARE brand for laboratory research (not for diagnostic or therapeutic use), and will eventually offer products for veterinary applications under the Vet-FLARE brand. CRV launched its flagship open-space imaging system, the Lab-FLARE Model R1 (see Fig. 3) and its first 11 NIR fluorescent contrast agents at the 2015 World Molecular Imaging Congress (September 2, 2015; Honolulu, HI). It will soon launch its first minimally invasive imaging system, the RF1, at the European Molecular Imaging Society

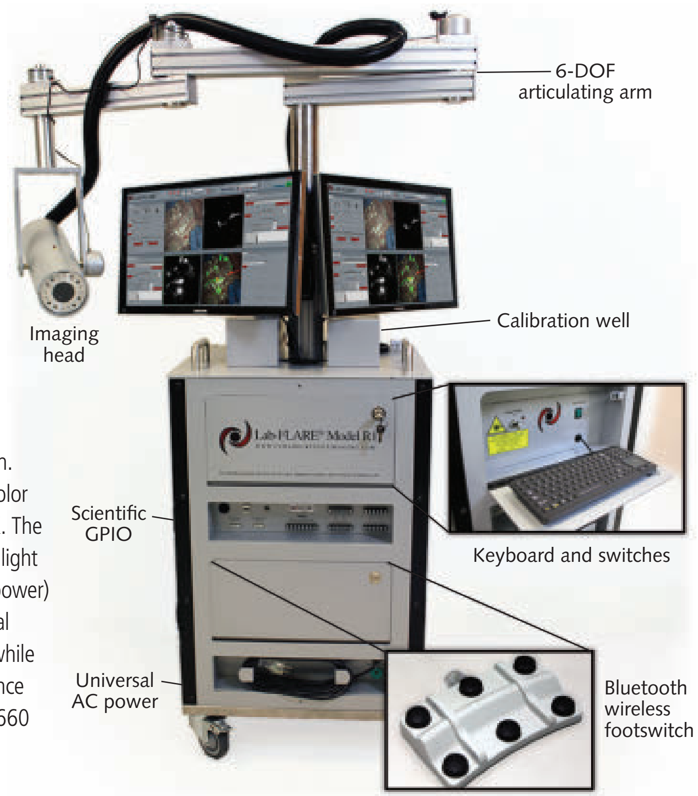

FIGURE 4. The fully mobile, 3R guideline-compliant Lab-FLARE Model R1 Open Space Imaging System for Laboratory Research features a long-reach articulated arm that positions the imaging head in 3D space. The white light source provides illuminance of ≥ 20,000 lux at 15 in. WD; ≥ 85 CRI; and a color temperature of 4500 K. The laser source generates light at 660 nm (4 W total power) and 760 nm (10 W total power) wavelengths, while the NIR excitation fluence rate is ≥ 4 mW/cm^2 at 660 nm and ≥ 10 mW/cm^2 at 760 nm.

meeting (March 2016). Over the coming year, CRV will expand its first 11 contrast agents for laboratory research to over 40 agents capable of a variety of NIR fluorescence imaging tasks *in vitro* and *in vivo*, and it will continue its efforts aimed at bringing the Vet-FLARE line of imaging systems for veterinary surgery to market.

The ultimate goal of FLARE is to empower surgeons to perform better surgery. All FDA- and EMA-regulated products for human use are being developed by Curadel's second subsidiary, Curadel Surgical Innovations (CSI). CSI plans to offer imaging systems and contrast agents under the Med-FLARE brand. At present, however, none of CSI's products have been approved by regulatory bodies, but efforts are currently underway to obtain marketing authorization.

For Dr. Frangioni, this has been a 15-year road that has been neither straight nor flat: "When we first started, we were told that it was a waste of time to develop the FLARE imaging system because there weren't enough contrast agents to use on it. So, once we developed the imaging system, we turned our attention to contrast agents and invented both zwitterionic NIR fluorophores and structure-inherent targeting. Now we're told that there is no market for optical imaging, and bringing contrast agents to regulatory approval will be too difficult and expensive. Well, OK, but after proof of principle of the technology in clinical trials involving over 500 patients worldwide, and with all studies published in peer-reviewed journals, naysayers are running out of excuses."

The promise of NIR fluorescence guidance are procedures that are faster, better, and cheaper. Only time will tell if these goals are met, but at least for the time being, NIR fluorescence is finally seeing the light of day.

ACKNOWLEDGEMENTS

FLARE, Lab-FLARE, Vet-FLARE, Curadel, Curadel Surgical Innovations, and Curadel ResVet Imaging are registered trademarks of Curadel, LLC.

REFERENCES

1. R. G. Pleijhuis et al., *Ann. Surg. Oncol.*, 16, 10, 2717–2730 (Oct. 2009).
2. M. D. Michaelson et al., *CA Cancer J. Clin.*, 58, 4, 196–213 (Aug. 2008).
3. W. A. Macrae, *Br. J. Anaesth.*, 101, 1, 77–86 (Jul. 2008).
4. S. Gioux, H. S. Choi, and J. V. Frangioni, *Mol. Imaging*, 9, 5, 237–255 (Oct. 2010).
5. H. Hyun et al., *Mol. Imaging Biol.*, doi:10.1007/s11307-015-0870-4 (Jun. 18, 2015).
6. H. S. Choi et al., *Nat. Biotechnol.*, 31, 148–153 (Feb. 2013).
7. H. S. Choi et al., *Angew. Chem. Int. Ed.*, 50, 28, 6258–6263 (Jul. 4, 2011).
8. H. Hyun et al., *Nat. Med.*, 21, 2, 192–197 (Feb. 2015).

David J. Burrington, *M.Ed., is quality system manager with the Translational Cancer Imaging Facility at Beth Israel Deaconness Medical Center (Boston, MA); e-mail: centerformolecularimaging@bidmc.harvard.edu; www.centerformolecularimaging.org/tcif.*

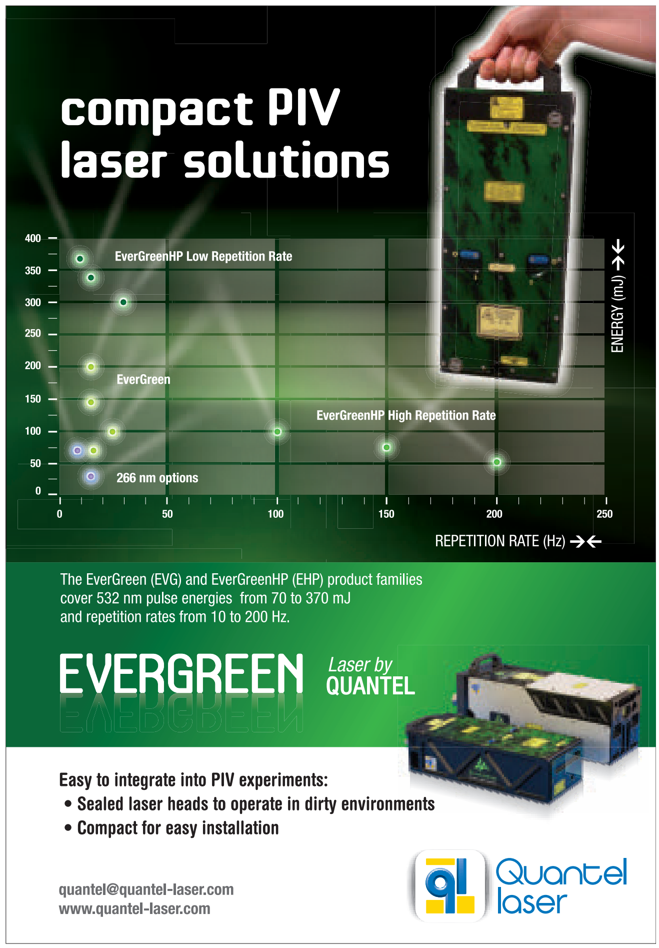

New products

Would you like to be included? Please send your product description with high-resolution digital image to: lfwnewproducts@pennwell.com

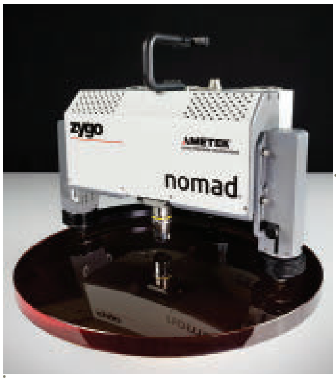

Portable optical profiler

The Nomad portable optical profiler enables 3D noncontact metrology on samples that were previously impossible or impractical to measure. It uses the company's Coherence Scanning Interferometry (CSI) and SureScan technologies for vibration robustness, its range of parfocal objectives from 1.4 to 100x magnification, and its Mx software for enhanced data visualization and quantification of step heights, texture, and volumetric features.

Zygo
Middlefield, CT
www.zygo.com

Tunable optical filter

The OSG100 is an ultrahigh isolation-programmable optical filter that enables the creation of arbitrary filter shapes, with isolation exceeding 60 dB for testing and experimentation. The filter allows tuning of frequency, passband, and power level in spectrum slices of 12.5 GHz centered on the ITU grid, and is controlled using an intuitive but powerful graphical user interface for generating arbitrary filter shapes.

InLC Technology
Gwangju, Korea
www.inlct.com

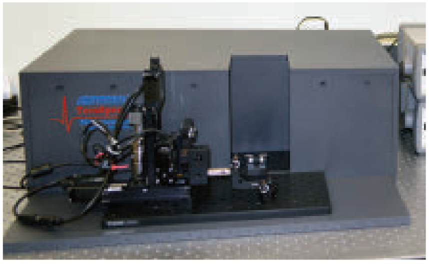

Terahertz time-domain spectrometer

A terahertz time-domain spectrometer integrates sub-surface scanning and 3D imaging functionalities. Featuring a proprietary dendrimer dipole excitation (DDE) continuous-wave (CW) terahertz source, the spectrometer has use in molecular investigations.

ARPhotonics
Harrisburg, PA
http://arphotonics.net

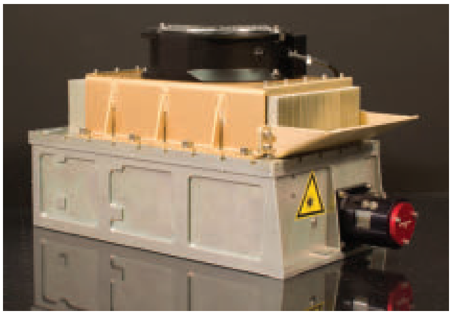

DPSS laser system for lidar

The HLS DPSS laser system is designed for airborne lidar data collection. It combines a proprietary short-pulse laser with Yb-doped fiber and Nd:YVO_4 amplifiers for up to 2 mJ pulse energies at 532 nm, with M^2<1.5 TEM_{00} beam quality at 10 kHz and above. It produces a stable temporal pulse shape of <1.5 ns pulse width at <100 ps jitter.

CEO Laser
St. Charles, MO
http://cuttingedgeoptronics.com

3X zoom lens

The MicroMate 3X Zoom lens system images onto a 4/3 in. sensor and retains the same pixel resolution across the entire field. It images onto sensors with diagonals up to 22.5 mm with no vignetting. With a large field of view and fixed pupil position, the lens offers a fixed NA over the entire zoom range.

Navitar
Rochester, NY
www.navitar.com

High-speed camera

The FASTCAM Mini AX100 high-speed camera offers light sensitivity of ISO 40,000 for monochrome and ISO 16,000 for color. It provides 1024 × 1024 pixel resolution at up to 4000 frames/s and 540,000 frames/s at reduced resolution. Weighing 1.6 kg, the one-piece camera has 4, 8, and/or 16 GB memory options.

Photron
San Diego, CA
www.photron.com

UV-enhanced silver mirror coatings

The #4000 and #4100 silver-based UV-enhanced mirror coatings overcome the inherent reflectivity limitation of silver below 450 nm and deliver broadband reflectivity >98% from 400 nm to the mid-IR wavelength range. These coatings are suited for military optics, telescopes, spaceflight hardware, analytical instruments, and ultrafast Ti:sapphire lasers.

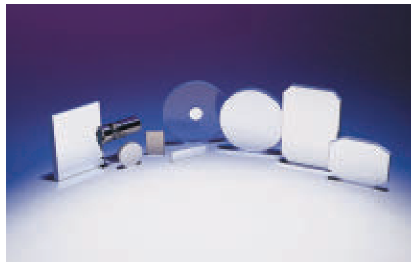

Acton Optics
Acton, MA
www.actonoptics.com

Servo amplifier

The QD-2000 servo amplifier is a class-0 servo amplifier that features a single output power amp with up to 30 W output power, dual push/pull output, and analog input (+10). Available in single-axis and open-frame configurations, it has over/under voltage protections for laser systems and scanning mirrors.

Nutfield Technology
Hudson, NH
www.nutfieldtech.com

Scientific OPO platform

A scientific optical parametric oscillator (OPO) platform for fully automated, synchronously pumped OPOs features redeveloped control and software architecture, automated tuning and control via a PC, and extensive log files and remote access. It is available for the Levante IRNSPfs, Levante EmeraldNSP, and Ti:sapphire pumped OPONSP-X.

APE
Berlin, Germany
www.ape-berlin.de

Optical design software

TracePro v7.7 optical design software features a Candela plot viewer

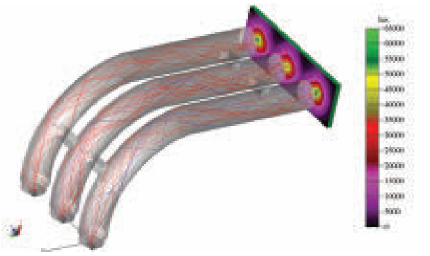

and an automotive lighting toolkit. Photorealistic rendering capability has been improved for 3D visualization of the output performance of luminaire or light pipe design. Users may now choose whether to use simulation or analysis modes for ray tracing.

Lambda Research
Littleton, MA
www.lambdares.com

Imaging spectrographs

The MS260i 1/4 m imaging spectrograph is designed for applications in the 200–1350 nm spectral range. Each pre-configured model comes with a

high-line-density ruled triple grating and input slit. Available options include slit type, number of output ports, and communication interfaces.

Oriel Instruments
Irvine, CA
www.newport.com/MS260i

Miniature positioning system

The DK-M3-RS-U-1M-20 piezoelectric mirror positioning system has a galvo-scanner form factor and measures 12 mm in diameter, including the embedded closed-loop controller. The

smart stage rotates the pre-mounted aluminum-coated mirror ±20° at up to 1100°/s. Applications include medical lasers and imaging systems, industrial measurement and spectroscopy instruments, and laser printing and engraving.

New Scale Technologies
Victor, NY
www.newscaletech.com

SLM picosecond laser

The Pico series laser delivers 10 W of TEM_{00} (M^2<1.3) at 1064 nm with 150 ps pulses at up to 300 kHz. The output is single longitudinal mode (SLM) with 10 pm linewidth. The laser requires 24 V DC input and is tap water-cooled. Applications include micromachining, ablation, scribing, lidar, nonlinear optics, and other industrial, medical, military, and R&D tasks.

RPMC Lasers
O'Fallon, MO
www.rpmclasers.com

UV-curable epoxy system

UV22 is a one-component, nanosilica-filled UV-curable epoxy system that

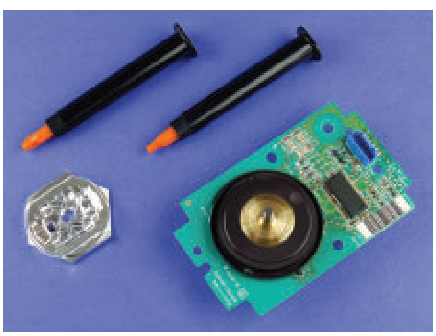

meets NASA low outgassing specifications. At 75°F, the system offers viscosity of 1000–8000 cps, tensile strength >7000 psi, abrasion resistance, optical clarity, and thermal stability up to 350°F. It cures quickly when exposed to a UV light source via a cationic reaction.
Master Bond
Hackensack, NJ
www.masterbond.com

Bidirectional IL/ RL test system

The OP940-OP725 bidirectional IL/RL test system has had new revisions to the insertion and return loss meter, allow-

ing direct control via USB link. Operators may obtain real-time IL/RL results or reflectance scans in either direction. The system can also be used as a 2 × 2 optical switch with the company's software, making any source unit bidirectional.

OptoTest
Camarillo, CA
www.optotest.com

High-speed video camera

The Hyper Vision HPV-X2 high-speed video camera features a FTCMOS burst image sensor that increases photosensitivity by six times more than previous models. It features high-speed recording at 10 million frames/s. It has use in observing phenomena, such as the interaction of cancer cells, the automotive fuel injection process, and the printer ink ejection process.
Shimadzu
Kyoto, Japan
www.ssi.shimadzu.com

Plasma profiling instrument

The Plasma Profiling time-of-flight mass spectrometer (PP-TOFMS) provides chemical composition as a function of depth of solid materials. It provides standard-free, instantaneous semi-

quantification analysis of a sample with an atomic concentration range spanning orders of magnitudes in a single measurement. It can analyze conductive and non-conductive materials from inorganic to hybrid.
Horiba Scientific
Edison, NJ
www.horiba.com/scientific

Adjustable rigid post mounts

The HZP Series adjustable rigid post mounts have use in electrophysiology applications. Compatible with upright and inverted microscopes and available in four different heights, they work with Sensapex zero-drift solid-state and other

common micromanipulators. They offer a 60° sliding dovetail for stable positioning, and are compatible with 1/4-20 and 6 mm optical breadboards.
Prior Scientific
Rockland, MA
www.prior.com

Light-shaping diffusers for simulation library

Proprietary Light Shaping Diffusers (LSDs) have been added to OPTIS's SPEOS optical modeling and simulation library. This adds simulations with light using holographic patterns imbedded on polycarbonate, acrylic, and polyester substrates. The diffusion ability allows engineers to design energy-efficient and low-profile subsystems with high uniformity.
Luminit
Torrance, CA
www.luminitco.com

Hyperspectral sensor systems

AisaKESTREL pushbroom hyperspectral sensor systems are designed for UAVs and other platforms of limited payload

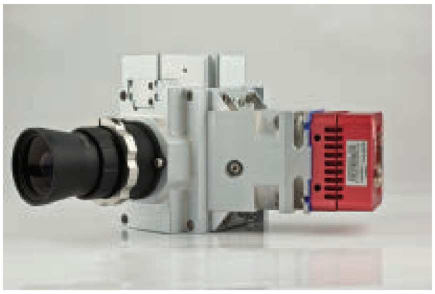

size. The 5 kg sensor detects vegetation, water, or soil attributes of minute spectral differences, providing radiometrically and spectrally stable data with high signal-to-noise ratio and spatial resolution of 2048 pixels. The AisaKESTREL10 is for 400–1000 nm and the AisaKESTREL16 for 600–1640 nm.
Specim
Oulu, Finland
www.specim.fi

X-Y stage

The KT210-EDLM X-Y Stage features an internal motor and controller. Measuring

50 × 210 mm, it offers travel of 100 × 100 mm and includes low-profile, direct-drive ironless linear motors. Suited for life science, semiconductor, fiber optics, and micromachining applications, accuracy is 13.6 μm with repeatability of 2.7 μm.

Steinmeyer
Burlington, MA
www.steinmeyer.com

Fiber laser

The Highlight FL series fiber laser delivers output powers to 4 kW. Using a modular architecture, OEM customers and system integrators may select turnkey systems or build custom fiber laser systems. Available at all power levels with various output delivery fiber options, they are optimized for cutting and welding metals and alloys.

Coherent
Santa Clara, CA
www.coherent.com

High-speed cameras

The Phantom v2512, v2012, v1612, and v1212 1 Mpixel ultra-high-speed cameras are now available with 72, 144, or 288 GB of memory. The cameras use 1 and 2 TB CineMag IV to quickly record data to a large amount of non-volatile storage. All models are equipped with 10 GB Ethernet and are able to transfer data at up to 500 MB/s on optimized systems.

Vision Research
Wayne, NJ
www.visionresearch.com

Tunable lasers

The TSL-550 tunable laser features mode-hop-free tuning with output power of 10 dBm and signal-to-noise ratio of 90 dB/0.1 nm. A unique cavity design is used to lower the optical ASE noise. The fully programmable laser is designed for precision optical testing in the 1260–1360/1500–1630 nm wavelength ranges.

Santec
Komaki, Japan
www.santec.com

Optical shaft measurement system

Designed to provide fully automatic measurement of smaller shafts and turned parts directly on the shop floor, the

MarShaft SCOPE 250 plus features a matrix camera with four million pixels. It measures parts up to 250 mm long and 40 mm in diameter with a maximum permissible error (MPE) of <1.5 μm + L/40 for diameter and <3 μm + L/125 for length.

Mahr Federal
Providence, RI
www.mahr.com

OTDR platform

A suite of optical time-domain reflectometry (OTDR) solutions for embedded network monitoring applications achieves instrumentation-level performance in a compact form factor. Designed for both central office and field monitoring applications, the platform provides a high dynamic range and spatial resolution using low optical power.

II-VI
Pittsburgh, PA
www.ii-vi-photonics.com

Positioning stage

The Lintech 610 series positioning stage provides a 7780 lb. load capacity and is available in stroke lengths from 6 to 60 in. The enclosed, screw-driven slide uses a low-friction, preloaded, recirculating linear ball bearing system riding on precision ground linear rail guides.

LinTech
Monrovia, CA
www.lintechmotion.com

Pulse generator

The Model 577 digital delay/pulse generator offers 4 or 8 channels, with each output individually configurable with its own trigger, gate, delay, and width settings. It provides precise timing up to 1000 s, with 250 ps width and delay

resolution and < 200 ps internal jitter. Optical electrical outputs and inputs are available.

Saelig
Fairport, NY
www.saelig.com

Coordinate measuring machine

The XM Series handheld probe coordinate measuring machine is designed to be easily installed in any environment and allow operators to perform accurate 3D measurements. Operation does not require any foundation or ancillary

equipment, and operating ranges are 50°–95°F and 20–80% RH. The system automatically records and saves all measurements.

Keyence
Itasca, IL
www.keyence.com/XMPR09

Nanopositioner

The PIHera Z flexure-guided piezo nanopositioning stage has travel ranges of 50 to 250 μm or 400 μm open-loop. Flexure-guided piezo positioning stages provide vibrationless motion. It is equipped with absolute-measuring, direct-metrology capacitance sensors and provide resolution down to 0.1 nm in a compact, FEA-optimized package for high stiffness and long lifetime.

PI (Physik Instrumente)
Auburn, MA
www.pi-usa.us

Interferometer

The SP1500 C interferometer from SIOS Messtechnik GmbH has a measuring range of > 15 m and has been designed for high-precision length, angle, and straightness measurements of linear axes. It uses a rotatable measuring

reflector consisting of hollow retro reflectors and a rotatable Wollaston prism. Calibration software and a USB interface are included.

Armstrong Optical
Northampton, Northamptonshire, England
www.armstrongoptical.co.uk

SXR spectrometer

The Model 251MX soft x-ray spectrometer includes a new gold-coated diffraction for work from 20 to 80 nm, for measurements of soft x-ray, extreme ultraviolet, and vacuum ultraviolet spectra. It includes an adjustable-width slit and adjustable detector mount. It operates at 10^{-6} torr vacuum, with a 10^{-10} torr version available.

McPherson
Chelmsford, MA
www.mcphersoninc.com

Manufacturers' Product Showcase

SuperGamut™ High-performance Spectrometer

BaySpec's high-performance ***SuperGamut***™ spectrometer is designed to cover the full spectral range of 200-2500 nm or your specific wavelength range with optimized performance and resolution. The unique turn-key system allows single acquisition for the entire wavelength range with ultrafast speed (up to 5K Hz). Utilizing BaySpec's patented VPG® grating technology, the spectrometer features compact size, high throughput with low stray light, and no moving parts with superb stability and reliability. Numerous ***SuperGamut*** have been shipped to date covering broad application areas such as OEM integration, light source measurement, radiometry and optical metrology.

BAYSPEC
Pervasive Spectroscopy

www.bayspec.com
sales@bayspec.com

Narrowband Optical Power Measurement

Ophir Photonics, global leader in precision laser measurement equipment and a Newport Corporation Company, introduces a new system for narrowband optical power measurement, the 3A-IS Optical Power Sensor and AUX-LED Self-Absorption Accessory. The 3A-IS is a compact, easy-to-use integrating sphere and photodiode sensor system. It is designed to measure the optical power of divergent, narrowband light sources from 350nm–1100nm, such as lasers and LEDs.

OPHIR® Photonics
A Newport Company
Spiricon® OPHIR Photonics
A Newport Company

sales@us.ophiropt.com • +1 435-753-3729
www.ophiropt.com/photonics

A Quantum Leap in Piezo Nanopositioning

Aerotech's QNP Series piezo nanopositioning stages offer nanometer-level performance in a compact, high-stiffness package for X, XY and Z axis applications. A variety of travel and feedback options make them ideal for applications from microscopy to optics alignment. Best-in-class stiffness and resonant frequency enable high process throughput and fast closed-loop response, and unparalleled geometric performance. The Ensemble QLAB stand-alone, piezo motion controller provides up to four axes of open- or closed-loop control. The front panel interface allows quick execution of simple operations such as jogging and moving to fixed positions. Onboard memory stores programs for more complex operations.

AEROTECH

www.aerotech.com

1919-R High Performance Optical Power Meter

Newport's new 1919-R High Performance Optical Power Meter will be released in October. It features on-board processing for advanced math and statistics functions, a color screen, and a comprehensive menu structure allowing an easy access to key functions.

Newport.
Experience | Solutions

(800) 222-6440
www.newport.com

New Laser Spectrum Analyzer

Bristol Instruments has introduced the model 771, a unique instrument that operates as both a high-accuracy wavelength meter and high-resolution spectrum analyzer. It is for researchers who need to know the spectral properties of their CW and high-repetition rate pulsed lasers that operate from 375 nm to 12 μm. Absolute laser wavelength is measured to an accuracy as high as ± 0.0001 nm, and the laser's spectrum is determined to a resolution as high as 2 GHz. What's more, these specifications are guaranteed by continuous calibration with a built-in wavelength standard, thereby ensuring the most meaningful experimental results.

Bristol Instruments

585-924-2620 • www.bristol-inst.com
info@bristol-inst.com

TracePro

Award-Winning Illumination Design, Analysis, and Optimization Software

- Luminaire Design
- LED Integration
- Light Pipe Design
- Design Optimization
- Biomedical Optics
- Stray Light Analysis

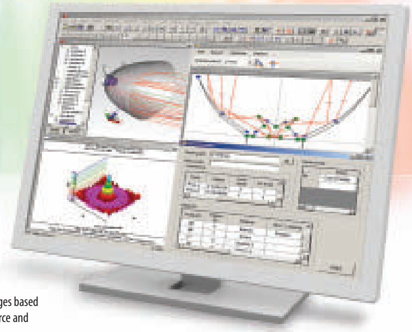

TracePro streamlines your prototype-to-manufacturing process with:

Photorealistic Rendering
Displays luminance and radiance maps as true color, images based on wavelength or as a photorealistic rendering using source and optical properties of the model

Light Source
Includes catalogs of LED surface sources from major manufacturers and imports source manufacturer ray files

2D & 3D Optimization
Sophisticated 2D and 3D optimizers provide complete and interactive control

CAD Interface
Enables geometry layout with familiar CAD tools and gadgets

Materials & Surfaces
Applies range of material and surface properties to objects and surfaces

REQUEST A FREE 30-DAY TRIAL TODAY www.lambdares.com

25 Porter Road | Littleton, MA 01460 USA
Phone: +1 978-486-0766 | Web: lambdares.com
sales@lambdares.com

LAMBDA RESEARCH CORPORATION

Mid-IR Optical Isolators

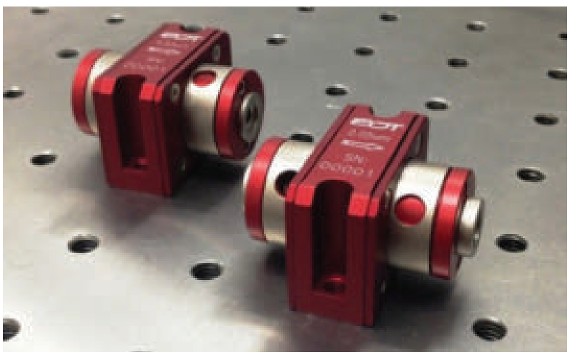

EOT's Mid-IR Optical Isolators maintain excellent beam quality while protecting lasers from back reflections. Our 2μm Faraday Isolator is designed for use with thulium and holmium lasers in the 1900-2100nm region. It provides >30dB isolation for power levels up to 30W with a pulsed damage threshold of 5J/cm^2 at 10ns. Our 4.55μm Faraday Isolator is designed for use with QCLs in the 4500 to 4600nm region. It provides >30dB isolation for power levels up to 2.5W and >65% transmission at 22°C.

EOT®

Electro-Optics Technology, Inc.
(231) 935-4044 | sales@eotech.com | www.eotech.com

LaserFocusWorld®

ONLINE

www.laserfocusworld.com

PennWell®

Manufacturers' Product Showcase

Pulsed Laser Diode Drivers from Avtech

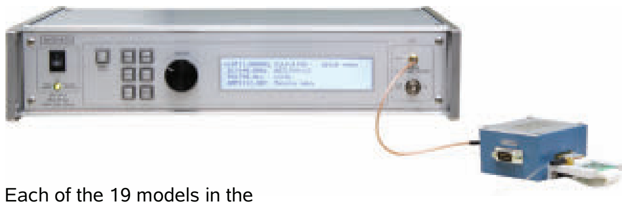

Each of the 19 models in the Avtech **AVO-9 Series** of pulsed laser diode drivers includes a replaceable output module with an ultra-high-speed socket, suitable for use with sub-nanosecond pulses.

Models with maximum pulse currents of 0.1A to 10A are available, with pulse widths from 400 ps to 1 us.

GPIB, RS-232, and Ethernet control available.

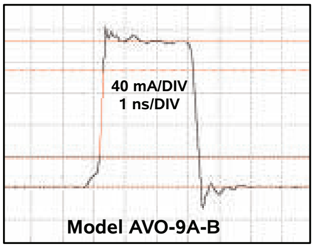

AVTECH

Pricing, manuals, datasheets at
http://www.avtechpulse.com/laser
More information: info@avtechpulse.com

MICRO Spectra Laser spectrum analyzer

- *7-20 pm resolution*
- *7-20 pm abs. accuracy*
- *Long-life calibration*
- *630-1083 nm range*

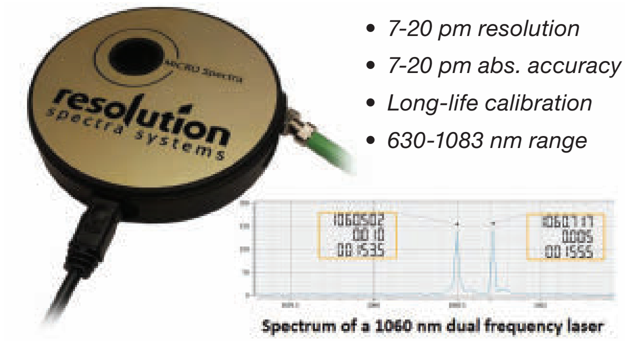

The MICRO Spectra is best in class in **high resolution, steady calibration** and **compactness**.

Characterize and control your **pulsed** and **cw lasers** (ECDL, DFB, DBR, VCSEL and many more) with this accurate and reliable tool.

resolution spectra systems

info@resolutionspectra.com • www.resolutionspectra.com

Q-Max Compact Precision Servo Stage

Q-Max series are stages with a compact envelope suitable for high precision and high stability positioning. The multi-directional high moment loading capability allows payloads of various envelope configurations, including overhanging CG, also in vertical Z-Axis installations.

A high resolution linear encoder provides position feedback with standard 50nm resolution and optional 1,2 nanometer for application specific high performance positioning.

The custom designed fine pitch ballscrew drive with preloaded nut mechanism guarantees elevated stiffness and secures excellent repeatability. The protective cover assures long term sustained positioning performance.

For the high rigidity guide system custom needle bearings rails are deployed featuring 4 rolling motion guide planes and non-recirculating continuous rolling motion elements. Achieves low mechanical noise, high rigidity, near infinite life expectancy and practically zero heat generation.

nutec MECHATRONIC SYSTEMS

www.nutec1.com • 631 242 1225 • info@nutecomp.com

Business Resource Center

Advertiser index

This ad index is published as a service. The publisher does not assume any liability for errors or omissions.
Send all orders & ad materials to: Ad Services Specialist, Laser Focus World, 1421 S. Sheridan, Tulsa OK 74112

LaserFocusWorld®

ADVERTISING SALES OFFICES

MAIN OFFICE
98 Spit Brook Road, LL-1, Nashua, NH 03062-5737
(603) 891-0123; fax (603) 891-0574

Publisher
Alan Bergstein
(603) 891-9447; alanb@pennwell.com

Executive Sales and Marketing Assistant
Julia Campbell
(603) 891-9174; juliac@pennwell.com

Digital Media Sales Operations Manager
Tom Markley
(603) 891-9307; thomasm@pennwell.com

Ad Services Manager
Alison Boyer-Murray
(918) 832-9369; fax (918) 831-9153
alisonb@pennwell.com

Director, List Sales
Kelli Berry
(918) 831-9782; kellib@pennwell.com

NORTH AMERICA

North America: East & Central
Jeff Nichols, National Sales Manager
(413) 442-2526; fax (413) 442-2527
jeffn@pennwell.com

North America: West & Mountain
AnneMarie St. John-Brooks,
(510) 606-0630; annemarie@pennwell.com

INTERNATIONAL

Austria, France, Germany, Switzerland, Russian Federation, United Kingdom
Holger Gerisch
+49-(0)8801-9153791; fax +49-(0)8801-9153792
holgerg@pennwell.com

Hong Kong/China Adonis Mak
852-2-838-6298; fax 852-2-838-2766
adonism@actintl.com.hk

India Rajan Sharma
91-11-686-1113; fax 91-11-686-1112
rajan@interadsindia.com

Israel (Tel Aviv) Dan Aronovic
972-9-899-5813; aronovic@actcom.co.il

Japan Masaki Mori
81-3-6721-9890; masaki.mori@ex-press.jp

Taiwan Diana Wei
886-2-2396-5128 ext. 270; fax: 886-2-2396-7816
diana@arco.com.tw

For all other international sales, please contact: Alan Bergstein, Publisher (see contact info. above)

For assistance with marketing strategy or ad creation, please contact:

Marketing Solutions
Vice President Paul Andrews
240.595.2352
pandrews@pennwell.com

Laser Focus World® (ISSN 1043-8092), Volume 51, No. 11. *Laser Focus World* is published 12 times a year, monthly by PennWell® Corporation, 1421 S. Sheridan, Tulsa, OK 74112. Periodicals postage paid at Tulsa, OK 74112 and at additional mailing offices. **SUBSCRIPTION PRICES:** USA $162 1yr., $310 2 yr., $443 3 yr.; Canada $216 1 yr., $369 2 yr., $507 3 yr.; International $270 1 yr., $435 2 yr., $578 3 yr. **POSTMASTER:** Send address corrections to *Laser Focus World*, P.O. Box 3425, Northbrook, IL 60065-3425.

Effective communication is fundamental to success in photonics

MILTON CHANG

A recent article in a business magazine cited that more than 60% of companies polled in a survey consider communication skills as the top skill they look for in hiring a new employee. I am surprised it is not 99.9%.

Effective communication to bring one's point across can make such a big difference in everything we do because we constantly have to sell our ideas, exert influence, and have our way—to land a job, win a grant, get funding to start a company, and convince people to take our side.

MILTON CHANG of Incubic Management was president of Newport and New Focus. He is currently director of mBio Diagnostics and Aurrion. He is a Trustee of the California Institute of Technology and has served on the SEC Advisory Committee on Small and Emerging Companies and the Visiting Committee on Advanced Technology of the National Institute of Standards and Technology, and the authoring committee of the National Academies' Optics and Photonics: Essential Technologies for Our Nation. Chang is a Fellow of IEEE, OSA, and LIA. Direct your business, management, and career questions to him at miltonchang@incubic.com, and check out his book *Toward Entrepreneurship* at www.miltonchang.com.

I was fortunate to get input from two friends to help me with this essay on the importance of communications: David Tytell, manager of marketing and communications at MIT, and Jeff Hecht, a regular contributor to this magazine and to *New Scientist*. Their input is particularly germane because both are technologists-turned-professional writers. I paraphrased what they said and thank them for sharing their wisdom and insight.

Dave stared at me when I asked him how to begin and said, pause a moment to contemplate where you stand relative to your reader or listener before you start. Decide on the message from their perspective. Define which aspects of your discussion can make an impression and how you might best convey the message to get their full attention.

For that, you have to know something about your audience and how they view you. Then, he told me about a YouTube video showing a blind person begging on a street corner. His placard states "I am blind, please help me!" He was able to get a few coins from time to time. Then, a passerby—no doubt a marketing professional—changed the message to read, "It is a beautiful day, but I can't see." Coins rained down on him hence. This video may be staged, but does point out that how you make your case does matter—in this example by appealing to a passerby's emotion vs. stating a fact.

Here are a few useful generalizations I got from Dave and Jeff:

Tell a story. Begin with an outline as if you are telling a story—no matter what you are writing, even if it is a research paper. Make the story fun, exciting, and suspenseful, as you want to capture the reader's full attention. If possible, keep the punch line until the end so the reader will read on. Use the so-called Watt's eight-point story arc: The stasis (starting point or status quo), trigger (what sparks off the story), quest (build the story), surprise, critical choice (crucial decision), climax, reversal, and resolution. Feel free to use adjectives, and even go overboard on superlatives because you can always ratchet back. Always follow the adage, tell them what you're going to tell them, tell them, and then tell them what you told them.

Be brief. It is really important to be able to express yourself clearly without being verbose. Anything more than necessary to make your point only serves to distract the reader. Information overload drowns out the main message—worse, it provides thoughts for objection.

Write it, sleep on it, and edit it again and again. Even experienced writers have difficulty getting started on a text. Write down whatever lead sentences come to mind to choose from later without worrying about the wording or even the order of your thoughts because it is easy to make revisions and move text around. Keep going until the first draft is finished. Then, fine-tune the text again and again! You will see ways to tell the story succinctly to get your message across, especially if you wait a few hours between drafts to see the text with fresh eyes. A 20% reduction in length with each pass is not an unrealistic goal.

Write frequently. Practice makes perfect! You will even become a better speaker. E-mail writing presents an excellent opportunity to practice communication skills. A good discipline is to edit the draft at least twice and reduce the length by 40% before hitting the send button. In a future editorial, I will address how to put your writing skills to practical use—for example, pitching to investors.

Programmable DC Power Supplies to 20 kV

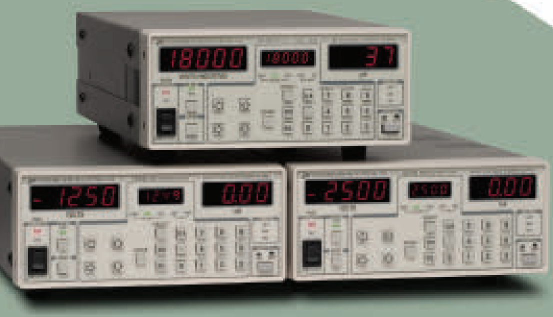

SRS has added four new high voltage power supplies to the PS300 series: −10 kV, +10 kV, −20 kV and +20 kV. All PS300 series supplies offer a wide range of features including programmable current and voltage limits, selectable overload response, short circuit protection, and a GPIB computer interface.

The combination of performance, features and price make the PS300 series the right choice.

www.thinkSRS.com/products/PS300.htm

- ***0.001 % regulation***
- ***0.05 % accuracy***
- ***1 volt resolution***
- ***0.0015 % output ripple***
- ***Programmable limits & trips***
- ***Voltage and current readouts***
- ***GPIB interface***

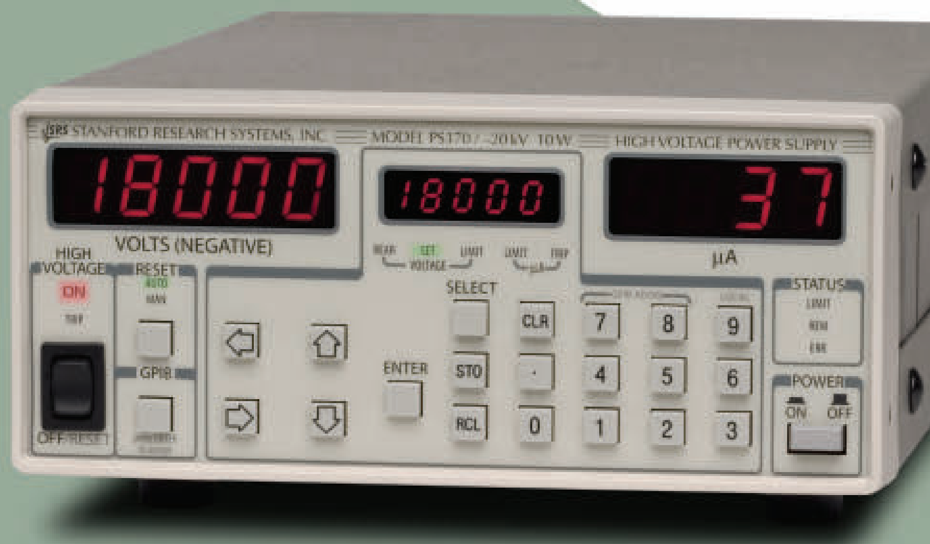

25 Watt Power Supplies ... $1395 (U.S. list)

- *PS310 ±1.25 kV*
- *PS325 ±2.5 kV*
- *PS350 ±5 kV*

10 Watt Power Supplies ... $2595 (U.S. list)

- *PS355 −10 kV*
- *PS365 +10 kV*
- *PS370 −20 kV*
- *PS375 +20 kV*

SRS ***Stanford Research Systems***

Phone: (408) 744-9040 Fax: (408) 744-9049 info@thinkSRS.com www.thinkSRS.com